Histological Assessment of Osteoarthritis Lesions in Mice

A DISSERTATION
SUBMITTED TO THE FACULTY OF THE GRADUATE SCHOOL
OF THE UNIVERSITY OF MINNESOTA
BY

Margaret Ann McNulty

IN PARTIAL FULFILLMENT OF THE REQUIREMENTS
FOR THE DEGREE OF
DOCTOR OF PHILOSOPHY

Cathy S. Carlson, Ph.D. Adviser

May, 2010

Acknowledgements

First and foremost I want to thank my adviser, Dr. Cathy Carlson, for all of her understanding, unwavering support, and advice throughout this journey, both in life and work. I wouldn't have survived without her.

Thank you to my committee: Dr. Richard Loeser, Dr. Liz Pluhar, and Dr. Al Beitz, whose support, input, and firm hand was just what I needed. Thanks to Josh Parker and Anne Undersander for all of their technical assistance; if left to my own devices I'd still be staring at a blank screen or microtome.

Thank you to Dr. Tom Fletcher, Dr. Vic Cox, Dr. Tina Clarkson, and Abby Rodriguez for allowing me to spend four fall semesters teaching in my academic "happy place", the gross anatomy lab. Thanks to the CMB faculty, staff, and students, especially the rest of the "Fab Five", Dr. Mary Mauzy, Dr. Erik Olson, & Lisa Hubinger.

I also would like to thank all of my family & friends for supporting me through this entire process and holding my hand through the crises. Dr. Kari Ekenstedt, your support & friendship has helped me through many a dark day. Dr. Brad Goupil, your love, support, & facetiousness the past few years has helped me more than you know. My four-legged & furry children: Mikie, Flash, Gizmo, Curious, Ronnie, Duncan, & Chester; most don't understand the support you provide, but I do, and I am eternally grateful for it. The biggest thank you of all goes to my father, Dr. John McNulty, whose unwavering love and support in everything I do started me on this remarkable path in life and convinced me that a love for science and gross anatomy is a genetic trait.

I would lastly like to thank all the mice who gave the ultimate sacrifice for this project.

This research was supported by grants from the National Institutes of Health and Arthritis Foundation.

Dedication

This dissertation is dedicated to my parents, Dr. John McNulty and Dr. Patricia Schwalm. Dad, this only marks the beginning of your duties in mentoring your daughter's career. Mom, wherever you are, I hope you are proud.

Abstract

The pathogenesis of osteoarthritis (OA) in both humans and animals is poorly understood. Histological assessment of tissue samples from joints is the most accurate way to diagnose OA severity. Unfortunately, current histological assessment grading schemes, such as the Mankin Histological-Histochemical Grading System (HHGS), are subject to observer variability and are unable to accurately distinguish varying levels of disease severity. The goals of this project were to: 1) develop a novel histological grading scheme to assess OA lesions in mice, 2) apply this scheme to several studies in which OA severity is expected to be influenced by treatment, and 3) compare the reliability and validity of this newly developed scheme to the widely used Mankin HHGS.

Histological sections from the knee (stifle) joints from 5 studies (n=158 joints), including 2 studies using a surgically induced model and 3 studies of naturally occurring disease, were globally examined for changes associated with OA. Changes that were consistent were evaluated using histomorphometry or assigned a grade based on severity. The final scheme that was developed included 13 quantitative and 2 semi-quantitative parameters that evaluated changes in articular cartilage, chondrocytes, subchondral & periarticular bone, and meniscus. Principal Components Analysis combined these 15 parameters into 5 factors that globally evaluated changes in articular cartilage integrity, chondrocyte viability, subchondral bone, periarticular osteophytes, and menisci. This newly developed scheme was then applied to five studies of murine OA, and comparisons among intervention groups in the 15 parameters and 5 factors were evaluated. In addition, the original Mankin HHGS was applied to these same sections. The newly developed scheme identified numerous changes in several tissues in both surgically induced and naturally occurring disease and was able to characterize several changes associated with OA severity in the mouse. While the Mankin HHGS was able to identify significant differences in the surgically induced models, it overlooked changes associated with naturally occurring disease. Finally, a direct comparison between the two schemes revealed that the newly developed scheme was more reliable than the Mankin HHGS, and was also able to correctly distinguish the severities of OA as well as the Mankin HHGS.

Table of Contents

List of Tables

List of Figures

List of Abbreviations

Abax OP	abaxial osteophyte	**GAG**	glycosaminoglycan
AC	articular cartilage	**H&E**	Hematoxylin & Eosin stain
AC area	articular cartilage area	**HRP**	horseradish peroxidase enzyme
AC thick	articular cartilage thickness	**ICC**	Intra-class Correlation
AC/chond	area of total articular cartilage per viable chondrocyte	**K&L**	Kellgren & Lawrence scale
ACLT	anterior (cranial) cruciate ligament tear model	**KIDA**	Knee Images Digital Analysis
ACS	articular cartilage structure score	**KOSS**	Knee Osteoarthritis Scoring System
AdLib	ad libitum	**Mankin HHGS**	Mankin Histological-Histochemical Grading System
AdLib W	ad libitum western diet	**Men area**	meniscal area
AdLib W LF	ad libitum western low-fat diet	**Men CCD**	area of chondrocyte cell death within the meniscus
ANOVA	analysis of variance	**MRI**	Magnetic Resonance Imaging
AUC	area under the curve	**MTL**	meniscotibial ligament
Ax OP	axial osteophyte	**NSAID**	non-steroidal anti-inflammatory drug
BLOKS	Boston Leeds Osteoarthritis Knee Score	**OA**	osteoarthritis
C57/Bl6	C57 Black 6 strain of mouse	**OARSI**	Osteoarthritis Research Society International
CCD	chondrocyte cell death	**OOCHAS**	Osteoarthritis Research Society International Cartilage Histopathology Assessment System
CCD%	percentage of chondrocyte cell death within the articular cartilage	**PCA**	Principal Components Analysis
CCD area	area of chondrocyte cell death within the articular cartilage	**PUFA**	poly-unsaturated fatty acid
CR	caloric restriction	**ROC**	receiver operating characteristic
CR W	caloric restriction western diet	**Saf-O**	Safranin-O staining score
CR W LF	caloric restriction western low-fat diet	**SCB**	subchondral bone
CT	computed tomography	**SCB area**	subchondral bone area
Ctrl	control group	**SCB thick**	subchondral bone thickness
DAB	3,3' diaminobenzidine	**TUNEL**	terminal deoxynucleotidyl transferase dUTP nick end labeling
DMM	destabilized medial meniscus	**VAC/chond**	area of viable articular cartilage per viable chondrocyte
DMOAD	disease modifying osteoarthritis drug	**WORMS**	Whole Organ Magnetic Resonance Imaging Score
EDTA	ethylenediaminetetraacetic acid	**WT**	wild-type

CHAPTER 1

INTRODUCTION & LITERATURE SEARCH

1.1 Osteoarthritis (OA)

Osteoarthritis (OA) is generally defined as a structural and functional failure of diarthrodial joints through progressive degeneration of bony and soft tissue components (1) and occurs when there is imbalance in the dynamic equilibrium between the breakdown and repair of joint tissues. (2) OA is commonly divided into primary OA and secondary OA, where primary (idiopathic) OA is of unknown cause, and secondary OA is initiated by an injury that creates instability or abnormal loading within a joint. OA is the most common form of arthritis in the US and affects approximately 15% of the overall population and over 85% of those aged 75 or over. (1) It is the most common cause of disability in those aged 18 years or older in the US. (3) Risk factors for primary OA include genetic inheritance, age, ethnicity, and female gender. (4) Altered load distribution patterns within a joint due to malalignment, obesity, joint injury, or altered muscle strength increase the risk for secondary OA. (5, 6) The disease commonly affects the knee, hands (specifically proximal and distal interphalangeal joints and the 1st carpometacarpal joint), hip, and lumbar spine, although the knee is one of the most commonly affected sites. (7)

Because OA is poorly understood and is diagnosed late in the course of the disease, no pharmacological interventions are available to delay progression or improve structural changes. Since pain is the most common symptom, currently available treatments for the disease mainly involve analgesics. For mild disease, over the counter topical analgesics and pharmacological drugs such as acetaminophen or non-steroidal anti-inflammatory drugs (NSAIDs) have historically been used to decrease pain

associated with OA and are commonly prescribed by practitioners. Intra-articular injections of corticosteroids & hyaluronic acid, and oral glucosamine & chondroitin have also been utilized in humans as well as other species. (8) There are surgical options available for those with moderate to severe OA, including arthroscopic surgery, osteotomy, and arthroplasty (joint replacement). (9, 10)

The main focus of research in OA currently is to identify a treatment that can slow or reverse the degradation of the articular cartilage and other structures within the joint. Since there is no cure for OA, researchers also have tried to identify methods of preventing the disease onset in addition to identifying more effective treatments for the disease. These research goals are based largely upon accurate assessment of OA severity in both humans and animals to determine if a given procedure or drug decreases progression of the disease.

1.2 Morphology of OA

OA is a very complex disease and the pathogenesis and initiating factors are not yet fully understood. It was once thought to be a disease solely of articular cartilage, however it has become clear that OA involves structures in the joint other than the articular cartilage, including surrounding bone and soft tissues. There are numerous changes and associated mechanisms that occur within the joint and these are too numerous to include in the current review. However, the changes that can be identified morphologically and are important in the histological evaluation of OA severity will be discussed in detail.

Articular Cartilage: Degradation and loss of articular cartilage is widely recognized as a major component of OA. Normal articular cartilage is composed of chondrocytes embedded within an extracellular matrix. This extracellular matrix can be divided into two components, the fibrillar matrix and extrafibrillar matrix. The fibrillar matrix is composed primarily of Type II collagen and the extrafibrillar matrix is composed of proteoglycans, the most abundant of these being aggrecan. (11) Aggrecan monomers are made up of glycosaminoglycan (GAG) side chains that have a high negative charge and attract water molecules, providing the biomechanical properties of cartilage that help withstand compressive loads. Characteristics of OA include fibrillation of, and clefting within, the articular cartilage, both of which may extend to the calcified cartilage and subchondral bone. The fibrillation and clefting in most species starts at the superficial surface of the articular cartilage and becomes increasingly more severe throughout the progression of the disease. Microscopic degradation of the fibrillar and extrafibrillar matrix components are evident in the early stages of the disease and eventually progress to complete disorganization of the collagen network, resulting in the loss of articular cartilage that is characteristic of OA. The depletion of the proteoglycans in osteoarthritic tissue has been shown to be a central factor in the pathogenesis of OA. (12) The exact relationship between the degradation of the collagen network and loss of proteoglycans within the articular cartilage is not known; however, a loosening of the collagen network leads to a loss of proteoglycans and further degradation of the collagen network which may then lead to an increase in water content and subsequent swelling of the articular cartilage. (13)

Chondrocytes: Chondrocytes are the cells within the articular cartilage matrix. They are derived from mesenchymal progenitor cells and are responsible for synthesis and maintenance of the extracellular matrix of cartilage. Chondrocytes have a low metabolic activity and survive in a hypoxic avascular environment within articular cartilage; they also possess little capacity to regenerate. Articular cartilage, in humans as well as animals, undergoes several changes during aging, including a decrease in chondrocyte number. (14) Apoptosis, or "programmed cell death", is a mechanism for removing damaged or harmful cells within an organism. It has been shown that chondrocyte apoptosis in cartilage increases with age in rodents (14), and during disease progression in surgically induced OA in animal models. (15) Other studies have indicated that apoptosis in OA cartilage is rare, however, suggesting that it is not a widespread phenomenon in the disease. (16) This discrepancy is likely due to the methods used to detect apoptotic cells in the earlier studies, where the researchers only used TUNEL (terminal deoxynucleotidyl transferase dUTP nick end labeling; a method to detect DNA fragmentation by labeling the terminal end of nucleic acids) to identify apoptotic cells. Results of the TUNEL assay are dependent on technical parameters such as enzyme concentration and are prone to errors. (17) The earlier studies also did not include proper specificity controls in their experiments, such as the growth plate. (16) More recent studies are examining potential inducers and pathways of chondrocyte apoptosis, including: nitric oxide (18); pro-inflammatory cytokines such as interleukin-8 and tumor necrosis factor (TNF)-α (19); and protein p-53 (20), which is indicated to play a role in numerous other diseases (21). Necrosis may also occur within the articular cartilage. One

of the differences noted between apoptosis and necrosis is that apoptosis affects individual cells, whereas necrosis affects groups of cells within a tissue. (22) However, necrotic chondrocytes have not been as well documented and studied as apoptotic chondrocytes within articular cartilage. Whether by apoptosis or necrosis, as the disease progresses, large areas of cell death and eventually acellularity can be seen within the articular cartilage. In addition to chondrocyte cell death, chondrocyte clones (aggregates of chondrocytes), are often found in OA cartilage. These chondrocytes have been found to be metabolically active. (23) In addition, clones may also suggest a level of recognition of the damage being caused and an attempt to repair it, as the majority of proliferative cells are found in the superficial zones of osteoarthritic articular cartilage where fibrillation and clefting of the extracellular matrix is found in early stages of the disease. (16)

Calcified Cartilage: The calcified cartilage is a mineralized zone of cartilage that serves as a transitional tissue between articular cartilage and the underlying subchondral bone. (24) One of the classic morphological changes within the joint during OA pathogenesis is duplication of the tidemark, which is the line of demarcation between the unmineralized articular cartilage and calcified cartilage. The tidemark experiences ongoing calcification and endochondral ossification that may cause the layer of calcified cartilage to thicken and subsequently alter the load distribution within the joint. (25) It is thought that the advancement of the tidemark and increase in calcified cartilage thickness subsequently decreases the thickness of articular cartilage which will lead to greater loss of articular cartilage as the disease progresses. However, while thickening of the calcified

cartilage and subchondral bone in the femoral heads of dogs with moderate or severe OA has been noted, no association between those changes and a loss of articular cartilage were identified. (26)

Subchondral Bone: The surrounding bone also plays a role in the morphological changes associated with the progression of OA, although the extent of this role has not been clearly delineated. Thickening of the subchondral bone is often associated with OA and always present in severe disease, but it was unclear whether this thickening is a primary feature of the disease and adds to the mechanical compression forces on articular cartilage therefore helping to exacerbate cartilage damage (27), or if the subchondral bone thickening is secondary and in response to the degradation of articular cartilage. The reactivation of the secondary center of ossification within the joint at the level of the calcified cartilage, which creates this thickening of subchondral bone, is indicated by duplications of the tidemark. (28) This increase in the number of tidemarks will decrease the thickness of the articular hyaline cartilage by replacing it with bone and lead to further loss of articular cartilage. (29) Subchondral bone is innervated by afferent sensory nerves, however, so an increase in thickness may have a more important role in the pain associated with OA. (30)

Osteophytes: Osteophytes are bony growths that are often associated with OA. They form within the periosteum at the junctions between cartilage and bone, most often at the joint margins, and are an important radiographic indication of OA, particularly end-stage disease. (31) It is not understood whether osteophytes are a pathological response or a functional adaptation and normal bone remodeling due to changes in joint

biomechanics secondary to OA. (31) One theory is that osteophytes develop to further stabilize the joint and protect it from additional damage by limiting the motion of the joint. (31) Both the periosteum and the synovial lining play a role in osteophyte formation. Mesenchymal stem cells within the periosteum or synovial lining are thought to be the precursor cells for osteophyte development. The growing osteophyte is continually covered with fibroblasts, which contribute to the growth by proliferation and differentiation to chondrocytes. The chondrocytes within the developing osteophyte then hypertrophy, leading to endochondral ossification and deposition of bone. (31)

Synovium: Synovium (synovial membrane) is the structure that lines synovial joints. It has two layers, the subintima (fibrous) and intima (cellular). The function of the synovium is to produce synovial fluid that helps lubricate synovial joints, and provide a boundary to maintain fluid within the joint. Synoviocytes are the main cell type within the intimal layer of the synovium. There are two types of synoviocytes: Type A (macrophagic cells) and Type B (fibroblast-like cells). (32) Type A cells phagocytose debris and cellular waste within the joint cavity, and Type B cells produce hyaluronan and lubricin that effectively lubricate the joint. (32) The synovium also has a blood supply that provides nutrients for the synovium and the avascular articular cartilage. As OA progresses, the synovial membrane thickens, synoviocytes become activated, and the synovial membrane becomes infiltrated with inflammatory cells. In addition, the synovial fluid experiences a decrease in hyaluronan, the molecule responsible for lubrication and shock absorption in synovial fluid, in response to an increase in OA. Although inflammation of the synovium is correlated with pain and other clinical outcomes of OA

in humans (33), and has been correlated with damage to knee articular cartilage as determined by arthroscopy (34), it is considered by most researchers to be a secondary reaction to the disease rather than a cause.

Meniscus: The menisci are semicircular fibrocartilagenous structures located in the articulation of the knee joint in the medial and lateral joint compartments and are firmly attached to the tibia by anterior and posterior (cranial and caudal) horns. The menisci are composed 98% of Type I collagen and have a much smaller proteoglycan content than does articular cartilage. (35) The collagen fibers within the menisci are oriented in a circumferential pattern and are important for providing strength and for holding the meniscus in place during loading. (36) The menisci have several functions within the normal joint, including providing stability for the convex femoral condyles on relatively flat tibial plateaus, lubrication (37), proprioception (38), load transmission (39), and shock absorption (40). Each meniscus covers approximately two thirds of the corresponding tibial plateau and weight-bearing articular cartilage. (36) It is widely known that there is a strong correlation between meniscal damage and the subsequent development of secondary OA, due to the menisci's important role in joint stabilization. Traumatic tears often occur in younger individuals and result in the fibers separating parallel to the circumferential fibers (36), and presence of these tears is strongly associated with knee OA. (41) Degenerative meniscal lesions are more common with older age and preexisting OA. (42) Osteoarthritic knee joints rarely have intact menisci, suggesting a correlation between the disease and the meniscus (36), however the relationship between the two is complex and poorly understood.

1.3 Animal models of OA

Naturally occurring (primary) OA occurs in species other than humans, including non-human primates, horses, dogs, guinea pigs, and other rodents. OA can also be surgically induced in many species by a variety of methods that destabilize the joint, causing abnormal loading patterns that are known to lead to secondary OA. There are many benefits to using animal models over human tissue. Firstly, animal models provide the opportunity to collect normal tissue, whether from the contralateral joint of the same animal or age-matched control animals. In addition, larger animals such as non-human primates and horses have large joints that allow for large tissue samples to be taken (e.g. synovial fluid, etc) for other analysis. Smaller animals, such as rodents, have smaller joints that can be evaluated intact. Secondly, the researcher knows the time of onset of disease in the case of a surgically-induced model, and can monitor the disease progression over several time points. Diet, exercise, medications, and other factors that may affect OA pathogenesis can be controlled. Finally, with the advances in molecular techniques, transgenic mouse models exhibiting numerous phenotypes are commercially available. The biggest drawback to using animal models is the uncertainty of whether the underlying processes of OA in animals, especially surgically induced animal models, closely match that of humans. Unfortunately pain, which is the major symptom of OA in humans, is not commonly evaluated in OA studies utilizing animal models of OA and therefore evaluation of OA severity in animal models has focused largely on structural damage within the joint due to OA. (43) There are species differences in the pathogenesis

of OA. For example, mice and guinea pigs often have tidemark clefts associated with severe disease (44), which are not seen in humans.

Naturally Occurring Models: Naturally occurring disease occurs in several animal species including: non-human primates, guinea pigs, and mice. The Dunkin-Hartley guinea pig model is widely used, as these animals consistently develop OA of the medial joint compartment of the stifle. About 50% of animals reaching the age of 3 months and a weight of 700 grams will have mild focal changes in the areas of the medial tibial plateau and femoral condyle that are not protected by the meniscus. (45) When the guinea pigs reach the age of 6 months and approximately 900 grams, 90-100% of the animals have mild to moderate lesions in the medial tibial plateau. (45) This model, while widely utilized, affects young animals and has a very rapid onset of disease, which does not model naturally occurring human disease as well as other models, such as disease in non-human primates. In rhesus macaques, prevalence of spontaneous disease matches that of humans, and is also associated with an increase in the number of tidemarks. Naturally occurring OA has also been identified and evaluated in cynomolgus macaques and the histological lesions that develop closely mimic those that are found in humans. (46-48) Naturally occurring models of mice are often used in research, mainly due to the availability of numerous transgenic and knock-out models. Spontaneous OA occurs in several mouse strains, including the SRT/Ort (49), SRT/IN (50), and the C57/Bl6 (51). Transgenic models include knock-outs for various collagens found within the articular cartilage: Type IX collagen deficient mice experience an increase in disease severity; A Disintegrin And Metalloproteinase with Thrombospondin motifs-5 (ADAMTS-5, an

aggrecanase enzyme) knockout in which the animals are protected from OA; and an IL-6 knockout, where the animals are also protected from OA, (52) among many others.

Surgically Induced Models: Surgically induced models of OA are meant to mimic traumatic joint damage in humans and are widely used. The cranial cruciate ligament (anterior cruciate ligament) transection (ACLT) model in the stifle joint (knee joint) of dogs is a very common model that produces moderate to severe lesions in a relatively short amount of time, with detectable OA changes occurring within the joint as early as 4 weeks post surgery. (53) In rabbits, removal or destabilization of all or part of either meniscus (54, 55) is commonly utilized, in addition to transection of the cranial cruciate ligament (55). Osteoarthritis has also been induced in the equine carpal joint by creating an osteochondral fragment that has been documented to create clinical lameness at 4 weeks post surgery. (56) These surgical models tend to rapidly create severe lesions within the joint. Therefore, other models have been developed to model mild to moderate OA lesions. One of these models is the Destabilized Medial Meniscus (DMM) (57) model in mice that creates moderate OA lesions within eight weeks.

There are advantages and disadvantages to surgically induced vs. naturally occurring animal models of OA. Surgically induced models have a known time point of disease onset, and by sacrificing animals at specific time points post-surgery, researchers can track disease progression. In addition, researchers can have some control over the severity of the disease by choosing the appropriate model and modifying timepoints to sacrifice of the animal and collection of tissues. A drawback to surgically induced models is that these create disease secondary to destabilization of the joint, which accounts for

only a small percentage of human disease. Primary OA commonly affects humans, and it is unclear whether the pathogenesis of primary and secondary OA is the same. Therefore surgically induced models of OA in animals may not mimic the disease progression of naturally occurring OA in humans. Nonetheless, both surgically induced and naturally occurring animal models have proven useful in studying the underlying mechanisms of OA and in the development and testing of potential disease modifying OA drugs (DMOADs). However, care should be taken in choosing the correct animal model to suit the needs of the study. Considerations such as housing, severity & location of OA lesions, and size of the joint should all be addressed by the researcher.

1.4 Evaluation and Imaging of OA

Accurate assessment of OA severity is critical for treating patients with the disease and for research studies focused on the evaluation of pharmacological interventions on disease severity. The goal of imaging techniques (radiography, MRI, & CT) is to evaluate OA severity *in vivo*, usually in a clinical setting, whereas other macroscopic and microscopic assessments are suited for evaluating samples *ex vivo*, commonly acquiring samples during partial or complete arthroplasty in humans or at the time of sacrifice in the case of animal models. The American College of Rheumatology has created criteria for evaluating idiopathic osteoarthritis *in vivo* of the knee (58), hip (59), and hand (60) in humans. These criteria have formed the basis for identifying OA in human subjects using clinical, radiographic, and laboratory evaluations (e.g. erythrocyte sedimentation rate to measure non-specific inflammation), and are widely used in studies

of OA in humans. Joint pain is a criterion that is included in all three classifications. Additional requirements for knee joint evaluation include age of the patient greater than 50 years, stiffness, osteophytes, and bony tenderness in addition to other criteria.

Macroscopic Evaluation: Macroscopic assessment of OA severity in autopsy or surgically retrieved samples was refined by Collins and McElligott. (61) This assessment is composed of 5 semi-quantitative grades that evaluate the loss of articular cartilage grossly. Grade 0 represents a normal joint with smooth cartilage, Grade 1 includes superficial fibrillation within cartilage, Grade 2 represents deeper fibrillation within cartilage, Grade 3 includes areas of total loss of articular cartilage and obvious osteophytes, and finally Grade 4 represents large areas of completely denuded bone with prominent osteophytes. The original study found a correlation between increased $^{35}SO_4$ uptake in articular cartilage chondrocytes and an increase in histological grades. (61) The Collins & McElligott scale is used often to macroscopically categorize OA severity in humans. Although it is highly subjective and provides only a superficial assessment of disease severity, it is very widely used in studies evaluating OA severity and is often utilized to separate joint specimens into varying stages of disease. In larger joints, such as those from dogs, humans, and non-human primates, an overall macroscopic assessment of the articular cartilage may be utilized using India Ink staining. (62, 63) India Ink allows visualization of areas of fibrillation within the articular cartilage and will assist researchers in identifying a focal area within the joint having the most severe articular cartilage lesions.

Radiography: In humans, radiographs have been traditionally used to diagnose OA and radiography is often referred to as the gold standard for imaging joints to evaluate OA severity. To evaluate outcomes in research studies, subchondral bone, joint space width, and presence of osteophytes have been the focus of evaluation schemes that have been developed for radiographic findings. The Kellgren & Lawrence (K&L) scale (64) has been the most commonly and widely used radiographic evaluation scheme in humans. This is a semi-quantitative evaluation scheme of the knee joint that includes joint space narrowing, presence of osteophytes, and subchondral bone sclerosis as parameters. Other schemes that incorporate measurements as opposed to semi-quantitative scales also have been devised, such as KIDA (Knee Images Digital Analysis). (65) KIDA includes measurements of joint space width, subchondral bone density, osteophyte size, tibial eminence height, and joint angles. In at least one study, significant differences between these parameters were identified between healthy and osteoarthritic knees, and correlations between these measurements and K&L grade were significant. (65)

Magnetic Resonance Imaging (MRI): With recent technological advancements in the sensitivity of MRI, several groups have worked to put together evaluation schemes for OA severity using MRI images. These include Whole-Organ MRI Score (WORMS) (66), the Knee Osteoarthritis Scoring System (KOSS) (67), and the Boston-Leeds Osteoarthritis Knee Score (BLOKS) (68). The WORMS method was developed for use with 1.5T MRI magnets and semi-quantitatively evaluates 14 different features that include changes in articular cartilage, subchondral bone, osteophytes, menisci, cruciate

ligaments, collateral ligaments, and synovium. (66) This system is widely used in studies utilizing MRI assessment of OA severity in humans. The KOSS scoring system was also developed for 1.5T magnets and evaluates lesions within the articular cartilage, osteophytes, subchondral bone changes, and meniscal changes using semi-quantitative scores. (67) Finally, the Boston Leeds Osteoarthritis Knee Score (BLOKS) is composed of semi-quantitative scores that evaluate bone marrow lesions, loss of articular cartilage, size of osteophytes, synovial volume, meniscal extrusion and tears, and presence or absence of ligamentous tears and periarticular features. (68) While these systems were developed for use in 1.5T MRI magnets, the measurements can easily be conducted on images taken with a 3.0T MRI magnet system or higher and will likely be more accurate due to the increase in quality of the images of the structures, however comparisons between the accuracy of the various evaluation schemes using more advanced MRI techniques have not yet been done.

1.5 Histology of OA

Histology is the method that is most precise in determining OA severity in specific sites in humans and other species. In larger animals and humans, cartilage biopsy samples may be taken from the joint *in vivo* and examined histologically. In smaller animals, often the joint is too small for sampling and therefore the entire joint needs to be evaluated. The location within the joint that is to be examined histologically needs to be determined based on the species and model of OA being utilized in the study. In some models, lesions are more severe in the medial tibial plateau as opposed to the lateral tibial

plateau or femoral condyles. In these cases, macroscopic evaluations described above, such as the Collins & McElligott scheme (61) or India Ink can be utilized to identify the area where lesions are most severe. In surgically induced models of OA, very focal lesions may appear before widespread loss of articular cartilage throughout the tibial plateau or femoral condyle occurs. These focal lesions can then be sectioned and stained for histological evaluation. For smaller joints such as in mice, the joints are small enough so that sections can be taken at regular intervals throughout the entire joint and can be subsequently assessed with a simpler method to determine the location of the most severe lesions.

As noted previously, there are morphological changes within many different bony and soft tissues within the joint that are associated with the pathogenesis of OA and can be identified histologically. While most of these changes, such as cartilage fibrillation and chondrocyte cell death, can be identified with a simple Hematoxylin & Eosin stain, the structure of articular cartilage in animal and human models has often been assessed by cationic stains that bind to proteoglycans within the articular cartilage and include Toluidine Blue, Safranin-O, and Alcian Blue. Toluidine Blue & Safranin-O are the most commonly utilized stains in OA studies. Safranin-O is a cationic dye that binds to glycosaminoglycans, staining a bright red color, and is often used with a counterstain of Fast Green. (69) Toluidine Blue also stains proteoglycans within the articular cartilage, but with a deep blue/purple color. A loss of the Safranin-O or Toluidine Blue staining indicates a decrease in glycosaminoglycans within the articular cartilage.

Factors involved in section preparation may affect the histological assessment of any joint tissue. Problems may arise during sectioning of the joints if they are improperly decalcified. Artifactual "chatter" of the calcified bony tissue will result in tears that may be interpreted as true lesions within the articular cartilage or surrounding bone and soft tissue. Artifactual tearing of tissue, especially articular cartilage, by other means such as a dull knife or improper mounting can closely resemble structural damage to the articular cartilage matrix due to OA and may result in an inaccurately higher histological score. Therefore great care needs to be taken when sectioning and staining the tissue that is to be evaluated in order to avoid any damage that may decrease the quality of the section to be evaluated, especially if the histological evaluation relies only on one or two sections per joint. Other factors that need to be considered include tissue orientation (plane of section) and staining techniques. Joints must be embedded correctly to achieve optimal orientation for evaluating hyaline cartilage. Fibrocartilage that is normally present along the joint margins is only weakly stained by Safranin-O and Toluidine Blue stains. This lack of positive staining in the joint margins may be mistaken for a loss of either of these stains in hyaline cartilage in joints that are embedded incorrectly and display a large amount of fibrocartilage along the joint margins. Finally, the Safranin-O and Toluidine Blue stains, where a lack of staining is considered a positive result, are subject to staining variation if sections are not stained at the same time and using the same reagents. Therefore it is important to stain all sections at the same time to minimize this variation. Most histological schemes are appropriate only for studies in which optimal sectioning & staining techniques have been used.

1.6 Histological Assessment of OA

Despite advances in imaging technology, none of these methods provide the morphological detail that can be obtained histologically. Thus, histological evaluation is the gold standard method of accurately evaluating the severity of OA in humans and animals. Unfortunately, there is little agreement regarding the optimal scheme to use for these evaulations. Several researchers have developed histological grading schemes that evaluate OA severity (57, 70, 71), but each has limitations and none have been able to accurately separate the mild and moderate changes associated with early stage disease. These early changes are critical in determining if a potential OA treatment is effectively modifying disease severity. Because it is highly unlikely that treatments will be developed that will reverse the changes that are induced in the OA process, the best hope for a successful treatment for this disease is one that will slow or halt the degenerative changes that occur in this disease when the treatment is administered over a long period of time. The development of this type of treatment and its assessment in animal models will require the use of a sensitive histological grading scheme.

Mankin HHGS: The histopathology of OA has traditionally been evaluated using the histological-histochemical grading system (HHGS) proposed by Mankin, et al, which was designed to evaluate changes in the articular cartilage of humans. (71) This grading scheme uses four subjective parameters to grade the severity of OA lesions in the joint, including evaluation of cartilage structure (range of grades: 0-6), cells (0-3), loss of Safranin-O or Toluidine Blue staining (0-4), and tidemark integrity (whether or not the

tidemarks are crossed by blood vessels; 0-1). The scores from each of the parameters are added together to get a final total score, 0 corresponding to normal articular cartilage, 14 corresponding to severe OA. Unfortunately, although it is widely used, this scheme suffers from a high level of subjectivity (72-74) and includes no quantitative evaluations. For the cartilage structure and loss of Safranin-O/Toluidine Blue staining categories, the range of grades that can be assigned is narrow and only the depth of the lesions is evaluated, with no consideration of the extent of the change. This scheme also employs wording such as "slight", "moderate", or "severe" but does not clearly define the criteria for these designations. In addition, the final joint score is a summation of the grades for all four categories even though the interrelationships of these changes are not known and the ranges of grades that can be assigned to the various categories are different. Finally, because the resulting data are not continuous, appropriate statistical analyses must use nonparametric methods.

Several studies have attempted to validate the Mankin HHGS. (72, 74) The first study completed by van der Sluijs & colleagues tested the scheme on a surgically induced model (medial menisectomy) or a plaster immobilization model of OA in rabbits. (72) Five observers evaluated 71 samples with the Mankin HHGS scheme twice with a 2 week interval in between each evaluation. Then, the same five observers repeated the study and re-evaluated the same samples with a two week interval between evaluations, however this time they utilized a modified Mankin HHGS that had more strict criteria for the four parameters and grades. The authors found that the true Mankin HHGS had intra-observer means that were similar, but the standard deviations were rather large, showing a large

amount of variation between the two evaluations for each observer. There was also variation found between observers when the sections were evaluated with the Mankin HHGS. When the observers evaluated the sections using the stricter modified Mankin scheme, there was a reduction in intra-observer and inter-observer reproducibilities. The authors also found no patterns among the four parameters and determined that all parameters contributed to the variation within the total score. Despite these results, the authors concluded that this scheme is an acceptable histological tool. This study did not have a method of determining levels of severity of OA, and only served to evaluate the reproducibility of the scheme using multiple observers.

A second study was conducted to evaluate the reproducibility and validity of the Mankin HHGS. (74) This study utilized articular cartilage from human femoral heads. Normal articular cartilage came from necropsies of sudden deaths (n=40), and OA cartilage came from joints that underwent complete arthroplasty and had Collins & McElligott grades of III or IV. In addition, areas of articular cartilage with less severe disease were obtained from these OA joints (Collins & McElligott grades of I &II) so that a total of 15 OA sections were obtained. Three observers, with varying degrees of experience in evaluating osteoarthritic tissue, evaluated the tissue twice with at least one week in between. Both intra-observer and inter-observer reproducibilities were found to be low, and the observer with less experience evaluating OA had a high variability when compared to the more experienced observers. The authors from this study did find patterns among the four parameters, where the Safranin-O score was the most reproducible but also tended to have higher scores, and the Tidemark Integrity score was

rarely utilized by the observers. In addition, the Mankin HHGS was not always able to significantly differentiate normal from OA cartilage, and varying grades were given to normal joints based on location from which the section was taken. Finally, 30% of the joints that were normal had overall grades higher than 5 (out of 14), whereas 47% of OA joints received scores greater than 5. These results do not support the previous paper which identified the Mankin HHGS as an acceptable method of histological evaluation of OA cartilage. The authors suggested that a macroscopic assessment, such as the Collins & McElliggott scale (61), be used in addition to a microscopic assessment such as the Mankin HHGS. Unfortunately, this is nearly impossible in the smaller joints of rodents, and most studies in rodents must rely entirely upon histological assessment of OA severity.

A third study also attempted to validate the Mankin HHGS. (73) This study was done by the same researcher as the previous study (74), and builds upon the study they initially performed to evaluate the reliability of the Mankin HHGS by using a more structured sampling technique to serve as the "gold standard" of OA severity since there is no such gold standard in existence. Once again, the same sampling technique as the previous study was used to obtain normal articular cartilage, however in this study the cartilage was obtained from the knee joint instead of the hip (either femoral condyles or tibial plateaus). OA cartilage was obtained from individuals who underwent total arthroplasty of the knee joint and had Collins & McElligott scores of III or IV. The samples that were obtained from these joints included an area of intact cartilage progressing to an area of completely denuded bone. These sections were then covered by

non-translucent tape so only a fourth of the area of the sample was visible, representing normal cartilage, and mild (superficial fibrillation), moderate (deep fibrillation), and severe (completely denuded bone) disease. This technique allowed comparisons of Mankin HHGS scores for varying degrees of disease severity. The observation procedure was the same as in the previous study. The researchers found in this study that while the Mankin scheme appears to be able to distinguish normal joint tissues from severely affected joints, it is not sensitive enough to distinguish more subtle differences, for example between mildly and moderately affected joints. Once again, the inter- and intra-observer reproducibilities were low with a wide variation in scores.

All three studies reported results that support the hypothesis that the Mankin HHGS is not an ideal method of evaluating OA severity. The goal of a histological grading scheme of OA is to accurately and reproducibly identify varying degrees of severity of OA lesions within articular cartilage, regardless of the species. Low inter- and intra-observer reproducibilities for the total Mankin HHGS score were detected in all three studies, and the third study additionally found this scheme was unable to accurately evaluate disease severity. In addition, the Mankin HHGS was developed to assess OA severity in humans, and changes in articular cartilage addressed by the Mankin HHGS do not always apply to all species, such as rodents that do not have distinctive zones of articular cartilage. The first study evaluated OA severity in rabbits, but the two other studies utilized human OA tissue, so this scheme has yet to be validated on OA severity in other commonly used species such as rodents. In addition, rodents lose articular cartilage by advancement of tidemark clefts (44) more so than superficial fibrillation of

the articular cartilage surface. Despite the limitations identified by several studies of the Mankin HHGS, it remains the histological grading scheme that is most commonly utilized and modified and to which all other potential histological grading schemes are compared.

OARSI Cartilage Histopathology Assessment System (OOCHAS): Other research groups have recognized these limitations in the Mankin HHGS and created additional histological grading systems that expand on the Mankin HHGS. Pritzker, et al, with a working group of the Osteoarthritis Research Society International (OARSI), developed a histological grading scheme based on five principles: simplicity, utility, scalability, extendibility, and comparability. (70) The authors believed that a histological grading scheme should be simple and reproducible, easily utilized in both clinical and experimental OA, produce data that is linear in comparison to severity, is able to accommodate needs of most researchers and studies, and is able to be compared to other histological grading schemes. What the authors developed was a grading scheme that includes changes in articular cartilage structure, proliferation and hypertrophy of chondrocytes, changes in staining patterns (Safranin-O & Toluidine Blue), bone cyst formation, remodeling and sclerotic subchondral bone, and osteophyte formation. These numerous changes were combined into seven grades with two sub-grades each that evaluate the depth of lesions into the articular cartilage and five stages that evaluate the extent of the joint involvement. This scheme attempts to simplify whole joint changes into one semi-quantitative histological grading scheme that accounts for depth of lesions into the plateau or condyle as well as extent throughout the tibial plateau. While this

scheme is an improvement upon the Mankin HHGS, it combines changes in articular cartilage, chondrocytes, and surrounding bone into a single grade, even though the severity of changes in each of these tissues may not be uniform at any given point in time.

A subsequent study evaluated the effectiveness of the OOCHAS system and compared it to the pre-established Mankin HHGS. (75) The tissue that was evaluated was from a study in which cartilage damage was induced by biomaterial articulation in goats in which the medial tibial plateau of the right stifle was replaced with a cobalt-chromium implant. One to two months after surgery the animals were euthanized and cartilage samples were collected from three standardized locations in the medial & lateral tibial plateaus and medial & lateral femoral condyles. However, the method of sampling the medial tibial plateau that contained the cobalt-chromium implant was not provided in the methods. Seventy-eight samples total were obtained, resulting in 936 sections with lesions ranging from almost normal to severely affected, and one section from each sample was used in the final evaluation. The authors found that the OOCHAS system had high intra- and inter-observer reproducibilities and positively correlated with the Mankin HHGS, however the hypothesized increases of inter- and intra-observer reproducibilities of the OOCHAS scheme compared to those of the Mankin scheme were not observed. Nevertheless, the reliability of the OOCHAS system was found to be higher than that of the Mankin HHGS. In addition, the OOCHAS system takes into account the extent of the lesion within the plateau or condyle in addition to the depth, whereas the Mankin HHGS only addresses the depth. However, the OOCHAS system also assumes a linear

progression of OA disease severity by grouping changes within several tissues into one grade. By grouping several changes into one grade, it makes the assessment more difficult in the instance when changes associated with multiple grades occur within the same joint. In addition, damage to the articular cartilage matrix is also assessed using the zones of articular cartilage as utilized in the Mankin HHGS. These zones are difficult, if not impossible, to distinguish in the small joints of rodents that are commonly used in OA research. Once again, differences in pathogenesis among species is not addressed, such as the fact that tidemark clefts occur only in rodents (44), so this makes the scheme difficult to apply to all species.

Glasson, et al scheme: Another histological grading scheme was developed by Glasson, et al (57) that is based on and very closely resembles a scheme developed by Chambers, et al (76). This scheme is simpler than even the Mankin HHGS, and focuses solely on changes within the articular cartilage structure, but was developed specifically for mice and utilizes multiple sections from one mouse joint that are spaced at 80μm intervals so that each joint yields approximately 13-16 slides for evaluation. The scheme itself is based on structural changes within the articular cartilage and Safranin-O staining. The grades are defined as: Grade 0, normal articular cartilage; Grade 0.5, loss of Safranin-O without structural lesions; Grade 1, small fibrillations; Grade 2, fibrillation deeper to the superficial layer; Grade 3, fibrillations extending into the calcified cartilage in less than 20% of the width; Grade 4, fibrillations extending into calcified cartilage in greater than 20% but less than 80% of the cartilage width; Grade 5, fibrillations extending into calcified cartilage in greater than 80% of the width. The scores are

gathered for all sections in both medial tibial plateaus and femoral condyles and evaluated as the maximum score and the sum of all scores. This grading scheme was able to detect significant differences between the two surgically destabilized groups, destabilized medial meniscus (DMM) and anterior (cranial) cruciate ligament transection (ACLT), and their respective control joints using both maximum and summed scores, but was not able to detect significant differences between the joints in the two surgical groups, indicating that it is useful to evaluate severity of lesions but not to better understand pathogenesis. (57)

Likely due to its simplicity, this scheme has gained popularity in evaluating OA severity in mice. A significant drawback of this scheme however, is that it only addresses changes within the articular cartilage matrix and does not include evaluation of any other tissues that are known to be affected during the progression of OA. It also has yet to be validated and inter- and intra-observer reproducibilities have not yet been determined. In addition, this scheme has not been compared to pre-established histological grading schemes. This scheme is also labor-intensive as numerous sections from each joint must be sectioned, stained, and finally evaluated, which is not commonly done when using other histological grading schemes that only evaluate one or two sections per joint. This also creates a hurdle in comparing this scheme to other pre-established histological schemes that only use one section in the evaluation process. However, a benefit of this scheme is that a researcher can evaluate the entire joint and does not need to have determined the location if the location of the most severe lesions for the particular model being utilized in the study. This scheme would be very useful as a global assessment of

OA severity in conjunction with a more precise and comprehensive evaluation of the area of the most severe lesions within the joint.

Articular Cartilage Repair: Other histological grading schemes have been developed to assess articular cartilage integrity, mostly during the repair process as opposed to progression of OA. A lesser-known histological grading scheme was developed by O'Driscoll et al to specifically evaluate the effect of an autogenous periosteal graft that was sutured into the base of a full-thickness defect created in the patellar groove of the femur in rabbits. (77) Three surgical groups were included in this study based on post-operative treatment of the defect: immobilization by cast for four weeks & 48 weeks of active motion in the cage, 52 weeks of active motion in the cage, or two weeks of continuous passive motion. This scheme utilizes approximately 20 sections taken from regular intervals; odd numbered sections are stained with Hematoxylin & Eosin and even numbered sections are stained with Safranin-O. The scheme initially only included four semi-quantitative parameters (range or available grades): surface regularity (1-3), structural integrity (1-3), bonding to the adjacent cartilage (1-3), and level of newly formed tissue (1-3). It was then subsequently modified and expanded to evaluate the effectiveness of autologous periosteal grafts in treating full thickness defects in rabbits one year postoperatively. (78) The modified scheme included nine semi-quantitative parameters (range): cellular morphology (0, 2, 4), Safranin-O staining of the matrix (0-3), surface regularity (0-3), structural integrity (0-2), thickness (0-2), bonding to the adjacent cartilage (0-2), hypocellularity (0-3), chondrocyte clustering (0-2), and freedom from degenerate changes in adjacent cartilage (0-3). In the first study, each of the parameters

was evaluated separately and reported as the percentage of joints that were assigned each score. The authors found significant differences among the three surgical groups in all four parameters, most notably in the bonding to adjacent tissue. The second study utilized a similar statistical approach by reporting the percent (and total number) of rabbits that were assigned each subparameter of the grading scale. In addition, average scores for each subparameter were calculated. Significant results were identified among treatment groups in several parameters, with the most significant differences noted in the thickness parameter.

Another scheme, developed by Pineda et al, evaluated articular cartilage repair following surgical production of two different sizes of full thickness defects. (79) The authors noted that the Mankin HHGS evaluates OA severity only and does not evaluate extent of healing from the disease within the joint. Therefore they set out to develop a scheme that would grade articular cartilage healing. In the scheme that was developed, four parameters were included (grades or range): filling of defect (1, 0, 1, 2, 3, 4; where a grade of 1 can either mean 125% filling of the defect or 75% filling of the defect), reconstruction of osteochondral junction (0-2), matrix staining (0-4), and cell morphology (0-4). Sections were cut from each condyle and stained with Hematoxylin & Eosin, Safranin-O, Mallory-Heidenhain (connective tissue stain), and Alcian Blue stains. Three high-quality sections from each joint were obtained and graded, and means and standard deviations were calculated for both individual parameters and the final total scores. The authors did not find significant differences in healing between sizes of the defects, but

were able to detect differences among the different timepoints of sacrifice and detected rapid cartilage repair between post-operative days 2 and 14.

The two schemes described above were compared by Moojen et al (80) utilizing an *in vivo* model of cartilage repair in the goat (81). Goals of this study were to compare the relatively complicated scheme described by O'Driscoll et al (78) to the simpler scheme developed by Pineda et al (79) and calculate previously unpublished inter- and intra-observer reproducibilities for both schemes. In addition, correlations between two schemes were evaluated. The authors expected that the Pineda, et al scheme would have higher reproducibilities due to the simplicity of the scheme, whereas the O'Driscoll, et al scheme would provide a higher power of discrimination due to the complexity of the scheme. Both grading schemes, however, had relatively high inter- and intra-observer reproducibilities; 0.92 and 0.87 respectively for the O'Driscoll scheme and 0.89 and 0.86 respectively for the Pineda scheme. The authors also found that the O'Driscoll, et al scheme was as reproducible as the Pineda, et al scheme, and explained that the large number of parameters in the O'Driscoll scheme may mask any small variations in inter- and intra-observer reproducibilities for a single parameter. The authors felt that both schemes were acceptable for evaluating articular cartilage repair and that no modifications to either scheme were necessary.

These schemes of articular cartilage repair are very similar to the semi-quantitative schemes that are established to evaluate OA severity. They also have the same pitfalls as described above for the other schemes, including subjective definitions for grades within certain parameters ("normal", "moderate", "slight", "none" for

Safranin-O staining of the matrix). In addition, the "Filling of Defect" parameter in the scheme developed by Pineda, et al (79), assigns the same grade to a defect that is filled 75% and 125% of the way, which gives the impression that these levels of repair are the same. The variability in using these schemes appears to be similar to values reported for the Mankin HHGS, which is expected since the three schemes are similar in terms of subjectivity of the parameters. However, O'Driscoll et al (78) used an interesting method of statistical evaluation by determining the total number or percentage of animals assigned each score in each treatment group and performing parametric statistical analysis on those values as opposed to the average histological scores for each treatment group. This eliminates the problem encountered with the Mankin HHGS and others that evaluate the non-parametric semi-quantitative grades with parametric statistical evaluations.

Overall Summary: It has been well established that, while the Mankin HHGS can be useful in identifying OA within joints, a great deal of improvement is needed to develop a scheme that will be useful in studies relying on accurate evaluation of OA severity. Other researchers have attempted to either modify the Mankin HHGS or devise new schemes that can accurately and reproducibly evaluate degradation of joint structures. (57, 70, 76, 82, 83) Furthermore, researchers have then modified these new schemes even further, which make comparing histological evaluation across studies almost impossible. Evaluations of the accuracy of these grading schemes are also quite difficult due to a lack of clear definitions of mild, moderate, and severe disease. Despite many modifications and improvements upon the Mankin HHGS and others, some of the

fundamental issues with histologically evaluating OA that were discussed earlier still remain. While the scheme devised by Glasson, et al, (57) has gained popularity, especially in evaluating OA severity in mice and other rodents, it is a very superficial method of evaluating OA and will not yield much information other than extent of damage to the extracellular matrix of articular cartilage. On the other hand, this method may be extremely useful as an initial evaluation of disease severity if the location of the most severe lesions is unknown in a particular model. A second, more comprehensive histological grading system may then be employed to further evaluate changes within the joint once the most severe lesions have been identified. The third study to validate the Mankin HHGS indicated that a simple numerical score would likely not be adequate in accurately identifying OA severity as it is a multifactorial disease with a complex pathogenesis. (44) A scheme that may be broken down into the individual parameters may be more useful to evaluate the complex pathogenesis of OA, as certain parameters may identify early changes and others may be more useful in determining end-stage disease. The same scheme may also be easily applied to other facets of articular cartilage biology, such as repair. The schemes for articular cartilage repair are similar to those for OA, and while they have been deemed “acceptable” to accurately evaluate articular cartilage repair (80), they may also benefit from similar modifications to those made to histological schemes that evaluate OA severity.

1.7 Histomorphometry

Bone is constantly remodeling in response to changes in mechanical forces and other factors. Histomorphometry is the study of the microscopic structure of a tissue and has been commonly used to evaluate changes in the microarchitecture of cortical and trabecular bone. The first attempts to quantitatively evaluate these changes were made in the late 1960's and early 1970's (84, 85) using a light microscope and an ocular grid. Since then, advances in technology have led to programs being developed especially for evaluating bone microarchitecture. A main focus of bone histomorphometry is the two-dimensional evaluation of number, width, and spatial organization of trabeculae using histological sections that are measured in millimeters or millimeters squared. Dynamic measurements of bone formation, such as mineral apposition and bone formation rate, may be evaluated in animals administered fluorochrome labels. (86) To standardize the nomenclature, symbols, and units utilized in bone histomorphometry, criteria for each was published by the American Society for Bone and Mineral Research. (87) Over 20 different measurements were standardized and are commonly utilized in the morphometric evaluation of bone. Algorithms have been devised to subsequently calculate trabecular thickness, number, and separation from two-dimensional measurements of trabecular area and thickness. (88) These measurements are commonly utilized in research studies of osteoporosis and renal diseases that affect bone density in both humans and animals. Histomorphometry is so commonly used to evaluate various pathological changes within bone that specific quantitative histomorphometric diagnostic criteria are used to definitively diagnose chronic kidney disease from bone biopsies in humans. (89) Some studies have started to utilize histomorphometry techniques to

evaluate changes within the joint that are associated with OA. Pastoureau and colleagues developed a histomorphometric scheme that evaluated cartilage thickness, fibrillation index, proteoglycan content, chondrocyte density, and subchondral bone plate thickness in a partial menisectomy model of OA in guinea pigs. (90) The authors found a significant increase in fibrillation index and subchondral bone plate thickness, and a significant decrease in chondrocyte density in the menisectomized joints when compared to the shams. Histomorphometry can be easily applied to tissues within the joint and changes that are associated with OA. It has been shown to be a reproducible technique that will potentially decrease some of the subjectivity in histological evaluation of OA severity.

1.8 Overall Summary

Overall, OA is a very common disease in the human population for which there is no cure or effective treatment. The pathogenesis of OA is not completely understood, which makes finding treatments for the disease quite difficult. Due to the symptoms of OA, the most common treatment for the disease includes addressing knee pain with NSAIDs or other analgesics. Current research focuses on other methods of treating pain and other symptoms in addition to addressing the causes and pathogenesis of OA. Determining methods to treat or prevent OA has become a main component of the research focused on the disease. In order to determine if the proposed methods are effective, accurate histological assessment of the joints to determine the extent and severity of OA is necessary. There are several types of studies that rely on the accurate

histological assessment of OA in this species, including evaluation of transgenic mice for OA lesions and studies that examine the effects of pharmaceuticals and nutraceuticals on OA severity in animal models prior to testing in humans. In humans, most studies focus on evaluating OA severity using radiographic or MRI-based grading schemes *in vivo*. Conversely, in animal models of OA histology is a critical component of studies evaluating the effect of different treatments on OA severity. Due to the ease of maintaining small animals and the increase in transgenic and surgical models of OA in mice, many researchers utilize mice and other small rodents in their studies. Development of a histological grading scheme that can accurately assess the morphological changes occurring in the joints and can distinguish between mild, moderate, and severe OA lesions in these mouse models is key to being able to detect differences between treatment groups should an intervention method be developed to slow or even stop the progression of OA in these animals. Unfortunately, commonly used histological grading schemes, such as the Mankin HHGS and others, do not provide adequate information on all changes that occur within the joint, nor do they take into account species differences in the pathogenesis of OA. In addition, they rely on subjective assessments and to a great deal of observer variability. Histomorphometry is commonly used to objectively evaluate bony changes, and can be applied to evaluate changes within the joint. The focus of this project was to develop a histological grading scheme that takes into account changes associated with OA in multiple tissues within the joint, utilizing both semi-quantitative grades and histomorphometry evaluations, and address specific changes that occur in mouse stifles.

1.9 Hypothesis and Specific Aims

Overall Hypothesis: The overall hypothesis for this project was that a semi-quantitative histological grading scheme combining both semi-quantitative grades and histomorphometric evaluations will be sufficiently accurate and precise to reliably distinguish normal knee (stifle) joints from those with mild, moderate, and severe OA in mice in which the lesions occur naturally or are surgically induced.

Specific Aim 1: Develop a histological grading scheme for osteoarthritis of the knee (stifle) joint in mice by characterizing changes associated with osteoarthritis in the stifle joint (in both surgically induced and naturally occurring models) that included a large number of joints and a wide range of lesions. Changes that are consistent among the joints can then either measured using histomorphometry or assigned a grade based on severity.

Hypothesis: A histological grading scheme can be developed that will reproducibly and quantitatively characterize changes in articular cartilage, meniscus, and subchondral bone occurring in OA.

Specific Aim 2: Apply this histological grading scheme that was developed in Specific Aim 1 to five studies (n= 158 joints) in which OA severity in both spontaneous and induced models of mice is expected to be influenced by treatment.

Hypothesis: An investigation using this scheme will be able to distinguish between mild, moderate, and severe OA lesions in several different mouse models of OA.

Specific Aim 3: Compare this new histological grading scheme with existing schemes to determine its accuracy and precision (sensitivity/specificity).

Hypothesis: The new histological grading scheme will, regardless of the identity of the observer, be able to distinguish mild, moderate, and severe OA lesions and will provide information regarding lesion location whereas the existing Mankin HHGS scheme will not when both schemes are applied to the same set of tissues.

1.10 References

1. Hunter DJ, Eckstein F. Exercise and osteoarthritis. J Anat. 2009 Feb;214(2):197-207.

2. Eyre DR. Collagens and cartilage matrix homeostasis. Clin Orthop Relat Res. 2004 Oct;(427 Suppl)(427 Suppl):S118-22.

3. Centers for Disease Control and Prevention (CDC). Prevalence and most common causes of disability among adults--united states, 2005. MMWR Morb Mortal Wkly Rep. 2009 May 1;58(16):421-6.

4. Felson DT. An update on the pathogenesis and epidemiology of osteoarthritis. Radiol Clin North Am. 2004 Jan;42(1):1,9, v.

5. Felson DT. Risk factors for osteoarthritis: Understanding joint vulnerability. Clin Orthop Relat Res. 2004 Oct;(427 Suppl)(427 Suppl):S16-21.

6. Roos H, Karlsson J. Anterior cruciate ligament instability and reconstruction. review of current trends in treatment. Scand J Med Sci Sports. 1998 Dec;8(6):426-31.

7. [homepage on the Internet]. . 2006. Available from: http://www.niams.nih.gov/Health_Info/Osteoarthritis/default.asp.

8. Bellamy N, Bell MJ, Goldsmith CH, Lee S, Maschio M, Raynauld JP, et al. BLISS index using WOMAC index detects between-group differences at low-intensity symptom states in osteoarthritis. J Clin Epidemiol. 2009 Nov 5.

9. NIH consensus statement on total knee replacement. NIH Consens State Sci Statements. 2003 Dec 8-10;20(1):1-34.

10. Lutzner J, Kasten P, Gunther KP, Kirschner S. Surgical options for patients with osteoarthritis of the knee. Nat Rev Rheumatol. 2009 Jun;5(6):309-16.

11. Aigner T, McKenna L. Molecular pathology and pathobiology of osteoarthritic cartilage. Cell Mol Life Sci. 2002 Jan;59(1):5-18.

12. Huang K, Wu LD. Aggrecanase and aggrecan degradation in osteoarthritis: A review. J Int Med Res. 2008 Nov-Dec;36(6):1149-60.

13. Maroudas AI. Balance between swelling pressure and collagen tension in normal and degenerate cartilage. Nature. 1976 Apr 29;260(5554):808-9.

14. Adams CS, Horton WE,Jr. Chondrocyte apoptosis increases with age in the articular cartilage of adult animals. Anat Rec. 1998 Apr;250(4):418-25.

15. Hashimoto S, Takahashi K, Amiel D, Coutts RD, Lotz M. Chondrocyte apoptosis and nitric oxide production during experimentally induced osteoarthritis. Arthritis Rheum. 1998 Jul;41(7):1266-74.

16. Aigner T, Hemmel M, Neureiter D, Gebhard PM, Zeiler G, Kirchner T, et al. Apoptotic cell death is not a widespread phenomenon in normal aging and osteoarthritis human articular knee cartilage: A study of proliferation, programmed cell death

(apoptosis), and viability of chondrocytes in normal and osteoarthritic human knee cartilage. Arthritis Rheum. 2001 Jun;44(6):1304-12.

17. Aigner T. Apoptosis, necrosis, or whatever: How to find out what really happens? J Pathol. 2002 Sep;198(1):1-4.

18. Abramson SB. Nitric oxide in inflammation and pain associated with osteoarthritis. Arthritis Res Ther. 2008;10 Suppl 2:S2.

19. Kim J, Xu M, Xo R, Mates A, Wilson GL, Pearsall AW,4th, et al. Mitochondrial DNA damage is involved in apoptosis caused by pro-inflammatory cytokines in human OA chondrocytes. Osteoarthritis Cartilage. 2009 Oct 1.

20. Hashimoto S, Nishiyama T, Hayashi S, Fujishiro T, Takebe K, Kanzaki N, et al. Role of p53 in human chondrocyte apoptosis in response to shear strain. Arthritis Rheum. 2009 Aug;60(8):2340-9.

21. Nayak SK, Panesar PS, Kumar H. p53-induced apoptosis and inhibitors of p53. Curr Med Chem. 2009;16(21):2627-40.

22. Kuhn K, D'Lima DD, Hashimoto S, Lotz M. Cell death in cartilage. Osteoarthritis Cartilage. 2004 Jan;12(1):1-16.

23. Kouri JB, Jimenez SA, Quintero M, Chico A. Ultrastructural study of chondrocytes from fibrillated and non-fibrillated human osteoarthritic cartilage. Osteoarthritis Cartilage. 1996 Jun;4(2):111-25.

24. Oegema TR,Jr, Carpenter RJ, Hofmeister F, Thompson RC,Jr. The interaction of the zone of calcified cartilage and subchondral bone in osteoarthritis. Microsc Res Tech. 1997 May 15;37(4):324-32.

25. Bullough PG, Jagannath A. The morphology of the calcification front in articular cartilage. its significance in joint function. J Bone Joint Surg Br. 1983 Jan;65(1):72-8.

26. Daubs BM, Markel MD, Manley PA. Histomorphometric analysis of articular cartilage, zone of calcified cartilage, and subchondral bone plate in femoral heads from clinically normal dogs and dogs with moderate or severe osteoarthritis. Am J Vet Res. 2006 Oct;67(10):1719-24.

27. Radin EL, Rose RM. Role of subchondral bone in the initiation and progression of cartilage damage. Clin Orthop Relat Res. 1986 Dec;(213)(213):34-40.

28. Brandt KD, Radin EL, Dieppe PA, van de Putte L. Yet more evidence that osteoarthritis is not a cartilage disease. Ann Rheum Dis. 2006 Oct;65(10):1261-4.

29. Burr DB. Anatomy and physiology of the mineralized tissues: Role in the pathogenesis of osteoarthrosis. Osteoarthritis Cartilage. 2004;12 Suppl A:S20-30.

30. Goldring MB, Goldring SR. Osteoarthritis. J Cell Physiol. 2007 Dec;213(3):626-34.

31. van der Kraan PM, van den Berg WB. Osteophytes: Relevance and biology. Osteoarthritis Cartilage. 2007 Mar;15(3):237-44.

32. Iwanaga T, Shikichi M, Kitamura H, Yanase H, Nozawa-Inoue K. Morphology and functional roles of synoviocytes in the joint. Arch Histol Cytol. 2000 Mar;63(1):17-31.

33. Hill CL, Gale DG, Chaisson CE, Skinner K, Kazis L, Gale ME, et al. Knee effusions, popliteal cysts, and synovial thickening: Association with knee pain in osteoarthritis. J Rheumatol. 2001 Jun;28(6):1330-7.

34. Ayral X, Pickering EH, Woodworth TG, Mackillop N, Dougados M. Synovitis: A potential predictive factor of structural progression of medial tibiofemoral knee osteoarthritis -- results of a 1 year longitudinal arthroscopic study in 422 patients. Osteoarthritis Cartilage. 2005 May;13(5):361-7.

35. Eyre DR, Wu JJ. Collagen of fibrocartilage: A distinctive molecular phenotype in bovine meniscus. FEBS Lett. 1983 Jul 25;158(2):265-70.

36. Englund M, Guermazi A, Lohmander SL. The role of the meniscus in knee osteoarthritis: A cause or consequence? Radiol Clin North Am. 2009 Jul;47(4):703-12.

37. MacCONAILL MA. The movements of bones and joints; the synovial fluid and its assistants. J Bone Joint Surg Br. 1950 May;32-B(2):244-52.

38. Assimakopoulos AP, Katonis PG, Agapitos MV, Exarchou EI. The innervation of the human meniscus. Clin Orthop Relat Res. 1992 Feb;(275)(275):232-6.

39. Walker PS, Erkman MJ. The role of the menisci in force transmission across the knee. Clin Orthop Relat Res. 1975;(109)(109):184-92.

40. Englund M. The role of the meniscus in osteoarthritis genesis. Med Clin North Am. 2009 Jan;93(1):37,43, x.

41. Englund M, Lohmander LS. Risk factors for symptomatic knee osteoarthritis fifteen to twenty-two years after meniscectomy. Arthritis Rheum. 2004 Sep;50(9):2811-9.

42. Noble J, Hamblen DL. The pathology of the degenerate meniscus lesion. J Bone Joint Surg Br. 1975 May;57(2):180-6.

43. Ameye LG, Young MF. Animal models of osteoarthritis: Lessons learned while seeking the "holy grail". Curr Opin Rheumatol. 2006 Sep;18(5):537-47.

44. Otterness IG, Chang M, Burkhardt JE, Sweeney FJ, Milici AJ. Histology and tissue chemistry of tidemark separation in hamsters. Vet Pathol. 1999 Mar;36(2):138-45.

45. Bendele AM. Animal models of osteoarthritis. J Musculoskelet Neuronal Interact. 2001 Jun;1(4):363-76.

46. Carlson CS, Loeser RF, Jayo MJ, Weaver DS, Adams MR, Jerome CP. Osteoarthritis in cynomolgus macaques: A primate model of naturally occurring disease. J Orthop Res. 1994 May;12(3):331-9.

47. Carlson CS, Loeser RF, Johnstone B, Tulli HM, Dobson DB, Caterson B. Osteoarthritis in cynomolgus macaques. II. detection of modulated proteoglycan epitopes in cartilage and synovial fluid. J Orthop Res. 1995 May;13(3):399-409.

48. Carlson CS, Loeser RF, Purser CB, Gardin JF, Jerome CP. Osteoarthritis in cynomolgus macaques. III: Effects of age, gender, and subchondral bone thickness on the severity of disease. J Bone Miner Res. 1996 Sep;11(9):1209-17.

49. Mason RM, Chambers MG, Flannelly J, Gaffen JD, Dudhia J, Bayliss MT. The STR/ort mouse and its use as a model of osteoarthritis. Osteoarthritis Cartilage. 2001 Feb;9(2):85-91.

50. Schunke M, Tillmann B, Bruck M, Muller-Ruchholtz W. Morphologic characteristics of developing osteoarthrotic lesions in the knee cartilage of STR/IN mice. Arthritis Rheum. 1988 Jul;31(7):898-905.

51. Glasson SS. In vivo osteoarthritis target validation utilizing genetically-modified mice. Curr Drug Targets. 2007 Feb;8(2):367-76.

52. de Hooge AS, van de Loo FA, Bennink MB, Arntz OJ, de Hooge P, van den Berg WB. Male IL-6 gene knock out mice developed more advanced osteoarthritis upon aging. Osteoarthritis Cartilage. 2005 Jan;13(1):66-73.

53. Boileau C, Martel-Pelletier J, Abram F, Raynauld JP, Troncy E, D'Anjou MA, et al. Magnetic resonance imaging can accurately assess the long-term progression of knee structural changes in experimental dog osteoarthritis. Ann Rheum Dis. 2008 Jul;67(7):926-32.

54. Messner K, Fahlgren A, Ross I, Andersson B. Simultaneous changes in bone mineral density and articular cartilage in a rabbit meniscectomy model of knee osteoarthrosis. Osteoarthritis Cartilage. 2000 May;8(3):197-206.

55. Wachsmuth L, Keiffer R, Juretschke HP, Raiss RX, Kimmig N, Lindhorst E. In vivo contrast-enhanced micro MR-imaging of experimental osteoarthritis in the rabbit knee joint at 7.1T1. Osteoarthritis Cartilage. 2003 Dec;11(12):891-902.

56. Frisbie DD, Kawcak CE, Werpy NM, Park RD, McIlwraith CW. Clinical, biochemical, and histologic effects of intra-articular administration of autologous conditioned serum in horses with experimentally induced osteoarthritis. Am J Vet Res. 2007 Mar;68(3):290-6.

57. Glasson SS, Blanchet TJ, Morris EA. The surgical destabilization of the medial meniscus (DMM) model of osteoarthritis in the 129/SvEv mouse. Osteoarthritis Cartilage. 2007 Sep;15(9):1061-9.

58. Altman R, Asch E, Bloch D, Bole G, Borenstein D, Brandt K, et al. Development of criteria for the classification and reporting of osteoarthritis. classification of osteoarthritis of the knee. diagnostic and therapeutic criteria committee of the american rheumatism association. Arthritis Rheum. 1986 Aug;29(8):1039-49.

59. Altman R, Alarcon G, Appelrouth D, Bloch D, Borenstein D, Brandt K, et al. The american college of rheumatology criteria for the classification and reporting of osteoarthritis of the hip. Arthritis Rheum. 1991 May;34(5):505-14.

60. Altman R, Alarcon G, Appelrouth D, Bloch D, Borenstein D, Brandt K, et al. The american college of rheumatology criteria for the classification and reporting of osteoarthritis of the hand. Arthritis Rheum. 1990 Nov;33(11):1601-10.

61. COLLINS DH, McELLIGOTT TF. Sulphate (35SO4) uptake by chondrocytes in relation to histological changes in osteoarthritic human articular cartilage. Ann Rheum Dis. 1960 Dec;19:318-30.

62. Kobayashi K, Amiel M, Harwood FL, Healey RM, Sonoda M, Moriya H, et al. The long-term effects of hyaluronan during development of osteoarthritis following partial meniscectomy in a rabbit model. Osteoarthritis Cartilage. 2000 Sep;8(5):359-65.

63. Luther JK, Cook CR, Cook JL. Meniscal release in cruciate ligament intact stifles causes lameness and medial compartment cartilage pathology in dogs 12 weeks postoperatively. Vet Surg. 2009 Jun;38(4):520-9.

64. KELLGREN JH, LAWRENCE JS, BIER F. Genetic factors in generalized osteo-arthrosis. Ann Rheum Dis. 1963 Jul;22:237-55.

65. Marijnissen AC, Vincken KL, Vos PA, Saris DB, Viergever MA, Bijlsma JW, et al. Knee images digital analysis (KIDA): A novel method to quantify individual radiographic features of knee osteoarthritis in detail. Osteoarthritis Cartilage. 2008 Feb;16(2):234-43.

66. Peterfy CG, Guermazi A, Zaim S, Tirman PF, Miaux Y, White D, et al. Whole-organ magnetic resonance imaging score (WORMS) of the knee in osteoarthritis. Osteoarthritis Cartilage. 2004 Mar;12(3):177-90.

67. Kornaat PR, Ceulemans RY, Kroon HM, Riyazi N, Kloppenburg M, Carter WO, et al. MRI assessment of knee osteoarthritis: Knee osteoarthritis scoring system (KOSS)--inter-observer and intra-observer reproducibility of a compartment-based scoring system. Skeletal Radiol. 2005 Feb;34(2):95-102.

68. Hunter DJ, Lo GH, Gale D, Grainger AJ, Guermazi A, Conaghan PG. The reliability of a new scoring system for knee osteoarthritis MRI and the validity of bone marrow lesion assessment: BLOKS (boston leeds osteoarthritis knee score). Ann Rheum Dis. 2008 Feb;67(2):206-11.

69. Rosenberg L. Chemical basis for the histological use of safranin O in the study of articular cartilage. J Bone Joint Surg Am. 1971 Jan;53(1):69-82.

70. Pritzker KP, Gay S, Jimenez SA, Ostergaard K, Pelletier JP, Revell PA, et al. Osteoarthritis cartilage histopathology: Grading and staging. Osteoarthritis Cartilage. 2006 Jan;14(1):13-29.

71. Mankin HJ, Dorfman H, Lippiello L, Zarins A. Biochemical and metabolic abnormalities in articular cartilage from osteo-arthritic human hips. II. correlation of morphology with biochemical and metabolic data. J Bone Joint Surg Am. 1971 Apr;53(3):523-37.

72. van der Sluijs JA, Geesink RG, van der Linden AJ, Bulstra SK, Kuyer R, Drukker J. The reliability of the mankin score for osteoarthritis. J Orthop Res. 1992 Jan;10(1):58-61.

73. Ostergaard K, Andersen CB, Petersen J, Bendtzen K, Salter DM. Validity of histopathological grading of articular cartilage from osteoarthritic knee joints. Ann Rheum Dis. 1999 Apr;58(4):208-13.

74. Ostergaard K, Petersen J, Andersen CB, Bendtzen K, Salter DM. Histologic/histochemical grading system for osteoarthritic articular cartilage: Reproducibility and validity. Arthritis Rheum. 1997 Oct;40(10):1766-71.

75. Custers RJ, Creemers LB, Verbout AJ, van Rijen MH, Dhert WJ, Saris DB. Reliability, reproducibility and variability of the traditional Histologic/Histochemical grading system vs the new OARSI osteoarthritis cartilage histopathology assessment system. Osteoarthritis Cartilage. 2007 Nov;15(11):1241-8.

76. Chambers MG, Bayliss MT, Mason RM. Chondrocyte cytokine and growth factor expression in murine osteoarthritis. Osteoarthritis Cartilage. 1997 Sep;5(5):301-8.

77. O'Driscoll SW, Keeley FW, Salter RB. The chondrogenic potential of free autogenous periosteal grafts for biological resurfacing of major full-thickness defects in joint surfaces under the influence of continuous passive motion. an experimental investigation in the rabbit. J Bone Joint Surg Am. 1986 Sep;68(7):1017-35.

78. O'Driscoll SW, Keeley FW, Salter RB. Durability of regenerated articular cartilage produced by free autogenous periosteal grafts in major full-thickness defects in joint surfaces under the influence of continuous passive motion. A follow-up report at one year. J Bone Joint Surg Am. 1988 Apr;70(4):595-606.

79. Pineda S, Pollack A, Stevenson S, Goldberg V, Caplan A. A semiquantitative scale for histologic grading of articular cartilage repair. Acta Anat (Basel). 1992;143(4):335-40.

80. Moojen DJ, Saris DB, Auw Yang KG, Dhert WJ, Verbout AJ. The correlation and reproducibility of histological scoring systems in cartilage repair. Tissue Eng. 2002 Aug;8(4):627-34.

81. Saris DB, Lafeber FP, Bijlsma JW, Dhert WJ, Verbout AJ. Cartilage repair by tissue engineering not successful in arthritic knees. Proc Orthop Res Soc. 2001:0200.

82. Laprade RF, Wentorf FA, Olson EJ, Carlson CS. An in vivo injury model of posterolateral knee instability. Am J Sports Med. 2006 Aug;34(8):1313-21.

83. Olson EJ, Wentorf FA, McNulty MA, Parker JB, Carlson CS, LaPrade RF. Assessment of a goat model of posterolateral knee instability. J Orthop Res. 2008 May;26(5):651-9.

84. Whitehouse WJ. The quantitative morphology of anisotropic trabecular bone. J Microsc. 1974 Jul;101(Pt 2):153-68.

85. Wakamatsu E, Sissons HA. The cancellous bone of the iliac crest. Calcif Tissue Res. 1969;4(2):147-61.

86. Chavassieux P, Meunier PJ. Histomorphometric approach of bone loss in men. Calcif Tissue Int. 2001 Oct;69(4):209-13.

87. Parfitt AM. Bone histomorphometry: Proposed system for standardization of nomenclature, symbols, and units. Calcif Tissue Int. 1988 May;42(5):284-6.

88. Dalle Carbonare L, Valenti MT, Bertoldo F, Zanatta M, Zenari S, Realdi G, et al. Bone microarchitecture evaluated by histomorphometry. Micron. 2005;36(7-8):609-16.

89. Miller PD. The role of bone biopsy in patients with chronic renal failure. Clin J Am Soc Nephrol. 2008 Nov;3 Suppl 3:S140-50.

90. Pastoureau P, Leduc S, Chomel A, De Ceuninck F. Quantitative assessment of articular cartilage and subchondral bone histology in the meniscectomized guinea pig model of osteoarthritis. Osteoarthritis Cartilage. 2003 Jun;11(6):412-23.

CHAPTER 2

DEVELOPMENT OF A COMPREHENSIVE HISTOLOGICAL GRADING SCHEME FOR OSTEOARTHRITIS IN MICE

The purpose of the present study was to develop a histological grading scheme to accurately assess the severity of osteoarthritis (OA) in mice. Coronal sections of paraffin embedded stifle joints from 158 mice with naturally occurring or surgically-induced OA were prepared. Two representative midcoronal sections were stained with Hematoxylin & Eosin (H&E) and Safranin-O stains. All slides were randomized and evaluated to characterize the changes present within the joints. A grading scheme that includes both measurements and semi-quantitative scores was developed to characterize changes of OA in murine stifle joints. Correlation analysis and Principal Components Analysis (PCA) identified significant associations among parameters and reduced the large number of correlated parameters to a smaller number of factors. Correlation analysis revealed highly significant correlations between the two semi-quantitative parameters (Articular Cartilage Structure and Safranin-O staining scores) and 6 continuous parameters ($p \leq 0.0001$ for all) in the medial tibial plateau. Correlations among these parameters were weaker in the lateral tibial plateau where the lesions were less severe. Five factors were retained by PCA using data from the medial tibial plateaus, accounting for 74% of the total variance in the data. The five factors had substantial contributions (factor loadings > 0.40) from parameters describing 1) articular cartilage integrity, 2) chondrocyte viability, 3) subchondral bone changes, 4) meniscus changes, and 5) periarticular changes. This grading scheme and resulting factors characterize joint changes in murine stifle joint that are associated with OA.

2.1 Introduction

Accurate morphological assessment of osteoarthritis (OA) severity in both human and animal tissues is critical for evaluation of results from studies that are designed to slow the progression of the disease. Several research groups have developed methods to quantify and standardize morphological changes of OA in humans using radiographic, MRI, and arthroscopic evaluations. (1-5) Because of the many issues (e.g., cost; variations in environmental factors, diet, and activity; concurrent medications, etc.) involved in conducting human OA studies, researchers have used animal models of OA to assess the effectiveness of various disease-modifying OA drugs (DMOADs) prior to testing in humans. The use of animal models ensures a more uniform population of subjects for study and provides the ability to euthanize animals at the end of the study to allow histological assessment of the joint tissues, providing data regarding specific structural features that are not obtainable using *in vivo* methods.

For many years, the Mankin Histological-Histochemical Grading System (HHGS) (6), which was initially developed for evaluation of human joint tissue but has been adopted for use in numerous animal species, has been the most widely-used grading scheme for assessing articular cartilage parameters of OA severity. Species differences in cartilage (7, 8), bone morphology (9), and in the development of OA, however, suggest that grading schemes for this disease should be tailored to individual species. The Mankin HHGS includes evaluation of four parameters (Structure, Cells, Safranin-O staining, & Tidemark integrity) that identify changes within the articular cartilage of the joint. Although this scheme is widely used, previous studies identified limitations such as

observer variability and a lack of specificity (i.e., the scheme is able to distinguish normal from severely affected articular cartilage, but is unable to distinguish among intermediate disease severities). (10, 11) These limitations are likely due, at least in part, to the imprecise definitions that are used for assigning scores, as well as to the narrow range of available scores within individual parameters. For example, the "Safranin-O" staining score (to evaluate extent of proteoglycan loss from cartilage matrix) defines scores of 1 through 3 as mild, moderate, and severe reduction in stain and are highly subject to individual interpretation and experience. In addition, the "Structure" score takes into account the depth, but not the extent, of the lesions across the plateau or condyle. Therefore, according to the definitions of the scores used for this parameter, a single cleft extending to the tidemark line (junction of articular cartilage and calcified cartilage) would receive the same score as a joint with complete loss of articular cartilage. In addition, one gradation of the Structure score includes the presence or absence of pannus tissue (grade 2 out of 6), which is a characteristic of rheumatoid arthritis, is not commonly found in osteoarthritic tissue, and is never present in the early stages of the disease.

Species differences in OA are also important considerations when using the Mankin HHGS. For example, mouse articular cartilage is too thin to allow identification of the designated zones (transitional & radial) that are included in the "Structure" parameter of this scheme. In addition, mice along with other rodents develop tidemark clefts as a feature of OA (12), and these are not included in the Mankin HGGS.

The Mankin HHGS also does not include changes that may be present in tissues other than articular cartilage, such as subchondral and periarticular bone, synovium, and menisci, which are also relevant to the pathogenesis of OA. (13-16) Once the grades from all four parameters are determined, they are added together to create a total joint score; however, doing so weights parameters that have a higher range of scores (e.g., Structure score; 0-3) over those that are evaluated by the presence or absence of a feature (e.g. Tidemark integrity score; 0-1). The Mankin HHGS fails to take into account the possibility that each of the parameters may be related in some way to the others. Parametric statistical methods (e.g., ANOVA) are often performed on data generated by the Mankin HHGS; however, the limited range of values for the total score (0–14) indicates that non-parametric methods are more appropriate.

Other schemes, such as those developed by Glasson, et al (17), and the Osteoarthritis Research Society International (OARSI) (18), aim to improve upon the Mankin HHGS and create an easier and more effective way of evaluating OA in animal models. The scheme developed for use in mice by Glasson, et al., evaluates the structural integrity of the articular cartilage (range of grades 0-6) in sections cut at 80μm intervals through the entire joint. (17) This scheme has the advantage of allowing the researcher to evaluate articular cartilage changes over the entire joint surface; however, it does not include evaluation of tissues other than articular cartilage. The OARSI Osteoarthritis Cartilage Histopathology Assessment System (OOCHAS), evaluates changes in articular cartilage, chondrocytes, and surrounding bone and groups these changes into grades (range 0-6, including sub-grades) and stages (range 0-4) where grade includes the depth

of the most severe lesion and stage includes the horizontal extent of the most severe lesion. (18) The grade and stage are then combined to generate a final score, which represents the overall OA severity of a tibial plateau or condyle. The OOCHAS scheme includes changes in articular cartilage and the surrounding joint tissue and expands on the Mankin scheme to include depth and extent of lesions; however, it combines changes in chondrocytes, articular cartilage, and surrounding bone into a single grade, even though the severity of changes in each of these tissues may not be uniform at any given point in time.

The purpose of the present study was to develop a histological grading scheme that includes changes in articular cartilage, subchondral and periarticular bone, and meniscus that are consistently observed during the development of OA in mice. The results from this scheme are then combined into uncorrelated factor scores that have high potential for distinguishing among mild, moderate, and severe OA utilizing parametric statistical methods.

2.2 Materials & Methods

Mouse models of osteoarthritis

In order to develop a scheme that would be broadly applicable to studies of OA in mice, animals from multiple studies and including a wide range of ages were evaluated in order to maximize the range of lesion severities. Thus, the mice used for the present study were from five separate OA studies in which the disease either occurred naturally (3 studies) or was surgically induced (2 studies).

Studies 1 and 2: Eleven mice, aged 10 weeks, and 15 mice, aged 14 weeks (C57/Bl6 strain) at the start of the experiment underwent surgical destabilization of the stifle joint (destabilized medial meniscus, DMM (17)) and were sacrificed for collection and evaluation of both hind limbs after 8 weeks of free cage movement.

Study 3: Thirty normal C57/Bl6 mice were sacrificed for collection and evaluation of both hind limbs at ages 17 (n=17) and 23 (n=13) months.

Study 4: Sixteen D257A mice having a mutation in a mitochondrial DNA polymerase (resulting in accelerated aging in specific tissues (19)) were sacrificed for collection and evaluation of one hind limb. Both homozygotes (n=8) and wild-type (n=8) mice, ranging from 10.5 to 14 months of age (mean= 12.8 months), were included.

Study 5: Thirty-three normal 16-month-old C57/Bl6 mice were sacrificed and one hind limb was collected and evaluated.

Histological preparation and assessments

Intact stifle joints (n=158 joints from 105 mice) were routinely fixed in 10% formalin, decalcified in 10% EDTA, processed, and embedded intact into paraffin. Three joints were excluded from their respective studies due to surgical complications (sham joint may have underwent destabilization) or improper embedding. Joints were then serially sectioned in a coronal plane and 4-5 representative midcoronal sections that were of high quality and spanned approximately 100μm (same level used for all stifles) were selected based on bony and soft tissue landmarks as determined by a characteristic wedge shape of both medial and lateral menisci and presence of articular cartilage on both tibial

plateaus and femoral condyles. Selected sections were stained with Hematoxylin & Eosin (H&E) and Safranin-O stains for evaluation.

The first step in the development of a grading scheme for these joints was to evaluate all of the sections and describe the changes that were present. To do this, 4-5 midcoronal sections from each of the 158 stifles from all five studies were randomized and relabeled to prevent observer bias. All sections were then carefully examined histologically and all changes were recorded, with particular focus on the following parameters: abnormalities in chondrocytes (e.g., number, viability, and morphology); abnormalities in the matrix of articular cartilage and menisci (e.g., variability in Safranin-O staining, structural changes such as fibrillation, clefting, and tidemark clefts); changes in synovial membrane (e.g., inflammation, fibrosis); and abnormalities in subchondral and periarticular bone (e.g., increased thickness, osteophytes). After changes were recorded for each stifle, those changes that were consistent among stifles (vs. an isolated finding involving one or a very low number of stifles) were further characterized with measurements using an Osteomeasure bone histomorphometry system (described below) or were assigned semi-quantitative grades according to severity. Then two representative midcoronal sections from each stifle, one stained with H&E and one stained with Safranin-O, were selected for final evaluation.

The following parameters were measured on the H&E stained section of each joint using an Osteomeasure bone histomorphometry system (Osteometrics, Atlanta, GA): areas and average thickness of articular cartilage, calcified cartilage, and subchondral bone in each medial and lateral tibial plateau; areas of weight-bearing medial

and lateral menisci; areas of chondrocyte cell death in each medial and lateral tibial plateau and meniscus; osteophyte areas; and number of viable chondrocytes in the articular cartilage. All measurements were taken at a magnification of 20X using a 700μm X 800μm grid that was centered on the tibial plateau and included 75-100% of the length of each plateau, or was centered over the area of interest for osteophyte & meniscal measurements. Articular cartilage (AC) area was defined as the area between the superficial surface of articular cartilage and the most superficial tidemark; calcified cartilage area was the area between the most superficial tidemark and the calcified cartilage-subchondral bone junction; and subchondral bone (SCB) area was the area between the calcified cartilage-subchondral bone junction and the most superficial boundary of the marrow spaces (Figure 2.1A). Several rules were followed in order to consistently measure the lower boundary of the subchondral bone. First, adjacent marrow spaces were connected by tracing horizontally across the bone trabeculae at the point where the width of the trabecula was constant or began to narrow. Second, marrow spaces were excluded if the size of the marrow space was less than the distance between marrow spaces. In instances where no marrow spaces were present, the lower measurement included all bone tissue in the epiphysis, with the upper margin of the growth plate serving as the deep face of the subchondral bone plate. The area of weight-bearing meniscus (Men area) was defined by drawing a straight line connecting the most medial or lateral aspect of the tibial plateau and the femoral condyle and outlining the meniscus axial to that line (Figure 2.1B). Total area composed of dead chondrocytes within the articular cartilage and meniscus were measured by tracing all areas within

which 2 or more chondrocytes were dead, as determined by visual assessment of loss of nuclear staining with H&E (Figure 2.1C), and summing these areas together. Percentages of chondrocyte cell death area relative to total area of articular cartilage within the measurement box (CCD%) and weight-bearing meniscus (Men CCD%) also were calculated. The number of viable chondrocytes (#chond) in the articular cartilage was counted and the area of articular cartilage/viable chondrocyte (AC/chond) was determined, as was the viable articular cartilage area (total articular cartilage minus total area of chondrocyte cell death) per viable chondrocyte (VAC/chond). In cases where there was complete loss of articular cartilage, CCD% was recorded as 100% and the remainder of the articular cartilage & chondrocyte measurements were recorded as "0". Abaxial and axial osteophytes (Abax OP & Ax OP respectively) were measured as previously described for nonhuman primates. (20) In addition to these measurements, articular cartilage was evaluated using two semi-quantitative parameters. The Articular Cartilage Structure score (ACS, range 0-12) evaluates depth and extent of fibrillation and clefting within the articular cartilage, and the Safranin-O staining score (Saf-O, range 0-12), evaluated on the safranin O stained sections semi-quantitatively evaluates loss of Safranin-O staining within the articular cartilage (Table 2.1). Finally, the total number of tidemark clefts, as described by Otterness, et al (12), in each tibial plateau was counted.

Statistics

Correlation analyses were conducted separately for medial and lateral tibial plateau parameters. In addition, parameters from the medial joint compartments of all

joints were included in a Principal Components Analysis (PCA) to reduce the large number of correlated parameters to a smaller number of orthogonal linear combinations (factors) of these parameters that accounted for at least 70% of the total variance of the data. Parameters with factor loadings > 0.40 were considered to contribute substantially to the identified factors. The final results of PCA are standardized factor scores for each joint that was included in the analysis. These standardized factor scores have an approximately normal distribution and can appropriately be used in parametric statistical methods. SAS Version 9.1 (Cary, North Carolina) was used for all statistical analyses.

2.3 Results

Histological evaluation of these sections revealed a wide range of lesions (Figure 2.2), including a low number of sites with no evidence of any abnormalities (Figure 2.2A), a low number of sites with complete loss of articular cartilage to the level of subchondral bone (Figure 2.2C), and many sites containing intermediate lesions (Figure 2.2B). In addition, a wide range of loss of Safranin-O stain was also noted (Figure 2.3). In an overwhelming percentage of the sections, the lesions were more severe in the medial tibial plateau than any other site within the joint. Based on preliminary studies with these data as well as from previous experience, a total of 15 parameters were included in the final grading scheme for analysis (Table 2.2).

Unlike previous studies of OA in other species, many of the murine stifle joints in the present study contained locally extensive areas of chondrocyte cell death. These were often located in the central region of the tibial plateaus in naturally occurring OA in older

animals. However, in joints that underwent DMM surgery to induce OA, areas of chondrocyte cell death tended to localize either in the central or the abaxial region of the plateau. In mild disease, areas of chondrocyte cell death were small; however, they increased in size and extent as severity of OA increased (as indicated by higher scores for ACS and Saf-O). In cases where areas of chondrocyte cell death were extensive, they often were associated with tidemark clefts and/or surface fibrillation and clefting.

Correlation Analysis

Correlation analysis of the 15 parameters from the medial tibial plateaus of all joints revealed statistically significant fair to moderately strong correlations among numerous continuous and semi-quantitative parameters (Table 2.3). There were highly significant correlations ($p \leq 0.0001$) between the two semi-quantitative grades, Articular Cartilage Structure score (ACS) and Safranin-O (Saf-O) staining score, and several continuous parameters, including articular cartilage area (AC area), average articular cartilage thickness (AC thick), subchondral bone area (SCB area), percent of chondrocyte cell death within the articular cartilage (CCD%), the total number of viable chondrocytes (#chond), and abaxial osteophyte size (Abax OP). In addition, Articular Cartilage Structure score (ACS) and Safranin-O score (Saf-O) parameters were highly significantly correlated with each other ($p<0.0001$). Meniscal changes, which include area of weight-bearing meniscus (Men area) and area of chondrocyte cell death within the weight-bearing meniscus (Men CD) were significantly correlated with each other ($p<0.0001$). Meniscal area was also significantly correlated with the articular cartilage Saf-O score

($p<0.001$). The average size of abaxial osteophytes (Abax OP) was significantly correlated with percent of articular cartilage chondrocyte cell death (CCD%), number of viable chondrocytes (#chond), and area of axial osteophytes (Ax OP).

Correlation analysis on parameters from the lateral tibial plateau, where the lesions were considerably less severe, revealed substantially fewer significant correlations among the 15 parameters (data not shown) compared with the results from the medial tibial plateau; however, Articular Cartilage Structure (ACS) and Safranin-O (Saf-O) results in this site remained strongly correlated ($r=0.33$, $p<0.0001$).

Principal Components Analysis (PCA)

Principal Components Analysis of the 15 medial tibial plateau parameters resulted in retention of 5 factors that together accounted for 74% of the total variance in the data (Table 2.4). For clarity, each factor was named according to the major parameters it describes. Factor 1 (Articular Cartilage Integrity), accounted for 30.3% of the variance and had substantial contributions (factor loadings > 0.40) from AC area, AC thickness, CD%, total number of chondrocytes (#chond), viable area of articular cartilage per viable chondrocyte (VAC/chond), and the two semi-quantitative scores (Articular Cartilage Structure score & Safranin-O score). Factor 2 (Chondrocyte Viability) accounted for 18.8% of the total variance and had substantial contributions from chondrocyte cell death area (CCD area), per cent area of chondrocyte cell death (CCD%), total number of viable chondrocytes (#chond), total articular cartilage per viable chondrocyte (AC/chond), and viable area of articular cartilage per viable chondrocyte (VAC/chond). Factors 3, 4, and 5

accounted for 9.9%, 8.5%, and 7.0% of the variance and had substantial contributions from subchondral bone measurements, meniscal measurements, and osteophyte size (periarticular changes) respectively (Table 2.4). Thus, the large number of quantitative measurements and scores were reduced to a smaller number (5 in the present study) of orthogonal linear combinations (factors) which were then transformed to standardized scores for each individual joint (data not shown). The approximately normal distribution of the standardized scores allows for their use in parametrical statistical methods such as ANOVA, linear regression, and Student's t-tests.

2.4 Discussion

The main outcome from this study was the development of a comprehensive histological grading scheme that characterizes, in detail, the changes occurring in murine stifle joints in surgically-induced and spontaneously-occurring OA. Because of the unbiased manner in which the scheme was developed, the quantitative nature of the majority of the parameters used, and the comprehensive nature of the scheme, we believe that it will have a high degree of accuracy and reliability in distinguishing between normal stifle joints and those with mild, moderate, and severe OA in mice. This hypothesis will be tested in the second chapter, and the third will be devoted to comparing this new histological scheme to commonly used pre-established schemes.

The grading scheme that we have developed thoroughly and independently evaluates the articular cartilage, subchondral & periarticular bone, and weight-bearing menisci. Continuous measurements of changes within the joint were included in the new

scheme along with two semi-quantitative parameters that are modifications/expansions of two parameters from the original Mankin HHGS (Table 2.1) that take into consideration the depth and the extent of the lesion throughout the plateau or condyle.

Some changes were noted in the joints in this study that were not included in the final grading scheme, primarily because PCA does not work effectively when the majority of the scores/measurements for a particular parameter are zero. For example, thickening of the synovial membrane was noted in some joints but was restricted to those that were severely affected and was absent in earlier stages of the disease. In addition, tidemark clefts were not numerous enough to include in the final analysis. These were most prevalent in the most severely affected joints, ranging from small areas of separation to loss of 50% or more of the articular cartilage. The absence of this feature in mildly or moderately affected joints, however, eliminated it from inclusion in the scheme. Calcified cartilage thickness and area were not affected by intervention or age in these mice (data not shown) and also were not included in the final scheme.

Conversely, some lesions were expected but were not identified in this large sample of mouse stifle joints. Although the Mankin HHGS includes vessels crossing the tidemark as a parameter, this feature was not observed in any of sections. Similarly, no chondrocyte clones were identified in any of the joints. These features are common in other species, including humans; however, their absence in mice provides yet another reason why histological grading schemes for OA need to be individualized by species.

Finally, because the initial phase of the study identified many sections in which death of chondrocytes was a feature, this parameter was included in the scheme whereas

it has not been included in previous schemes for OA evaluation in humans or animals. Chondrocyte death was considered to be a real (not artifactual) lesion, evidenced by the common association of this change with other lesions of OA including articular cartilage fibrillation and tidemark clefting and the characteristic appearance of the affected cells. (21)

The grading scheme that has been developed is based on a thorough evaluation of one section, as opposed to a less rigorous evaluation focused on articular cartilage in multiple sections. This method of evaluation has the benefit of identifying changes not only in articular cartilage, but also in surrounding bone and soft tissues. When using this scheme, however, the researcher must know the location of the most severe OA lesions that are present in the particular model being evaluated. This is especially important when evaluating studies that utilize a surgical method of inducing OA, since the lesion location will likely differ for different surgical models. The site within the joint that will be evaluated should be pre-determined and should be consistent among all joints. It is also important when using this grading scheme, in which detailed measurements are made in a single section, to develop a standardized protocol for positioning & measuring slides that is consistent among all individuals who evaluate the lesions. It is also critical to use artifact-free sections that allow clear visualization of all structures within the joint, as areas of artifactual tissue loss cannot be measured or evaluated. For certain studies, in which a more detailed knowledge of the location of the lesions is important (e.g. a surgically-induced OA model in which severe lesions are created in localized areas, particularly in studies using a low number of animals), the tibial plateau can be divided

into three separate areas (axial, middle, and abaxial) and the scheme can be applied to each area individually. This approach was considered for the present study, but was not used due to the fact that a large number of sections that were evaluated. The OA lesions in the present study were consistently more severe in the medial tibial plateaus than the lateral tibial plateaus in mice from all five studies, suggesting that histological grading may be limited to the medial tibial plateau.

A benefit of using PCA is the ability to generate factor scores for each individual joint which are standardized and are approximately normally distributed. Intervention differences using the standardized factor scores can then be tested using parametrical statistical methods such as ANOVA, linear regression, and Student's t-tests. Prior studies have successfully used PCA to analyze OA lesions in other species using factor scores. (22, 23) All parameters evaluated need to be included in the PCA to generate the parameter loadings for each factor and create standardized scores. In the present study, standardized scores for the 5 factors for each individual medial plateau were calculated (data not shown) and will be used in future studies to compare intervention groups within studies as well as OA changes across the five studies that were utilized in the present study.

In future studies, the hypothesis that the grading scheme derived from this PCA approach will have a high degree of accuracy and reliability in distinguishing between normal stifle joints and those with mild, moderate, and severe OA in mice will be tested by using the standardized scores generated for each of the joints used in the present study to evaluate the effects of age and surgical intervention on OA severity in these animals.

The grading scheme will also be compared with the Mankin HHGS to determine if the proposed scheme provides a more sensitive analysis of OA severity than previously developed schemes.

Figure 2.1. Continuous measurements performed using the Osteomeasure bone histomorphometry system. Bar = 100µm. (A) A box (800µm X 700µm) was centered on the tibial plateau and the superficial and deep surfaces of articular cartilage (blue), calcified cartilage (yellow), and subchondral bone (red) were traced. (B) Weight-bearing meniscal area (green) was outlined. (C) Areas of chondrocyte cell death (red) were traced within the articular cartilage (blue).

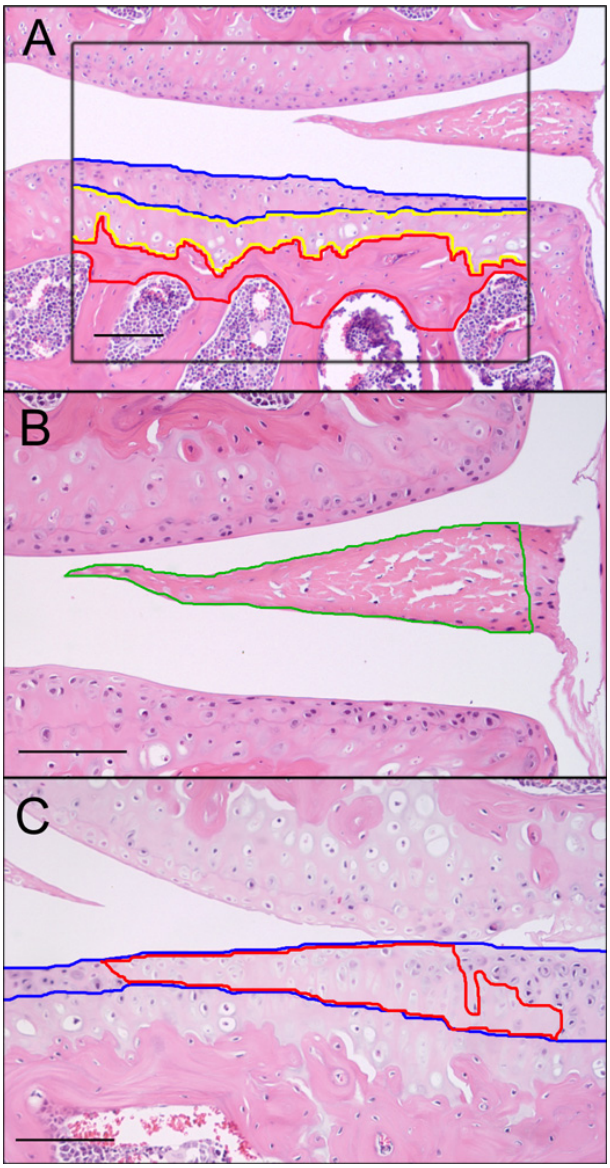

Figure 2.2. H&E stained sections from mouse medial stifle joint compartment demonstrating the wide range of severity of OA lesions. (A) Normal joint compartment containing no lesions of OA. (B) Moderate OA including a tidemark cleft and locally extensive loss of articular cartilage with locally extensive chondrocyte cell death in the remaining articular cartilage. (C) Severe OA with full thickness loss of articular cartilage over virtually the entire tibial plateau and femoral condyle.

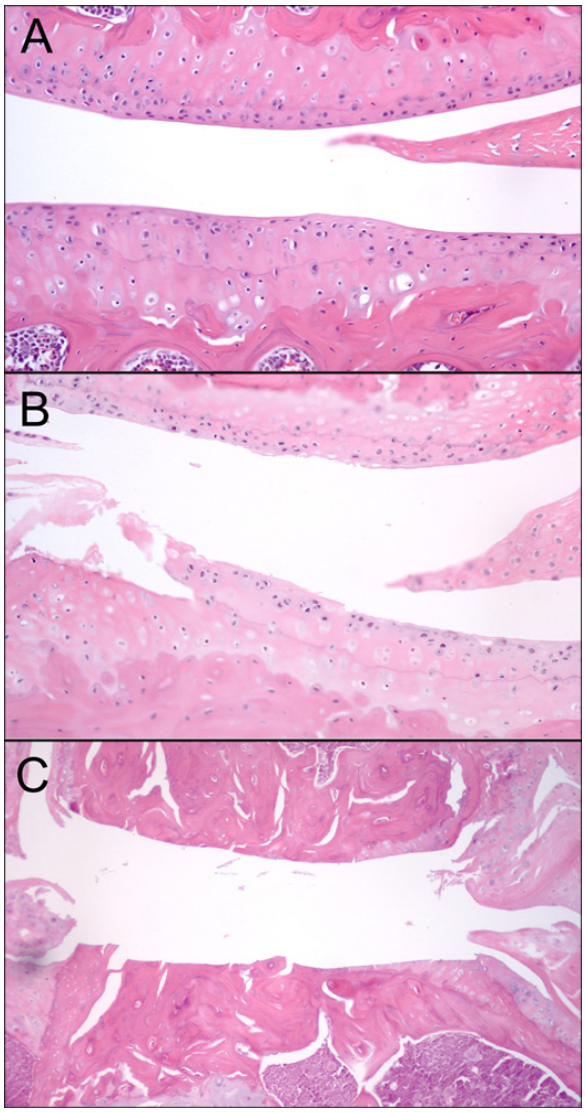

Figure 2.3. Safranin-O stained sections from mouse medial stifle joint compartment demonstrating the wide range of severity of loss of stain. (A) Normal joint compartment containing no loss of stain. (B) Moderate OA including superficial fibrillation and focal chondrocyte cell death with moderate loss of stain. (C) Severe OA with full thickness loss of articular cartilage with extensive loss of stain.

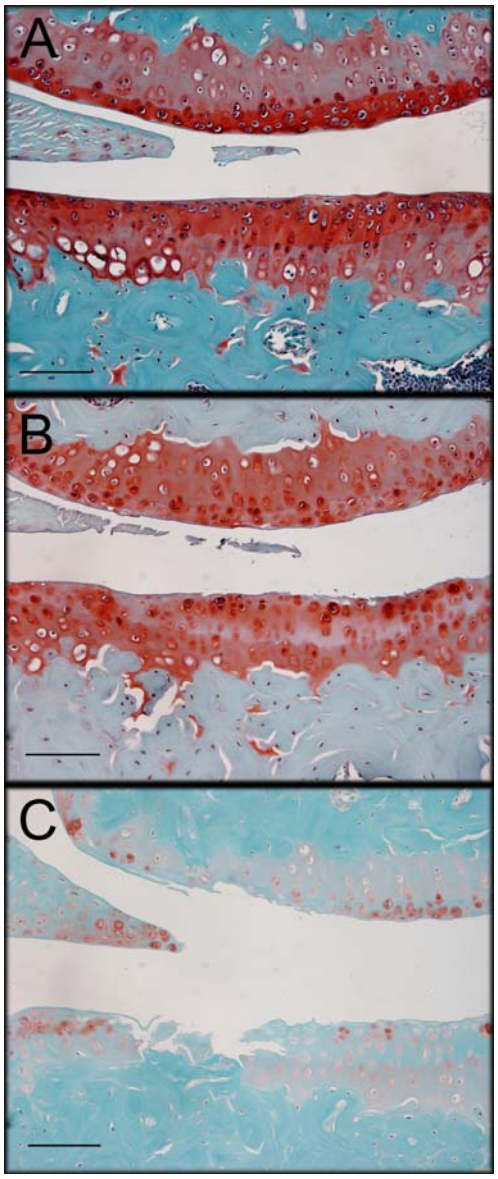

Table 2.1. Description of two semi-quantitative grades included in new histological grading scheme.

Histological Parameter	Description
Articular Cartilage Structure Score (ACS)	
Grade 0	Articular surface smooth and intact
Grade 1-3	Fibrillation and/or clefts and/or loss of cartilage involving 1/4 or less of articular cartilage thickness involving ≤1/3, >1/3 and ≤2/3 or >2/3 of the plateau or condyle respectively
Grade 4-6	Fibrillation and/or clefts and/or loss of cartilage involving 1/2 or less of articular cartilage thickness involving ≤1/3, >1/3 and ≤2/3, or >2/3 of the plateau or condyle respectively
Grade 7-9	Fibrillation and/or clefts and/or loss of cartilage involving >1/2 of articular cartilage but less than full thickness involving ≤1/3, >1/3 and ≤2/3, or >2/3 of the plateau or condyle respectively
Grade 10-12	Fibrillation and/or clefts and/or loss of cartilage involving the full thickness of articular cartilage involving ≤1/3, >1/3 and ≤2/3, or >2/3 of the plateau or condyle respectively
Safranin-O Staining Score (Saf-O)	
Grade 0	Uniform staining throughout the articular cartilage
Grade 1-3	Loss of staining in the matrix (but not cells) in ≤ 1/2 of the articular cartilage and involving ≤1/3, >1/3 and ≤2/3, or >2/3 of the plateau or condyle respectively
Grade 4-6	Loss of staining in the matrix (but not cells) in >1/2 of the articular cartilage and involving ≤1/3, >1/3 and ≤2/3, or >2/3 of the plateau or condyle respectively
Grade 7-9	Complete loss of staining in ≤ 1/2 of the articular cartilage involving ≤1/3, >1/3 and ≤2/3, or >2/3 of the plateau or condyle respectively
Grade 10-12	Complete loss of staining in >1/2 of the articular cartilage and involving ≤1/3, >1/3 and ≤2/3, or >2/3 of the plateau or condyle respectively

Table 2.2. Summary of 15 parameters that were included in the histological grading scheme, including abbreviations. Measurements were taken at a magnification of 20X using a 700µm X 800µm grid that was centered on the tibial plateau and included 75-100% of the length of each plateau, or centered upon area of interest (meniscus, osteophytes).

Parameter (units); Abbreviation	Definition
Articular cartilage (AC) area (μm^2); AC area	Total area of articular cartilage
Articular cartilage thickness (µm); AC thick	Average articular cartilage thickness
Subchondral bone (SCB) area (μm^2); SCB area	Total area of subchondral bone
subchondral bone thickness (µm); SCB thick	Average subchondral bone thickness
Chondrocyte cell death (CCD) area (μm^2); CCD area	Total area of articular cartilage with two or more necrotic chondrocytes
Percent of chondrocyte cell death (%); CCD%	Percent of CCD area over total AC area
Number of chondrocytes; #chond	Total number of viable chondrocytes
Total AC area per viable chondrocyte (μm^2); AC/chond	AC area divided by number of viable chondrocytes
Viable AC area per viable chondrocyte (μm^2); VAC/chond	Total area of AC subtracted by CCD area, divided by total number of viable chondrocytes
Size of axial osteophytes (μm^2); Ax OP	Total area of axial osteophytes (if present)
Size of abaxial osteophytes (μm^2); Abax OP	Total area of abaxial osteophytes (if present)
Meniscal area (μm^2); Men area	Total area of weight-bearing menisci
Meniscal cell death area (μm^2); Men CCD	Total area of chondrocyte cell death within weight-bearing menisci
Articular cartilage structure score (0-12); ACS	Semi-quantitative score of articular cartilage integrity
Safranin-O staining score (0-12); Saf-O	Semi-quantitative score of loss of Safranin-O staining

Table 2.3. Statistically significant ($p<0.05$) correlation coefficients between parameters using data from the medial tibial plateaus. AC, articular cartilage; SCB, subchondral bone; CCD, chondrocyte cell death; chond, viable chondrocytes; VAC, viable articular cartilage; OP, osteophyte; Men, meniscal; ACS, articular cartilage structure score; Saf-O, safranin-O staining score. Correlation coefficients with absolute value > 0.30 are highly significant ($p<0.0001$).

Parameter	AC area	AC thick	SCB area	SCB thick	CCD area	CCD %	# chond	AC / chond	VAC / chond	Ax OP	Abax OP	Men area	Men CCD	ACS	Saf-O
AC area		0.83	-0.17		0.32	-0.41	0.59		0.68		-0.19			-0.3	-0.38
AC thick			-0.22	-0.2	0.19	-0.44	0.52		0.63		-0.16			-0.4	-0.28
SCB area				0.49	0.20	0.48	-0.30	0.20	-0.23	0.19	0.24	-0.20	0.18	0.43	0.30
SCB thick						0.27	-0.17		-0.17					0.24	
CCD area						0.60	-0.43	0.72	0.35		0.20		0.17	0.18	
CCD%							-0.83	0.53	-0.24		0.33		0.21	0.62	0.50
#chond								-0.52			-0.30			-0.51	-0.53
AC / chond									0.50					0.24	0.21
VAC / chond														-0.22	
AxOP											0.29				
AbaxOP												-0.20		0.34	0.33
Men area													-0.30	-0.20	-0.28
Men CCD														0.24	
ACS															0.46
Saf-O															

Table 2.4. Components of Factors retained by PCA using data from the medial tibial plateaus (factor loadings in parentheses), including % variation accounted for by each factor (bottom row). Parameters with factor loadings >0.40 are highlighted in bold.

Factor 1 Articular Cartilage Integrity	Factor 2 Chondrocyte Viability	Factor 3 Subchondral Bone	Factor 4 Meniscus	Factor 5 Periarticular Bone
AC Area (0.942)	AC Area (0.082)	AC Area (-0.005)	AC Area (-0.074)	AC Area (-0.107)
AC Thick (0.898)	AC Thick (0.017)	AC Thick (-0.151)	AC Thick (-0.094)	AC Thick (0.010)
SCB Area (-0.195)	SCB Area (0.184)	**SCB Area (0.711)**	SCB Area (-0.282)	SCB Area (0.191)
SCB Thick (-0.086)	SCB Thick (0.063)	**SCB Thick (0.864)**	SCB Thick (0.076)	SCB Thick (0.027)
CCD Area (0.219)	**CCD Area (0.858)**	CCD Area (0.149)	CCD Area (-0.054)	CCD Area (0.015)
CCD% (-0.527)	**CCD% (0.689)**	CCD% (0.285)	CCD% (-0.170)	CCD% (0.149)
#Chond (0.604)	**#Chond (-0.692)**	#Chond (-0.042)	#Chond (0.051)	#Chond (-0.161)
AC/Chond (0.115)	**AC/Chond (0.902)**	AC/Chond (0.036)	AC/Chond (-0.051)	AC/Chond (-0.058)
VAC/Chond (0.707)	**VAC/Chond (0.445)**	VAC/Chond (-0.259)	VAC/Chond (-0.013)	VAC/Chond (-0.058)
Ax OP (-0.021)	Ax OP (-0.155)	Ax OP (0.141)	Ax OP (0.064)	**Ax OP (0.837)**
Abax OP (-0.159)	Abax OP (0.205)	Abax OP (0.031)	Abax OP (-0.174)	**Abax OP (0.716)**
Men Area (-0.044)	Men Area (-0.041)	Men Area (0.138)	**Men Area (0.866)**	Men Area (-0.069)
Men CCD (0.042)	Men CCD (0.046)	Men CCD (0.253)	**Men CCD (-0.656)**	Men CCD (-0.002)
ACS (-0.482)	ACS (0.315)	ACS (0.275)	ACS (-0.371)	ACS (0.207)
Saf-O (-0.492)	Saf-O (0.334)	Saf-O (-0.114)	Saf-O (-0.350)	Saf-O (0.290)
30.3%	18.8%	9.9%	8.5%	7%

2.5 References

1. Hunter DJ, Felson DT. Osteoarthritis. BMJ. 2006 Mar 18;332(7542):639-42.

2. Marijnissen AC, Vincken KL, Vos PA, Saris DB, Viergever MA, Bijlsma JW, et al. Knee images digital analysis (KIDA): A novel method to quantify individual radiographic features of knee osteoarthritis in detail. Osteoarthritis Cartilage. 2008 Feb;16(2):234-43.

3. Oka H, Muraki S, Akune T, Mabuchi A, Suzuki T, Yoshida H, et al. Fully automatic quantification of knee osteoarthritis severity on plain radiographs. Osteoarthritis Cartilage. 2008 Nov;16(11):1300-6.

4. Peterfy CG, Guermazi A, Zaim S, Tirman PF, Miaux Y, White D, et al. Whole-organ magnetic resonance imaging score (WORMS) of the knee in osteoarthritis. Osteoarthritis Cartilage. 2004 Mar;12(3):177-90.

5. Spahn G, Muckley T, Klinger HM, Hofmann GO. Whole-organ arthroscopic knee score (WOAKS). BMC Musculoskelet Disord. 2008 Nov 24;9:155.

6. Mankin HJ, Dorfman H, Lippiello L, Zarins A. Biochemical and metabolic abnormalities in articular cartilage from osteo-arthritic human hips. II. correlation of morphology with biochemical and metabolic data. J Bone Joint Surg Am. 1971 Apr;53(3):523-37.

7. Athanasiou KA, Agarwal A, Muffoletto A, Dzida FJ, Constantinides G, Clem M. Biomechanical properties of hip cartilage in experimental animal models. Clin Orthop Relat Res. 1995 Jul;(316)(316):254-66.

8. Schulze-Tanzil G, Muller RD, Kohl B, Schneider N, Ertel W, Ipaktchi K, et al. Differing in vitro biology of equine, ovine, porcine and human articular chondrocytes derived from the knee joint: An immunomorphological study. Histochem Cell Biol. 2009 Feb;131(2):219-29.

9. Price JS, Oyajobi BO, Russell RG. The cell biology of bone growth. Eur J Clin Nutr. 1994 Feb;48 Suppl 1:S131-49.

10. Moussavi-Harami SF, Pedersen DR, Martin JA, Hillis SL, Brown TD. Automated objective scoring of histologically apparent cartilage degeneration using a custom image analysis program. J Orthop Res. 2009 Apr;27(4):522-8.

11. Ostergaard K, Andersen CB, Petersen J, Bendtzen K, Salter DM. Validity of histopathological grading of articular cartilage from osteoarthritic knee joints. Ann Rheum Dis. 1999 Apr;58(4):208-13.

12. Otterness IG, Chang M, Burkhardt JE, Sweeney FJ, Milici AJ. Histology and tissue chemistry of tidemark separation in hamsters. Vet Pathol. 1999 Mar;36(2):138-45.

13. Ding C, Cicuttini F, Jones G. Tibial subchondral bone size and knee cartilage defects: Relevance to knee osteoarthritis. Osteoarthritis Cartilage. 2007 May;15(5):479-86.

14. Dore D, Ding C, Jones G. A pilot study of the reproducibility and validity of measuring knee subchondral bone density in the tibia. Osteoarthritis Cartilage. 2008 Dec;16(12):1539-44.

15. Englund M. The role of the meniscus in osteoarthritis genesis. Med Clin North Am. 2009 Jan;93(1):37,43, x.

16. Goldring SR. The role of bone in osteoarthritis pathogenesis. Rheum Dis Clin North Am. 2008 Aug;34(3):561-71.

17. Glasson SS, Blanchet TJ, Morris EA. The surgical destabilization of the medial meniscus (DMM) model of osteoarthritis in the 129/SvEv mouse. Osteoarthritis Cartilage. 2007 Sep;15(9):1061-9.

18. Pritzker KP, Gay S, Jimenez SA, Ostergaard K, Pelletier JP, Revell PA, et al. Osteoarthritis cartilage histopathology: Grading and staging. Osteoarthritis Cartilage. 2006 Jan;14(1):13-29.

19. Kujoth GC, Hiona A, Pugh TD, Someya S, Panzer K, Wohlgemuth SE, et al. Mitochondrial DNA mutations, oxidative stress, and apoptosis in mammalian aging. Science. 2005 Jul 15;309(5733):481-4.

20. Olson EJ, Lindgren BR, Carlson CS. Effects of long-term estrogen replacement therapy on bone turnover in periarticular tibial osteophytes in surgically postmenopausal cynomolgus monkeys. Bone. 2008 May;42(5):907-13.

21. Ytrehus B, Carlson CS, Ekman S. Etiology and pathogenesis of osteochondrosis. Vet Pathol. 2007 Jul;44(4):429-48.

22. Carlson CS, Loeser RF, Purser CB, Gardin JF, Jerome CP. Osteoarthritis in cynomolgus macaques. III: Effects of age, gender, and subchondral bone thickness on the severity of disease. J Bone Miner Res. 1996 Sep;11(9):1209-17.

23. Ham KD, Loeser RF, Lindgren BR, Carlson CS. Effects of long-term estrogen replacement therapy on osteoarthritis severity in cynomolgus monkeys. Arthritis Rheum. 2002 Jul;46(7):1956-64.

CHAPTER 3

HISTOPATHOLOGY OF NATURALLY OCCURRING AND SURGICALLY INDUCED OSTEOARTHRITIS IN MICE

Current histological assessments of osteoarthritis (OA) focus on articular cartilage lesions and are not designed to reproducibly evaluate more global changes in the mouse stifle joint. In addition, little work has been done to comprehensively characterize the morphology of OA lesions in naturally occurring or surgically induced mouse models of OA. The objective for the present study was to evaluate several models of mouse OA with the comprehensive histological grading scheme developed in Chapter 2. In the present study, the stifle (knee) joints in five separate studies (3 naturally occurring, 2 surgically induced) were examined with the novel histological grading scheme developed in Chapter 2 that included both quantitative measurements and semi-quantitative grades to evaluate changes in articular cartilage, periarticular bone, and meniscus. The data collected was analyzed using Principal Components Analysis (PCA) and factor scores for each individual joint were generated. Individual parameters and mean factor scores were compared between intervention groups in each study. In addition, these parameters and scores were compared among control animals across studies to examine changes associated with age. In addition, for comparison, the original Mankin Histological-Histochemical Grading System (HHGS) was applied to each joint. OA lesions overall were more severe on the medial tibial plateau than the lateral tibial plateau. The Mankin HHGS was able to detect significant differences among surgical groups in the surgically-induced models of OA, but was unable to detect changes related to dietary differences in naturally occurring models of OA or changes associated with age. Using the newly developed scheme, significant changes in articular cartilage and surrounding bone were found not only between surgical groups and their respective control groups, but also

among dietary intervention groups in naturally occurring models. In addition, changes with age were also noted in control joints. Chondrocyte cell death within the articular cartilage significantly increased with age, and was also significantly increased in surgically destabilized joints compared with their respective controls. Mean factor scores were closely associated with histomorphometric and semi-quantitative evaluations and provided a comprehensive evaluation of all joint changes. Overall, this study provided a comprehensive evaluation of OA lesions in several mouse models of OA and also identified age-related changes in the joint that have not been previously noted in *in vivo* wild-type mouse models of OA.

3.1 Introduction

Accurate histological assessment of osteoarthritis (OA) severity in animal models is critical in studies that evaluate effectiveness of agents designed to prevent or reduce the severity of the disease. The most commonly used histological grading scheme to evaluate OA severity, the Mankin Histological-Histochemical Grading System (HHGS), was initially developed in humans. (1) However, this scheme, whether in its original form or modified, is often applied to evaluate OA severity in animals, including mice. (2-5) There are limitations that prevent the Mankin HHGS from accurately assessing OA severity species other than humans, especially in rodent models which are increasingly utilized in OA research. Firstly, the Structure parameter in the Mankin HHGS relies on the ability to differentiate among the four zones of articular cartilage (superficial, transitional, radial, and calcified); however these are very difficult to consistently identify in rodents,

particularly mice, in which the articular cartilage is less than 75μm thick. In addition, the parameters of the Mankin HHGS and another scheme that was developed by Glasson, et al (6) do not take into account tidemark clefts that are a relatively consistent feature of OA in rodents but not in humans (7), and instead assume that articular cartilage degradation is initiated superficially. These schemes also only evaluate changes found within the articular cartilage and do not consider changes found in other structures such as surrounding bone and soft tissues. Finally, schemes such as the OARSI Osteoarthritis Cartilage Histopathology Assessment System (OOCHAS) (8) evaluate features occurring in multiple tissues in a single parameter, assuming that these are synchronous, and do not allow for changes in individual tissues to be evaluated separately.

In addition, very few studies have reproducibly and comprehensively characterized stifle (knee) joint changes associated with OA in mice in either naturally occurring or surgically induced models, despite the popularity of various transgenic and surgical mouse models of the disease. Histological characteristics of the stifle joint in several transgenic mouse models have been published. (9-13) However, these assessments commonly utilize the semi-quantitative histological evaluations described above. While these changes may closely resemble those found in wild type animals, a comprehensive histological evaluation of both primary and secondary OA lesions in wild type mice is needed. The goals of this study were to apply the newly developed scheme from Chapter 2 to several studies of naturally occurring and surgically induced OA in mice to further characterize changes within articular cartilage as well as surrounding bone and soft tissues within the joint.

3.2 Materials & Methods

Animal models of osteoarthritis

The tissues evaluated in this study were from five separate studies in which OA either was surgically induced (n=2) or occurred naturally (n=3) (Table 3.1).

Study 1: Purpose: Validate the destabilized medial meniscus (DMM) surgical model of OA in mice. (6) 11 mice (C57/Bl6 strain), aged 10 weeks at the start of the experiment, underwent DMM surgery by meniscotibial ligament (MTL) transection. One stifle served as either a sham (Sham) or transection surgery (MTL) and the other was left as an unoperated control (None [where contralateral stifle was sham] or Control [where contralateral stifle underwent MTL transection] groups). After 8 weeks of free cage movement, the mice were sacrificed and both hind limbs were collected for evaluation.

Study 2: Purpose: Further validate the DMM surgical model of OA in mice and examine the effects of a dietary intervention (muscadine grape extracts) on OA severity. 15 mice (C57/Bl6 strain), aged 14 weeks at the start of the experiment, underwent the DMM procedure utilizing the same study design as for Study 1. Mice were further randomized to a control, Noble (muscadine grape cultivar extract thought to be high in resveratrol), or Ison (muscadine grape cultivar extract thought to be low in resveratrol) diet. After 8 weeks of free cage movement the mice were sacrificed and both hind limbs were collected for processing.

Study 3: Purpose: Determine the effects of dietary interventions that included muscadine grape extracts or polyunsaturated fatty acids (PUFAs) on naturally occurring

OA in mice. Thirty C57/Bl6 mice that were 12 (n=17) or 18 months old (n=13) at the start of the experiment were randomized to one of two different muscadine grape extracts (Noble or Ison cultivars), or one of two PUFA diet groups (20% palm oil group or a 10% palm oil plus 10% fish oil group). After being maintained on the diets for 5 months, the mice were sacrificed at ages 17 and 23 months and both hind limbs were collected for processing.

Study 4: Purpose: Determine the severity of OA in mice with a mutation in the mitochondrial DNA polymerase (D257A mice). This mutation results in an accumulation of mitochondrial DNA mutations and an accelerated aging phenotype that is accompanied by increased apoptosis in certain tissues. (14) Homozygotes for the mutation have approximately half the lifespan of heterozygotes and wild-type mice. (14) Homozygotes (n=8) and wild-type (n=8) mice were sacrificed at 10.5-14 months of age (mean= 12.8), one hind limb was collected for processing.

Study 5: Purpose: Evaluate the effects of caloric restriction on naturally occurring OA in mice. Thirty-three 10 month old C57/Bl6 mice were randomized to one of 6 dietary intervention groups: Ad Libitum (AdLib) Western, AdLib Western Low-Fat (LF), AdLib Control, Caloric Restriction (CR) Western, CR Western LF, and CR Control. The Western diet contained 40.3% energy from fat vs. 12.2% in the Low-Fat Western diet which was similar to the control diet (12.4%). All animals were fed their assigned diet ad libitum for the first month of the study, after which they were either fed ad libitum or maintained on a caloric restriction diet, defined as 60% of their normal dietary intake, for

the remaining 5 months. The animals were then sacrificed and final body weights were taken and one hind limb was collected for processing.

Histological preparation and assessments

All stifle joints (n=158 joints from 108 mice) were routinely fixed in 10% formalin, decalcified in 10% EDTA, processed, and embedded intact into paraffin. Sectioning, staining, grading, and measuring of these sections have been described previously in detail in Chapter 2. In addition, the original Mankin HHGS grading scheme (1), was applied to the medial and lateral tibial plateaus of these same sections.

Immunohistochemistry

Because some of the sections contained relatively large numbers of dead chondrocytes, immunostaining studies were done to attempt to initially characterize this lesion. One section from three joints in which at least one tibial plateau contained >25% of dead chondrocytes was immunostained using an antibody directed against cleaved caspase-3 to determine if there was evidence for chondrocyte cell death occurring by apoptosis. Briefly, antigen retrieval was achieved by steaming slides in tris-EDTA buffer (pH 9.0) for 30 minutes followed by cooling for 20 minutes. Endogenous peroxidase was blocked with 3% hydrogen peroxide for 15 minutes at room temperature. The sections were incubated with universal protein block (DAKO) for 15 minutes, followed by a 60 minute room temperature incubation with a rabbit monoclonal antibody directed against human cleaved caspase 3 (Cell Signaling Technologies, clone Aspl75 5Al) diluted at

1:200. Binding of primary antibody was detected using an anti-rabbit HRP labeled polymer (DAKO) for 30 minutes at room temperature. The sections were developed with DAB chromagen for 8 minutes at room temperature and were counterstained with Mayer's Hematoxylin (DAKO). For negative control slides the primary antibody was substituted with Rabbit Immunoglobulin Fraction (DAKO).

Statistics

As has been described previously in Chapter 2, continuous measurements were completed and semi-quantitative grades were assigned for both the medial and lateral tibial plateaus of all joints. All histological data from the newly developed scheme (continuous measurements and semi-quantitative grades) from the medial tibial plateaus were subjected to Principal Components Analysis (PCA) as previously described in order to reduce 15 correlated OA parameters to 5 uncorrelated factors (principal components). The 5 factors generated by PCA were orthogonal linear transformations of the original observations and were each comprised of a group of parameters that were closely related to one another and were renamed to reflect these relationships. These included Articular Cartilage Integrity (Factor 1), Chondrocyte Viability (Factor 2), Subchondral Bone (Factor 3), Meniscus (Factor 4), and Periarticular Bone (Factor 5) (Table 3.2). In addition, each medial and lateral tibial plateau was scored using the Mankin HHGS.

All of the factor scores and select continuous measurements from each of the five studies were subjected to ANOVA & post-hoc analyses. The semi-quantitative grades and total Mankin HHGS scores from each tibial plateau were evaluated using non-

parametric statistical analyses. A total joint score also was calculated for each joint by adding the Mankin HHGS scores for each tibial plateau.

3.3 Results

Medial vs. Lateral Tibial Plateaus

In all five studies, histological lesions were most severe in the medial tibial plateaus in an overwhelming majority of the animals. Significant differences between the medial and lateral tibial plateaus in intervention as well as control groups were found. In general, the mean articular cartilage areas and thicknesses were smaller in the medial tibial plateaus than the lateral tibial plateaus. These differences were significant in Study 1 (MTL group, $p<0.01$ & $p<0.05$ respectively), Study 2 (MTL group, $p<0.001$ for both; Control group, $p<0.01$ for both), and Study 5 (AdLib Control group, $p<0.01$ for both). The overwhelming majority of intervention groups from all 5 studies also had significantly higher mean SCB areas and thicknesses in the medial tibial plateaus than the lateral tibial plateaus. In addition, several intervention groups from the 5 studies had significantly larger percentages of chondrocyte cell death (CCD) & smaller total number of viable chondrocytes in medial vs. lateral plateaus. These included Study 1 (MTL group, $p<0.01$ & $p<0.001$ respectively), Study 2 (MTL group, $p<0.0001$ for both), Study 3 (23 month group, $p<0.01$ & $p<0.001$ respectively), and Study 5 (AdLib Western, $p<0.05$ for both; CR Western, $p<0.05$ for both; AdLib Western LF $p<0.05$ for total number of viable chondrocytes). Medial meniscal area was significantly higher in the medial tibial plateaus in 3 intervention groups: Study 3 (17 & 23 month groups, $p<0.05$

for both) & Study 4 (WT, $p<0.05$). In contrast, the MTL group in Study 2 had significantly lower medial meniscal areas when compared to the lateral meniscus ($p<0.01$). In Study 3, both the 17 & 23 month groups had significantly higher areas of cell death within the medial meniscus when compared to the lateral meniscus ($p<0.05$).

Study 1

No differences were found between the Control (contralateral joint was an MTL joint) and None (contralateral joint was a Sham joint) surgical groups for the grades or measurements, therefore results from these two groups were combined to create a single Control group (n=11). Joints in the sham group were not included from the following analysis because no differences were identified between those joints and the control groups, and there were only 3 joints in this group.

Articular Cartilage: Mean AC area in the medial tibial plateau was significantly smaller in the MTL stifles compared with that of the Control stifles ($p<0.05$) (Figure 3.1).

Articular Cartilage Chondrocytes: The mean area of CCD was significantly larger in the medial tibial plateaus of the MTL stifles than the Control stifles ($p<0.001$), as was the percentage of chondrocyte cell death (CCD%) ($p<0.0001$) (Figure 3.2A). Similar results were seen in the lateral tibial plateaus ($p<0.05$ for both; data not shown). In both tibial plateaus, there was a significant decrease in the number of viable chondrocytes in the MTL joints compared to the Control joints ($p<0.001$ for medial & $p<0.05$ for lateral) (Table 3.3).

Meniscus & Periarticular Bone: No significant differences were identified among meniscal measurements. Three abaxial osteophytes were present in the medial tibial plateau of MTL joints (53,857μm^2 $\pm$ 27,000μm^2) (Figure 3.3). Five axial osteophytes were present in the lateral tibial plateau (22,297μm^2 $\pm$ 3,662μm^2) and 2 in the medial tibial plateau (26,473μm^2 $\pm$ 18839μm^2) and these were evenly divided among surgical groups.

Semi-quantitative Grades: The MTL group had a significantly higher Safranin-O (Saf-O) mean grade in the medial tibial plateau than the Control group ($p=0.02$) (Table 3.3).

Factor Scores: The Chondrocyte Viability factor scores were significantly higher (more severe OA) in the MTL group than the Control group ($p<0.001$) (Figure 3.2B).

Mankin HHGS: The MTL joints had a significantly higher mean Mankin HHGS score than the Control joints for the medial tibial plateaus ($p<0.01$) and the total joint score ($p<0.01$) (Table 3.3).

Study 2

As for Study 1, the results for Control and None surgical groups were closely similar for all measurements, grades, and factors. Therefore these groups were combined to create a single Control group (n=15). In addition, no differences among dietary groups were noted; therefore the data from the dietary intervention groups were combined into their respective surgical intervention groups.

Articular Cartilage: Mean AC area and thickness were significantly smaller in the medial tibial plateaus of the MTL stifles than the Control stifles ($p<0.001$ and $p<0.01$, respectively); area data shown in Figure 3.1.

Subchondral Bone: The medial tibial plateaus of the MTL joints had significantly larger areas of subchondral bone (SCB) than the Control joints ($p=0.05$) (Table 3.3).

Articular Cartilage Chondrocytes: The mean area of CCD in the medial tibial plateau was significantly larger in the MTL stifles than the Control stifles ($p<0.001$), as was the CCD% ($p<0.0001$, Figure 3.2A). The medial tibial plateaus of the MTL stifles also had a significantly smaller mean number of viable chondrocytes when compared to the Control stifles ($p<0.0001$) (Table 3.3).

Meniscus & Periarticular Bone: The medial meniscus had a significantly smaller mean area in the MTL joints vs. Control joints ($p<0.01$). Six abaxial osteophytes were identified; all were located on the medial tibial plateaus of the MTL stifles (87,403μm^2 $\pm$ 24,290μm^2) (Figure 3.3). Six axial osteophytes were identified (25,208μm^2 $\pm$ 12,688μm^2); all were located on the lateral tibial plateau and were distributed evenly among surgical groups.

Semi-quantitative Grades: The medial tibial plateau of MTL joints had significantly higher articular cartilage structure (ACS) & Saf-O grades than the Control joints ($p<0.01$ for ACS, $p<0.001$ for Saf-O). The MTL joints also had significantly higher total (results for medial & lateral tibial plateaus were summed) ACS & Saf-O scores than the Control joints ($p=0.02$ for ACS, $p<0.01$ for Saf-O) (Table 3.3).

Factor Scores: The mean Articular Cartilage Integrity was significantly lower (more severe OA) in the MTL joints vs. the controls ($p<0.01$), and Chondrocyte Viability factor scores were significantly higher (more severe OA) in the MTL joints vs. Controls ($p<0.001$) (Figure 3.2B). The mean Meniscus factor scores were significantly lower (more severe OA) in the MTL stifles compared to the Control stifles ($p<0.01$). Finally, the mean Periarticular Bone factor scores (more and larger osteophytes) were significantly higher in the MTL joints than the Control joints ($p=0.01$).

Mankin HHGS: The MTL joints had a significantly higher mean Mankin HHGS score than the Control joints for the medial tibial plateaus ($p<0.001$) and the total joint score ($p<0.001$) (Table 3.3).

Study 3

In Study 3, the only significant differences identified by ANOVA among the dietary intervention groups in either the 17 or 23 month old age group was a significant difference in the mean percentage of cell death in the medial menisci & Meniscal factor scores in the 17 month old age group ($p<0.01$, data not shown). Because these were the only significant findings out of many comparisons, the data from the dietary groups was combined into the respective age groups and further comparisons were made between these two groups.

Articular Cartilage Chondrocytes: The medial tibial plateaus of the 23 month old joints had significantly higher mean areas & percentages of CCD than those of the 17 month old stifles ($p<0.05$ for both) (Table 3.3). The medial tibial plateaus of the 23

month old stifles also had a significantly reduced number of total viable chondrocytes than the 17 month old stifles ($p<0.01$) (Table 3.3).

Periarticular Bone: Axial & Abaxial osteophytes were equally present in both age groups (axial: 16,255μm^2 $\pm$ 5,742μm^2; abaxial: 29,187μm^2 $\pm$ 24,632μm^2), however, 75% of axial osteophytes were located on the lateral tibial plateau and 89% of abaxial osteophytes were located on the medial tibial plateau.

Semi-quantitative Grades: The 23 month old joints had significantly higher mean Saf-O scores, both in the medial tibial plateau and when scores from medial & lateral plateaus were summed than the 17 month old joints ($p<0.01$ for both) (Table 3.3).

Factor Scores: The 23 month old animals had significantly higher mean factor scores for Chondrocyte Viability (more severe OA) than the 17 month old age group ($p<0.01$, data not shown). In addition, the 23 month old animals had lower mean factor scores for Subchondral Bone (less severe OA) than the 17 month old animals ($p<0.05$) (data not shown).

Mankin HHGS: The medial tibial plateaus of the 23 month old joints had significantly higher Mankin HHGS scores than those of the 17 month old joints ($p<0.05$). This was also true for the total joint score ($p<0.05$) (Table 3.3).

Study 4

Subchondral Bone: The D257A homozygote mice had significantly smaller areas and average thicknesses of SCB than the WT mice in both medial ($p<0.01$ for both) and lateral tibial plateaus ($p<0.05$ for both) (Figure 3.4).

Articular Cartilage Chondrocytes: In the medial tibial plateaus, the D257A mice had significantly higher areas & percentages of CCD within the articular cartilage than the WT mice ($p<0.05$ for both) (Table 3.3).

Periarticular Bone: Eight axial osteophytes were identified (18,636μm^2 $\pm$ 4,684μm^2), 7 of which were located in the WT stifles. Two abaxial osteophytes were identified (13,780μm^2 $\pm$ 3,840μm^2), one in a D257A stifle and the other in a WT stifle.

Factor Scores: The D257A joints had significantly lower mean factor scores for Subchondral Bone than the WT mice ($p<0.01$, data not shown).

Mankin HHGS: No significant differences were noted (Table 3.3).

Study 5

ANOVA revealed differences in final body weights among the intervention groups ($p<0.0001$): the AdLib Western group had significantly higher final body weights (mean: 60.7g) than the other 5 dietary groups (range of means: 22.1g-43.5g; $p<0.001$).

Subchondral Bone: ANOVA revealed significant differences among the intervention groups in SCB area in the medial tibial plateaus ($p<0.01$) (Table 3.3). Both AdLib Control group and the AdLib Western LF had significantly larger mean subchondral bone area than the CR Western LF group ($p<0.05$ for both) (Table 3.3). In addition, the AdLib Western group had significantly larger mean subchondral bone areas than the CR Western LF and the CR Western groups ($p<0.01$ for both) (Table 3.3).

Articular Cartilage Chondrocytes: ANOVA revealed significant differences among the intervention groups in the following: CCD% in both medial (Table 3.3) &

lateral tibial plateaus ($p=0.02$, $p<0.001$ respectively); total number of viable chondrocytes in both medial (Table 3.3) & lateral tibial plateaus ($p=0.02$, $p<0.05$ respectively); and mean CCD areas in the lateral tibial plateaus ($p<0.001$, data not shown). In short, the AdLib Western group had significantly larger percentages of CCD in both medial (Table 3.3) & lateral tibial plateaus ($p<0.001$ & $p<0.01$), significantly lower mean total viable chondrocytes ($p<0.05$), and significantly higher mean CCD areas ($p<0.05$) than the majority of the remaining 5 intervention groups. The AdLib Control group also had significantly higher mean percentages of CCD & areas of CCD (Table 3.3) ($p<0.01$ & $p<0.05$ respectively) than the majority of the remaining 4 intervention groups.

Periarticular Bone: Five abaxial osteophytes were found ($20{,}936\mu m^2 \pm 7{,}203\mu m^2$), 3 of which were located on the medial tibial plateau of the 3 joints in the AdLib Western group. The remaining 2 were located in the medial tibial plateau of two joints in the AdLib Control group. Eighteen axial osteophytes were found ($16{,}362\mu m^2 \pm 5{,}931\mu m^2$), all located in the lateral tibial plateau and evenly distributed among dietary intervention groups.

Semi-quantitative Grades: There were no significant differences among the ACS scores, however the AdLib Western group had a significantly higher Saf-O score than the CR Western LF group (Table 3.3).

Factor Scores: Significant dietary intervention differences were found in the Chondrocyte Viability ($p<0.001$) factor scores. The AdLib Western group had significantly higher mean Chondrocyte Viability factor scores (more severe OA) than all 5 other intervention groups ($p<0.01$).

Mankin HHGS: No significant differences between intervention groups were noted (Table 3.3).

Changes with Age, Naturally Occurring OA

Because of the striking and unexpected differences in Chondrocyte Viability factor scores and chondrocyte cell death measurements that were noted among groups in the previous analyses, this result was further evaluated using data from the control mice in each study (aged 18 weeks, 22 weeks, 16 months, 17 months, and 23 months) to examine changes in chondrocyte viability with age.

There were significant differences in total area of CCD and percentage of CCD within the articular cartilage in the medial and lateral tibial plateaus vs. age (ANOVA, $p<0.0001$ for medial, Figure 3.5A; ANOVA, $p<0.01$ for lateral). The youngest mice had the smallest area of CCD and this progressively increased with age. In the medial tibial plateau, all comparisons among age groups using total CCD area and percentage CCD were significant except for those involving the 16 month old mice, which were not significantly different from any other age group.

Because of this interesting result, other parameters were further evaluated to determine if these also were affected by age. Interestingly, there was a significant difference in the average AC thickness in the medial tibial plateaus (Figure 3.5B) & lateral tibial plateaus (ANOVA, $p<0.05$ for both) among age groups. In the medial tibial plateaus, the 18 week old joints had significantly thicker AC than the 16 month, 17

month, and 23 month old joints ($p<0.05$). There were, however, no significant differences in mean AC area among age groups.

Mean factor scores among the control joints in each age group were also evaluated and significant differences were found in the Chondrocyte Viability (ANOVA, $p<0.0001$) & Subchondral Bone (ANOVA, $p<0.001$) factor scores. The Chondrocyte Viability factors scores increased with age similar to the measurement data (data not shown). The differences among age groups were significant with the exception of the 18 & 22-week old joints and the 16 & 17 month old joints, which were not significantly different from each other. The 18 week old joints had a significantly smaller mean Subchondral Bone factor scores (less severe OA) than the other four age groups ($p<0.05$) (data not shown).

Immunohistochemistry

Immunohistochemistry did not reveal any chondrocytes that were immunopositive for cleaved caspase 3, however immunopositive cells were noted within the bone marrow of each section, indicating that the failure to detect immunopositive chondrocytes was not due to issues with methodology.

3.4 Discussion

This study was the first to apply a comprehensive OA grading scheme to a large number of mice with surgically induced and naturally occurring OA. The benefit of using this scheme is that the 15 histological parameters included in the new scheme can be

evaluated individually (to specifically examine certain parameters) or together as a whole (for a more global evaluation of OA changes) in the form of factor scores generated by PCA. Significant differences were indentified between intervention groups in each study using the continuous measurements, semi-quantitative scores, and factor scores.

Overall, the factor scores substantiated the results identified when separate parameters were evaluated but did not identify new relationships. A main benefit of the factor scores, however, is that they provide a method of combining semi-quantitative assessments with continuous measurements into one analysis and may provide a succinct method of summarizing changes found within the joint. In addition, factor scores are standardized and can allow comparisons across studies, assuming data from all studies is included in the initial PCA. A drawback to using PCA is that the PCA loadings and factor scores are data dependent and are not transferable to a new data set. In addition, the analysis requires a sample size including more than 30 units, which is uncommon in OA studies, which usually are underpowered, typically including only 5-7 joints per intervention or surgical group. However PCA may be extremely useful in studies in which comparisons among a large number of joints is desired.

For comparison, the Mankin HHGS was applied to both tibial plateaus in all joints. When the Mankin HHGS (1) was applied to these same studies, some significant intervention group differences were identified that were similar to those found using the newly developed scheme. For example: significant differences between surgical groups were found in Studies 1 & 2. However, there were significant changes that were identified using the newly developed scheme, such as an increase in disease severity in

the AdLib Western dietary group in Study 5, were not detected using the Mankin HHGS. In addition, changes in the subchondral bone in several studies, including Study 4 in which bone thickness and area was decreased in the D257A homozygotes, were not identified because the Mankin HHGS does not include a parameter to evaluate subchondral bone. This also is true for other histological grading schemes including the scheme developed by Glasson, et al. (6)

The present study revealed several new insights as well as supporting previous findings regarding spontaneous and surgically induced OA in mice. OA lesions, including a decrease in articular cartilage and an increase in chondrocyte cell death, were most severe in the medial tibial plateau vs. the lateral tibial plateau in the overwhelming majority of joints in all five studies, which has been demonstrated other mouse models and other animal species. (15-18) Studies 1 & 2 validated the DMM model (6) of OA in mice, and confirmed that it is a very reproducible model that can induce moderate to severe articular cartilage lesions in young mice within eight weeks post-operatively. In addition, an increase in osteophyte number and size was observed in the destabilized joints of Studies 1 & 2, which is common in other surgically induced models of OA. (19-21) The abaxial osteophytes identified in the present study largely occurred in the surgically-induced models as opposed to the naturally occurring models of OA, which indicates a strong correlation between destabilization of the stifle joint and formation of abaxial osteophytes. Axial osteophytes, on the other hand, were equally present among intervention and surgical groups, however these were more often found on the lateral tibial plateau. Tidemark clefts like those that have been previously identified and

characterized in hamsters (7) were also identified in these joints and were often associated with severe disease (Figure 3.6). A parameter evaluating the total number of tidemark clefts within a joint was initially included in the histological assessment, but they were only associated with severe disease and there were not enough tidemark clefts to include an entire parameter dedicated to them. Because these tidemark clefts result in full thickness loss of articular cartilage and are associated with chondrocyte cell death, it was concluded that tidemark clefts would be accounted for in other parameters such as articular cartilage thickness and chondrocyte cell death area measurements. The underlying mechanisms of the formation of the tidemark clefts, however, have not been identified in the mouse stifle joint, and their relationship to disease progression in the mice is unclear.

Highly significant changes were identified in articular cartilage chondrocyte viability and number, both between surgical groups and as an age-related change in control mice (Figure 3.7). Other than from findings in a single transgenic mouse model of OA (13), this change has not been noted. A significant decrease in the number of viable chondrocytes and increase in area occupied by dead chondrocytes was found in Chapter 2 to be closely correlated with an increase in the degradation of articular cartilage, including decrease in thickness and increase in ACS scores. Immunostaining of sections with large areas of chondrocyte cell death within the articular cartilage did not identify any of the dead chondrocytes to be apoptotic, and the morphology of these chondrocytes, as well as the large numbers identified (vs. individual cells), are similar to the areas of chondrocyte necrosis that have been observed in lesions of osteochondrosis in pigs (22)

that were described as necrotic chondrocytes. A recent study identified a similar increase in chondrocyte cell death in the articular cartilage of transgenic mice, however immunostaining for the apoptosis marker poly (ADP-ribose) polymerase (PARP)-p86 indicate the mechanism of cell death is by apoptosis. (13) Therefore, further studies will be necessary to characterize the pathogenesis of the chondrocyte cell death in these joints. In addition, chondrocyte cell death was often noted in the absence of changes in any other tissues, including articular cartilage (Figure 3.7). Therefore detecting changes in articular cartilage chondrocytes may be a method of identifying early osteoarthritic changes in mouse joints prior to the occurrence of other changes, such as degradation of the articular cartilage.

Overall, this study comprehensively evaluated lesions in the mouse stifle joint that are associated with OA. Significant changes in articular cartilage, chondrocytes, and subchondral and periarticular bone were identified in both surgically induced and naturally occurring models of OA. Several changes that were identified using the newly developed histological grading scheme were overlooked when using the Mankin HHGS, and the newly developed scheme was able to detect changes in a wider range of tissues.

Table 3.1. Summary of five mouse studies.

Study	Age at Start of Study	Number of Animals	Surgical Intervention	Age at Sacrifice
1	10 weeks	11	DMM	18 weeks
2	14 weeks	15	DMM	22 weeks
3	12 months	17	None	17 months
	18 months	13	None	23 months
4	N/A	16	None	mean: 12.8 months
5	10 months	33	None	16 months

Table 3.2. Summary of five factors retained from Principal Components Analysis, in order of percent variation accounted for by the factor, and relation to OA severity. *Dead chondrocytes have rarely been reported in murine OA literature; however, chondrocyte cell death was found with high frequency in the present study and was interpreted to represent early OA lesions.

Variation Explained (%)	Factor	Name	Description	Direction
30.3%	1	Articular Cartilage Integrity	Articular cartilage area and thickness, semi-quantitative grades	Lower factor score: more severe OA
18.8%	2	Chondrocyte Viability	Chondrocyte cell death area and percent, number of viable chondrocytes, viable articular cartilage area	Higher factor score: more severe OA*
9.9%	3	Subchondral Bone	Subchondral bone area and thickness	Higher factor score: more severe OA
8.5%	4	Meniscus	Weight-bearing meniscus area and chondrocyte cell death within the meniscus	Lower factor score: more severe OA
7.0%	5	Periarticular Bone	Size of axial and abaxial osteophytes, if present	Higher factor score: more severe OA

Table 3.3. Select continuous and semi-quantitative results (mean ± standard deviation) and total Mankin HHGS score from the medial tibial plateaus in all five studies, separated by intervention group. AC= articular cartilage, SCB= subchondral bone, CCD= chondrocyte cell death, #chondr= total number of chondrocytes, ACS= articular cartilage structure score, Saf-O=Safranin-O staining score. MTL= meniscotibial ligament transection group, AdLibW= AdLib Western diet group, AdLibW LF= AdLib Western Low-fat diet group, CR W= Caloric Restriction Western diet group, CR W LF= Caloric Restriction Western Low-fat diet group.

Intervention Group	AC area (μm^2)	AC thickness (μm)	SCB area (μm^2)	SCB thickness (μm)	CCD area (μm^2)	CCD%	#chondr	ACS	Saf-O	Total Mankin HHGS
Study 1										
MTL	31608 (7289)	40.6 (9.4)	88731 (28396)	73.4 (14.6)	6747 (3170)	20.9 (7.3)	75 (15)	1.8 (1.9)	8 (2.6)	11.6 (1.1)
Control	39607 (8715)	48.7 (10.2)	65079 (37173)	59.5 (27.2)	2041 (1946)	5.5 (5.5)	126 (27)	0.7 (1.2)	4.8 (1.7)	8.5 (2.7)
Study 2										
MTL	26925 (14181)	31.8 (18.5)	157502 (51220)	129.5 (43.5)	12150 (5299)	49.0 (15.0)	54 (27)	4.8 (4.0)	8.9 (2.1)	8.9 (3.7)
Control	41687 (6704)	49.7 (10.1)	112746 (60459)	96.0 (53.3)	5330 (3268)	12.9 (7.4)	119 (15)	1.2 (1.6)	1.7 (1.8)	2.8 (2.2)
Study 3										
17 month	37066 (8714)	45.0 (10.7)	111039 (49988)	121 (117)	9090 (7054)	26.6 (21.3)	91 (31)	3.1 (2.9)	2.4 (3.0)	8.0 (4.8)
23 month	37032 (11565)	44.1 (14.1)	94910 (30637)	87.4 (30.2)	13832 (8260)	39.0 (20.7)	70 (27)	2.5 (2.5)	4.6 (3.3)	10.1 (1.8)
Study 4										
WildType	34742 (9312)	50.0 (10.9)	112228 (44650)	88.8 (29.8)	7080 (3310)	20.3 (7.0)	109 (20)	2 (2)	5.4 (4.4)	6.9 (3.4)
D257A	32312 (8317)	37.5 (10.4)	48439 (14494)	43.6 (12.0)	3670 (2691)	10.9 (6.4)	113 (14)	.8 (.7)	1 (.8)	4.8 (1.8)
Study 5										
AdLib W	21170 (14136)	27.4 (18.6)	127995 (12373)	75.5 (20.7)	10692 (8981)	62.4 (12.2)	25 (18)	6 (5.3)	10.7 (1.2)	15 (1.7)
AdLib W LF	32958 (3673)	39.1 (4.9)	102222 (27610)	85.9 (24.6)	6836 (4046)	21.8 (14.0)	70 (20)	3 (2.7)	6.4 (1.5)	12.8 (3.6)
AdLib Ctrl	25973 (14668)	30.3 (17.2)	105130 (40427)	93.2 (36.4)	3467 (2926)	30.7 (39.3)	71 (41)	5 (4.1)	6.4 (3.4)	13.6 (4.7)
CR W	38074 (6249)	44.3 (8.8)	70843 (22508)	67.2 (19.2)	7064 (2480)	20.0 (9.2)	86 (16)	3.6 (2.3)	3.8 (2.2)	10.2 (2.6)
CR W LF	38042 (8723)	45.6 (11.6)	52462 (32512)	46.7 (23.5)	6387 (3902)	17.5 (10.1)	83 (21)	3.1 (3.0)	3.3 (2.5)	11.4 (3.5)
CR Ctrl	38655 (10714)	48.5 (13.7)	77854 (36235)	73.0 (26.2)	6317 (4507)	16.6 (11.1)	85 (18)	2.8 (2.6)	5 (1.4)	10.2 (3.9)

Figure 3.1. Mean articular cartilage (AC) area (μm^2) in the medial tibial plateaus of Studies 1 & 2. *=p<0.05, **=p<0.001.

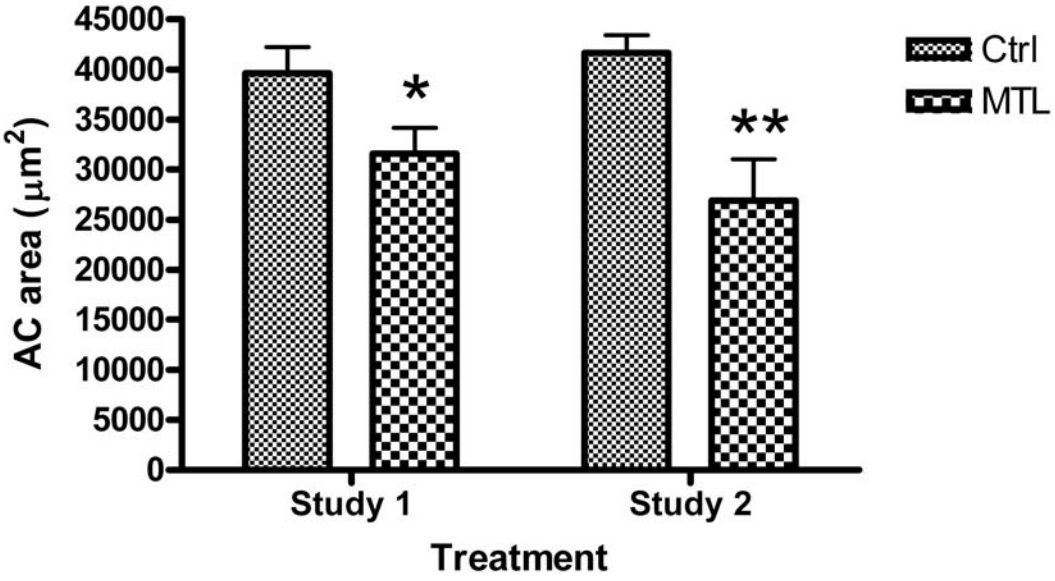

Figure 3.2. Evaluation of chondrocyte cell death in the medial tibial plateaus from Studies 1 & 2. (A) Mean percentage of chondrocyte cell death. **=p<0.0001 when compared to the Control joints of Study 1, ^^=p<0.0001 when compared to the Control joints of Study 2. (B) Mean Chondrocyte Viability factor scores. **=p<0.001 when compared to the Control joints of Study 1, ^^=p<0.001 when compared to the Control joints of Study 2.

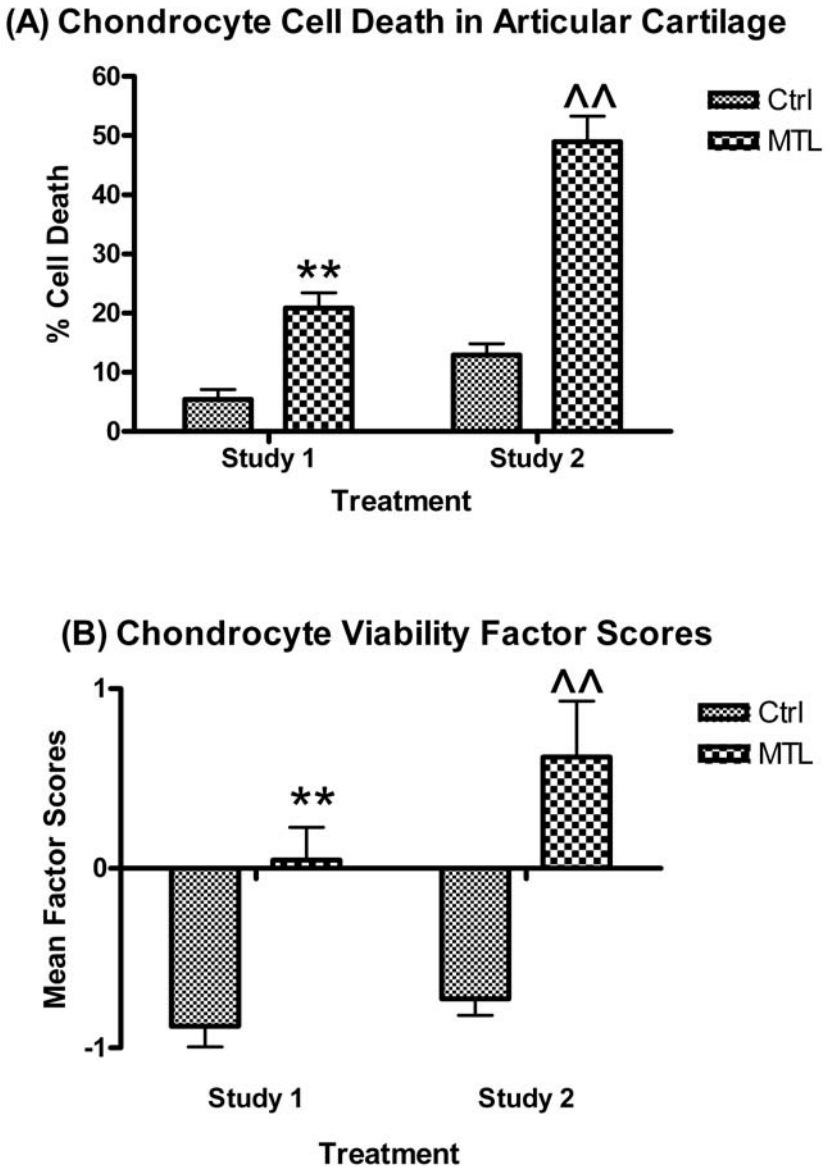

Figure 3.3. Histological sections demonstrating abaxial osteophytes located on the medial tibial plateaus of MTL joints. Bar = 100μm. (A) Abaxial joint margin of the medial tibial plateau from Control joint from Study 1. (B) Abaxial osteophyte on the medial tibial plateau of an MTL joint from Study 1. Arrows indicate original abaxial joint margin. (C) Abaxial osteophyte on the medial tibial plateau of an MTL joint from Study 2. Arrows indicate original joint margin.

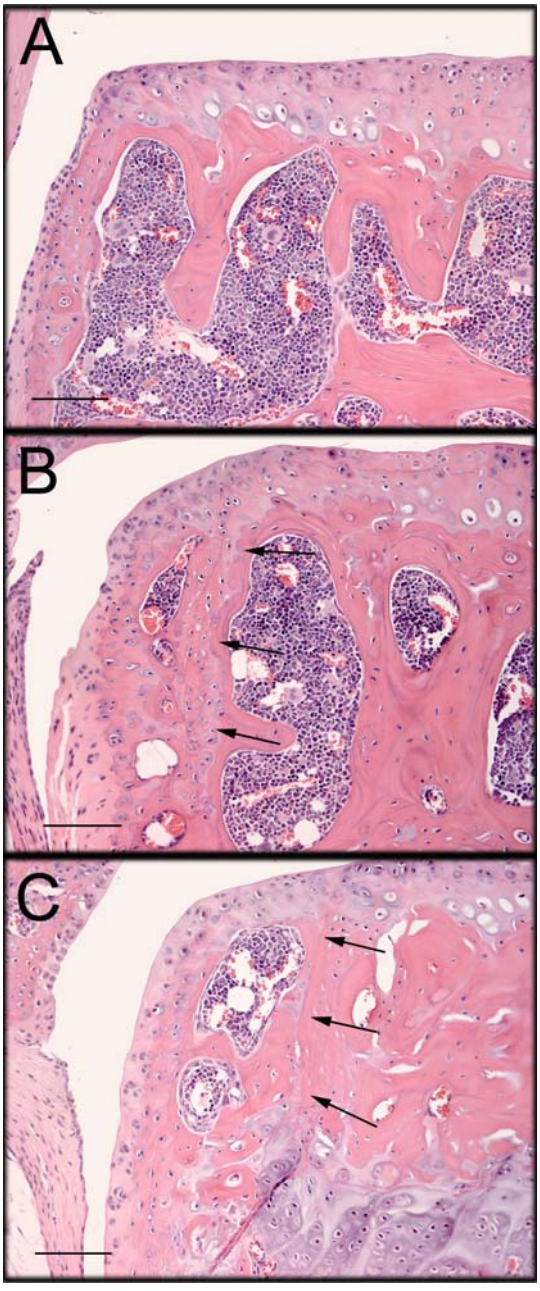

Figure 3.4. Mean subchondral bone (SCB) thickness from the medial tibial plateaus in the Wild Type (WT) and D257A joints in Study 4. *=p<0.05 when compared to the WT.

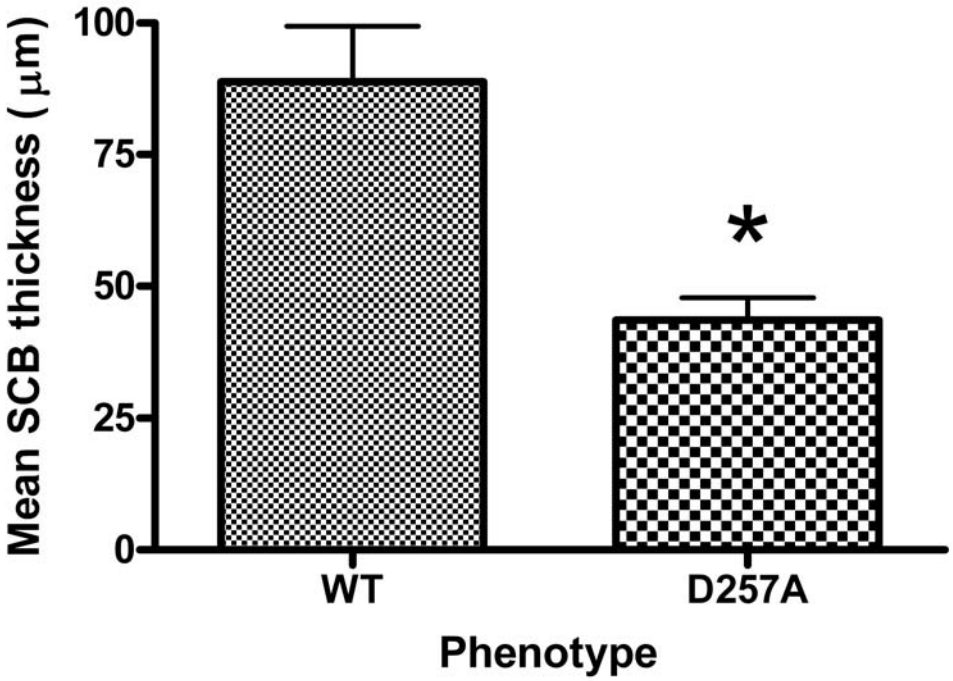

Figure 3.5. Changes in articular cartilage and chondrocyte cell death in C57/Bl6 mice by age, using the control joints from Studies 1, 2, 3, and 5. (A) Mean percentage of chondrocyte cell death (CCD) by age. *=p<0.01 when compared to 22 weeks, 17 months, and 23 months and p<0.05 when compared to 16 months; ^=p<0.05 when compared to 17 months and 23 months, and #=p<0.05 when compared to 23 months. (B) Mean articular cartilage (AC) thickness by age. *=p<0.02 when compared to 16 months, 17 months, and 23 months.

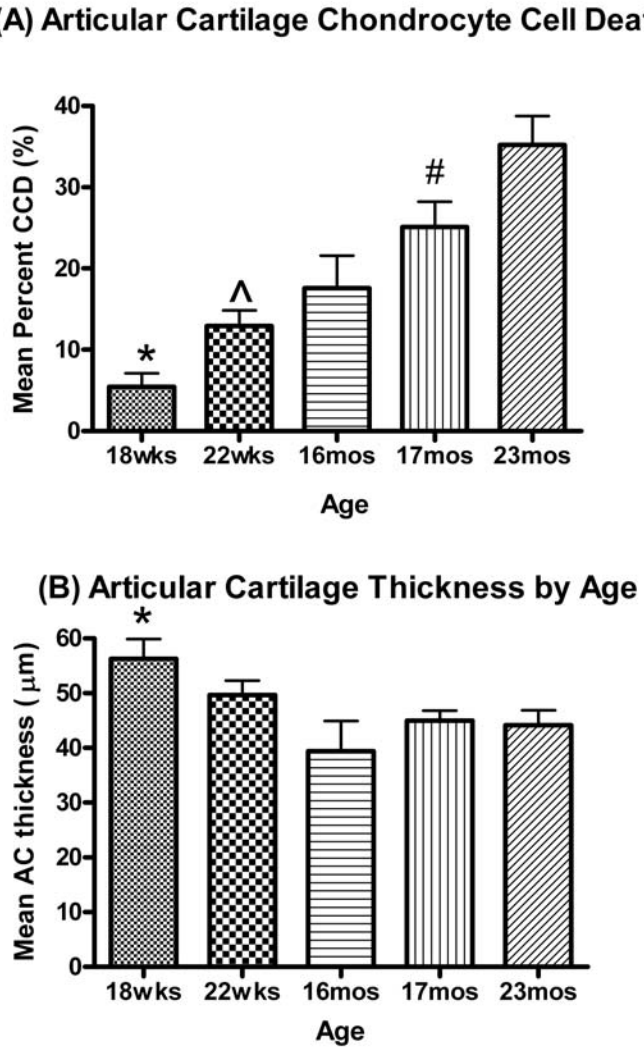

Figure 3.6. Histological sections demonstrating tidemark clefts (indicated by arrows) identified on the tibial plateaus of mouse stifle joints. Bar=100μm (A) Early stages of a tidemark cleft that is associated with cell death and thinning of articular cartilage with chondrocyte cell death in the articular cartilage adjacent to the tidemark. (B) A tidemark cleft that has extended almost the entire length of the tibial plateau, but has yet to separate, leaving the articular cartilage surface intact. (C) A tibial plateau missing approximately a large area of full thickness articular cartilage extending approximately half of the tibial plateau.

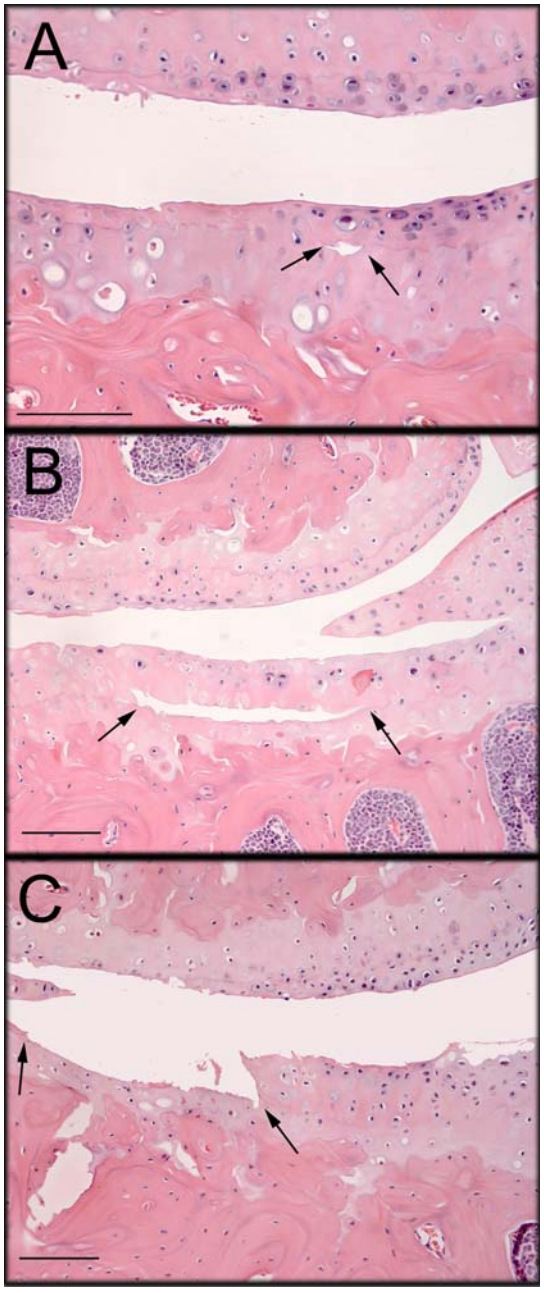

Figure 3.7. Histological sections demonstrating varying degrees of chondrocyte cell death (CCD) identified in the mouse stifle joints. Bar = 100µm. Black arrows indicate areas of CCD, black arrow heads indicate fibrillation and clefting of the articular cartilage, and green arrow heads indicate tidemark. (A) Small area of CCD on the tibial plateau not associated with any fibrillation and clefting of the articular cartilage. (B) Large area of CCD on the tibial plateau, associated with CCD on the femoral condyle and damage to the articular cartilage. (C) and (D) Areas of CCD on both the tibial plateau and femoral condyle associated with thinning of the articular cartilage. (E) CCD in both the tibial plateau and femoral condyle, associated with extensive thinning of the articular cartilage. (F) CCD in both the tibial plateau and femoral condyle, associated with extensive damage to the articular cartilage, including full thickness loss.

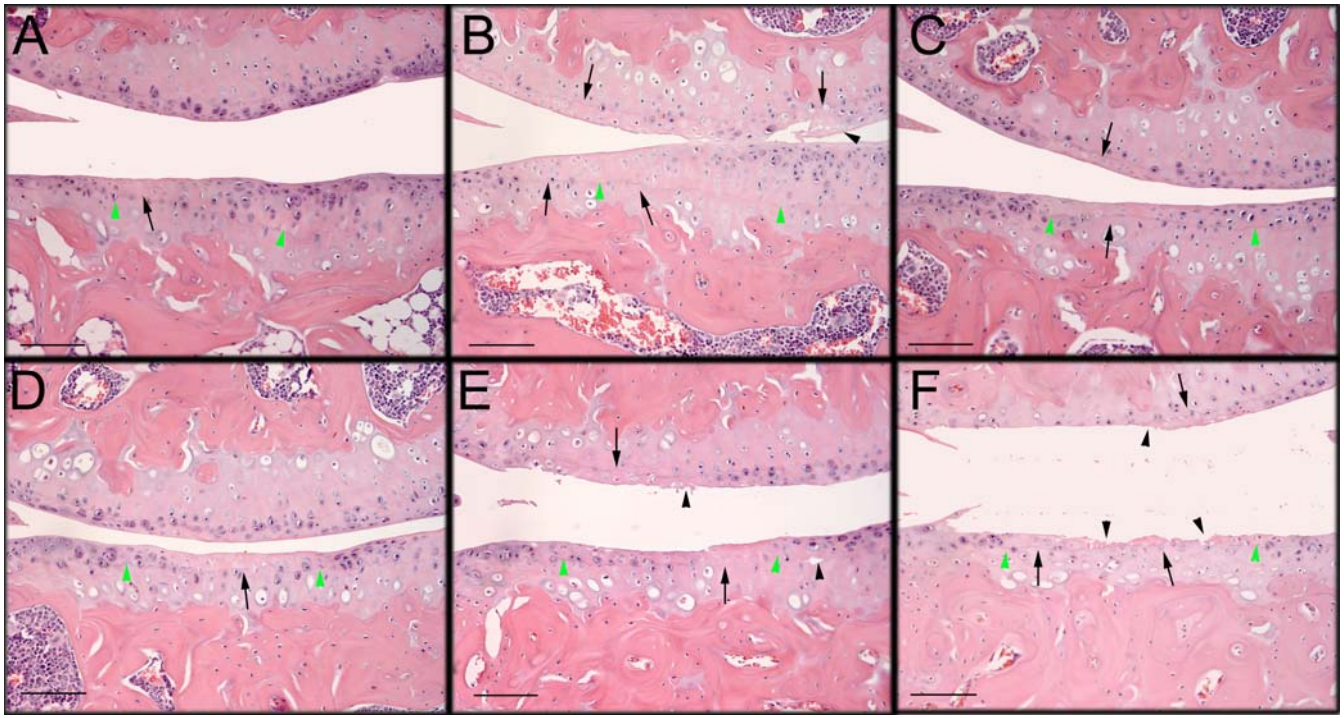

3.5 References

1. Mankin HJ, Dorfman H, Lippiello L, Zarins A. Biochemical and metabolic abnormalities in articular cartilage from osteo-arthritic human hips. II. correlation of morphology with biochemical and metabolic data. J Bone Joint Surg Am. 1971 Apr;53(3):523-37.

2. Lahm A, Uhl M, Erggelet C, Haberstroh J, Mrosek E. Articular cartilage degeneration after acute subchondral bone damage: An experimental study in dogs with histopathological grading. Acta Orthop Scand. 2004 Dec;75(6):762-7.

3. Lozano J, Saadat E, Li X, Majumdar S, Ma CB. Magnetic resonance T(1 rho) imaging of osteoarthritis: A rabbit ACL transection model. Magn Reson Imaging. 2009 Jun;27(5):611-6.

4. Griffin TM, Huebner JL, Kraus VB, Guilak F. Extreme obesity due to impaired leptin signaling in mice does not cause knee osteoarthritis. Arthritis Rheum. 2009 Oct;60(10):2935-44.

5. Naito K, Watari T, Muta T, Furuhata A, Iwase H, Igarashi M, et al. Low-intensity pulsed ultrasound (LIPUS) increases the articular cartilage type II collagen in a rat osteoarthritis model. J Orthop Res. 2009 Oct 6;28(3):361-9.

6. Glasson SS, Blanchet TJ, Morris EA. The surgical destabilization of the medial meniscus (DMM) model of osteoarthritis in the 129/SvEv mouse. Osteoarthritis Cartilage. 2007 Sep;15(9):1061-9.

7. Otterness IG, Chang M, Burkhardt JE, Sweeney FJ, Milici AJ. Histology and tissue chemistry of tidemark separation in hamsters. Vet Pathol. 1999 Mar;36(2):138-45.

8. Pritzker KP, Gay S, Jimenez SA, Ostergaard K, Pelletier JP, Revell PA, et al. Osteoarthritis cartilage histopathology: Grading and staging. Osteoarthritis Cartilage. 2006 Jan;14(1):13-29.

9. Bomsta BD, Bridgewater LC, Seegmiller RE. Premature osteoarthritis in the disproportionate micromelia (dmm) mouse. Osteoarthritis Cartilage. 2006 May;14(5):477-85.

10. Botter SM, Glasson SS, Hopkins B, Clockaerts S, Weinans H, van Leeuwen JP, et al. ADAMTS5-/- mice have less subchondral bone changes after induction of osteoarthritis through surgical instability: Implications for a link between cartilage and subchondral bone changes. Osteoarthritis Cartilage. 2009 May;17(5):636-45.

11. Mason RM, Chambers MG, Flannelly J, Gaffen JD, Dudhia J, Bayliss MT. The STR/ort mouse and its use as a model of osteoarthritis. Osteoarthritis Cartilage. 2001 Feb;9(2):85-91.

12. Schunke M, Tillmann B, Bruck M, Muller-Ruchholtz W. Morphologic characteristics of developing osteoarthrotic lesions in the knee cartilage of STR/IN mice. Arthritis Rheum. 1988 Jul;31(7):898-905.

13. Taniguchi N, Carames B, Ronfani L, Ulmer U, Komiya S, Bianchi ME, et al. Aging-related loss of the chromatin protein HMGB2 in articular cartilage is linked to reduced cellularity and osteoarthritis. Proc Natl Acad Sci U S A. 2009 Jan 27;106(4):1181-6.

14. Kujoth GC, Hiona A, Pugh TD, Someya S, Panzer K, Wohlgemuth SE, et al. Mitochondrial DNA mutations, oxidative stress, and apoptosis in mammalian aging. Science. 2005 Jul 15;309(5733):481-4.

15. Bendele AM. Animal models of osteoarthritis. J Musculoskelet Neuronal Interact. 2001 Jun;1(4):363-76.

16. Bendele AM, Hulman JF. Spontaneous cartilage degeneration in guinea pigs. Arthritis Rheum. 1988 Apr;31(4):561-5.

17. Carlson CS, Loeser RF, Jayo MJ, Weaver DS, Adams MR, Jerome CP. Osteoarthritis in cynomolgus macaques: A primate model of naturally occurring disease. J Orthop Res. 1994 May;12(3):331-9.

18. Mistry D, Oue Y, Chambers MG, Kayser MV, Mason RM. Chondrocyte death during murine osteoarthritis. Osteoarthritis Cartilage. 2004 Feb;12(2):131-41.

19. Boileau C, Martel-Pelletier J, Abram F, Raynauld JP, Troncy E, D'Anjou MA, et al. Magnetic resonance imaging can accurately assess the long-term progression of knee structural changes in experimental dog osteoarthritis. Ann Rheum Dis. 2008 Jul;67(7):926-32.

20. Hayami T, Pickarski M, Zhuo Y, Wesolowski GA, Rodan GA, Duong le T. Characterization of articular cartilage and subchondral bone changes in the rat anterior cruciate ligament transection and meniscectomized models of osteoarthritis. Bone. 2006 Feb;38(2):234-43.

21. Little CB, Barai A, Burkhardt D, Smith SM, Fosang AJ, Werb Z, et al. Matrix metalloproteinase 13-deficient mice are resistant to osteoarthritic cartilage erosion but not chondrocyte hypertrophy or osteophyte development. Arthritis Rheum. 2009 Dec;60(12):3723-33.

22. Ytrehus B, Carlson CS, Ekman S. Etiology and pathogenesis of osteochondrosis. Vet Pathol. 2007 Jul;44(4):429-48.

CHAPTER 4

VALIDATION OF A HISTOLOGICAL GRADING SCHEME FOR OSTEOARTHRITIS IN MICE

Studies attempting to validate commonly used histological grading schemes used to evaluate osteoarthritis (OA) severity have been previously identified limitations to these schemes, including lack of specificity and reproducibility. The goal of this study was to validate a new histological grading scheme for OA lesions in mice and compare it to the Mankin Histological-Histochemical Grading System (HHGS) which is the most commonly used histological grading scheme. Two midcoronal sections (stained with H&E and Safranin-O) from 30 tibial plateaus representing a wide range of disease severity were evaluated with both schemes by four observers with a wide range of experience. Principal Components Analysis (PCA)-derived factor scores were calculated for each individual joint based on the results obtained for each observer using the new histological grading scheme. The mean factor scores were then compared to the total Mankin HHGS score generated by each observer. The reliability of both schemes was calculated using Intraclass Correlation Coefficients (ICCs). Validity of both schemes was calculated using the area under the ROC curve. Finally, a correlation analysis was performed to identify correlations between individual parameters of the new histological grading scheme and the total Mankin HHGS score. The intra- and inter-observer reliabilities were higher in the newly developed scheme than the Mankin HHGS. Reliability of the Mankin HHGS also decreased as experience decreased, which was not true for the newly developed scheme. The validities of both schemes were similar; both schemes were able to distinguish normal from osteoarthritic cartilage and severe disease from lesser severities. Overall, the newly developed scheme proved to be more reliable

and as valid as the Mankin HHGS, and is able to characterize changes in a wider range of tissues.

4.1 Introduction

Validation of histological grading schemes that assess the severity of osteoarthritis (OA) is essential for determining their reliability and reproducibility. A histological grading scheme must accurately and reproducibly assess severity of the disease if it is to be beneficial, regardless of the species on which it is being used and the experience of the observer assessing the tissue. The Mankin Histological-Histochemical Grading System (HHGS) (1) is currently the most widely used histological grading scheme for osteoarthritis. It was initially developed for evaluation of OA in human articular cartilage, and is a semi-quantitative assessment of changes within the articular cartilage. The Mankin HHGS includes four parameters: degradation of the extracellular matrix, changes in chondrocyte number, loss of Safranin-O staining of proteoglycans, and tidemark integrity. Several studies have attempted to validate the Mankin HHGS, but none have succeeded. (2-4) Inter- and intra-observer reproducibilities of the scheme have been shown to be quite low, indicating that the scheme is neither reliable nor reproducible. (2-4) In addition, the reliability of this scheme to evaluate OA severity in rodents, including mice, has not been examined.

A new histological grading scheme to assess OA severity in mouse stifle joints was developed to attempt to overcome the limitations of the Mankin HHGS, indicated in Chapter 1, that include: subjectivity of the parameters evaluated, lack of quantitative

evaluations, and the fact that the scheme is restricted to evaluating only changes occurring within the articular cartilage. The parameters included in the new scheme are less subjective than the Mankin HHGS and include numerous quantitative evaluations of changes occurring not only within articular cartilage, but within multiple tissues of the joint, such as subchondral bone and the menisci. The development of the new scheme was outlined in Chapter 2, and results of its application to a large set of mouse stifle joints were included in Chapter 3. The goals of the present study were to 1) assess the reliability and validity of the PCA-derived scores as descriptors and identifiers of OA severity and 2) to compare the utility of the PCA-derived scores with the Mankin HHGS total score, which is the accepted standard assessment of OA severity. It is anticipated that the inclusion of continuous measurements of changes within the joint will make the new histological grading scheme more reproducible and reliable than the Mankin HHGS, and that the evaluation of multiple tissues within the joint will provide a more sensitive evaluation of milder changes associated with OA.

4.2 Methods

Articular Cartilage Samples

Sections from joints for this study were selected from the 158 mouse stifle joints utilized in Chapter 2. Thirty tibial plateaus from 21 joints were used (lateral n=12, medial n=18). Tibial plateaus were selected for evaluation based on a mid-coronal location, high quality of sectioning and staining of the tissue, and level of disease severity. In order to ensure that a wide range of OA lesions were represented, each tibial plateau was

independently assessed and assigned an OA severity level based on the semi-quantitative articular cartilage structure (ACS) score. (Table 4.1) Five levels of OA severity were created based on the ACS scores: 0 = "normal" (n= 8); 1-3 = "minimal" (n=8); 4-6 = "mild" (n=6); 7-9 = "moderate" (n=3); 10-12 = "severe" (n=5). Two mid-coronal sections were utilized for histological evaluation, one stained with H&E and one with Safranin-O stained.

Histological Evaluation

The 30 tibial plateaus were evaluated using both schemes (Tables 4.2 & 4.3) by four individual observers (Observers 1-4). Two of the observers had extensive experience in evaluating mouse OA and using an Osteomeasure histomorphometry system (Osteometrics, Atlanta, GA) (Observers 1 & 4), one observer had moderate experience (Observer 2), and one observer had little to no experience (Observer 3). Both slides for each tibial plateau were blinded and randomized to prevent observer bias. Each observer was given written definitions for both schemes and a figure outlining how measurements should be taken. In addition, observers were given a tutorial (approximately 20 minutes long) on how to use the Osteomeasure system for taking the measurements included in the new scheme. All measurements & histological grades were performed on the H&E stained section with the exception of the Safranin-O semi-quantitative grades in both the newly developed scheme and the Mankin HHGS. For the Safranin-O grades, a corresponding mid-coronal Safranin-O stained section was used. Observers evaluated all

30 sections using both schemes over a two day period (Time 1), after which the slides were re-randomized and re-evaluated by all four observers two weeks later (Time 2).

Statistics

In Chapter 2, Principal Component Analysis (PCA) was used to reduce the 15 correlated OA quantitative and semi-quantitative scores to 5 orthogonal (uncorrelated) linear combinations of these measurements. The PCA-derived scores for each of the 8 evaluations in this study (4 observers, 2 time points) were calculated by 1) standardizing each measurement using means and standard deviations from the original PCA; 2) multiplying these standardized measures by the PCA-derived factor score loadings from the original PCA; and 3) summing the weighted standardized measures into PCA-derived scores for this study.

Reliability: Intra- and Inter-observer reliability coefficients were estimated for each of the 5 PCA-derived scores and the total Mankin HHGS score using an Intraclass correlation coefficient (ICC). To estimate intra-observer reliabilities, ICCs were calculated for each evaluator using repeated measures of calculated PCA-derived scores and Mankin HHGS total scores. An inter-observer reliability analysis was completed using data from all four observers. In addition, a separate inter-observer reliability analysis was completed for the two experienced observers (Observers 1 & 4). ICCs of 0.80 or greater are generally identified as acceptable and ICCs of 0.90 or greater are recommended for diagnostic or intervention purposes. (5)

Validity: The accuracy of each PCA-derived score and HHGS score in identifying levels of OA severity was estimated by the area under the ROC curve (AUC) for each of the five OA severity levels: normal, minimal, mild, moderate, & severe. Combined data from each evaluator at each time were used in separate logistic regression models for each score (five PCA-derived scores and HHGS score) as a predictor of each level of assigned OA severity (five levels). It is known that the AUC ranges from 0.5 (no discrimination) to 1.0 (perfect discrimination), with values ranging from 0.70 to 0.9 indicating moderately accurate classification, and values >0.90 representing high classification accuracy. (6) Sensitivity and specificity analysis were completed for scores that demonstrated acceptable levels of inter- and intra-observer reliability (ICCs >0.90) as well as moderately acceptable validity (AUC >0.80). Data used to calculate cut points associated with varying levels of sensitivity and specificity were generated from the same logistic regression models used to calculate AUC for the ROC curves.

Correlation Analysis: As a further evaluation of validity of the PCA-derived score scheme to quantify OA severity, correlation analysis was done between each PCA-derived score at Time 1 and the total HHGS score as well as HHGS score components at Time 1 for each evaluator (separate analyses by evaluator). Additional correlation analyses to compare the HHGS total score with quantitative parameter measures having factor loadings $\geq$0.40 on either the Articular Cartilage Integrity and/or Chondrocyte Viability factors (outlined in Chapter 2) were done. Non-parametric Spearman rank correlation coefficients were calculated as appropriate for the semi-quantitative total Mankin HHGS and individual parameter scores.

4.3 Results

Observers took between 2 and 6 hours to complete the histological evaluations of the 30 tibial plateaus using both schemes. The time taken to evaluate the sections depended primarily on level of experience with the Osteomeasure system. The amount of time per slide decreased as the observers became more comfortable with the Osteomeasure system and the schemes. The most experienced observer was able to finish all evaluations within two hours.

Reliability

Table 4.4 outlines intra-observer reliability coefficients for all five factors and the total Mankin HHGS score. Intra-observer reliability coefficients were acceptable (>0.90) for all evaluators for Articular Cartilage Integrity factor scores. Three evaluators (Observers 1, 2, & 4) had acceptable coefficients for the Mankin HHGS, and 2 evaluators (Observers 1 & 4) had acceptable coefficients for the Chondrocyte Viability scores. Only one evaluator had acceptable coefficients for the Subchondral Bone (Observer 1) and Meniscal (Observer 4) factor scores, and no evaluators had acceptable coefficients for the Osteophyte factor scores.

Table 4.5 includes the ICC for a single evaluator and the mean of multiple evaluators using data from all four evaluators and then from the two most experienced evaluators (Observers 1 & 4). The ICC for a single evaluator using data from all four observers indentified only one factor score, Articular Cartilage Integrity, that had

acceptable inter-observer reliability (0.95). The same ICC for a single evaluator was recalculated only using data from the two most experienced observers (Observers 1 & 4), and in this case three factor scores were deemed acceptable: Articular Cartilage Integrity (0.94), Chondrocyte Viability (0.95) and Subchondral Bone (0.90). The Mankin HHGS did not have acceptable inter-observer reliability scores for a single evaluator in either analysis (0.68 & 0.76, respectively). When the ICC was calculated as the mean of four evaluators using data from all four observers, 4 of the 5 factor scores with the exception of the Osteophyte factor score had acceptable inter-observer reliability scores, as did the total Mankin HHGS score. When the ICC was calculated as the mean of two evaluators using data from the two most experienced observers (Observers 1 & 4), three factor scores (Articular Cartilage Integrity, 0.97; Chondrocyte Viability, 0.97; and Subchondral Bone, 0.94) had acceptable inter-observer reliability scores; however, the Mankin HHGS did not have acceptable inter-observer reliability (0.86).

Validity

For evaluation of validity of both schemes, the area under the ROC curve was reported for each OA severity level using data from all four evaluators from the second evaluation. (Table 4.6) The Mankin HHGS was determined to be moderately accurate (AUC = 0.85) in discriminating normal articular cartilage from all levels of severity of osteoarthritic cartilage, and highly accurate (AUC = 0.94) in discriminating severe OA from normal, minimal, mild, and moderate OA. The Articular Cartilage Integrity score was moderately accurate (AUC = 0.82) in discriminating severe OA from normal,

minimal, mild, & moderate disease. The Chondrocyte Viability factor score was moderately accurate (AUC = 0.81) in distinguishing normal cartilage from all levels of osteoarthritic cartilage, and moderately accurate (AUC = 0.74) in distinguishing severe OA from normal, minimal, mild, & moderate disease. These results are consistent with the plots of OA severity level by average PCA-score stratified by evaluator at Time 1 (Figure 4.1).

Correlation Analysis

Spearman rank correlation coefficients between mean PCA scores for each of the 5 factors were compared to each of the 4 parameters of the Mankin HHGS and the total Mankin HHGS score. The Chondrocyte Viability factor was most consistently correlated with the 4 parameters of the Mankin HHGS, and was found to be significantly correlated with the total Mankin HHGS score for all four evaluators (data not shown). Strong ($r>0.80$) and statistically significant ($p<0.05$) correlation coefficients provide evidence that the factor scores are consistent with the current, albeit less than perfect, standards of OA severity assessment (total Mankin HHGS score and component scores). When individual parameters were separated and compared to the total Mankin HHGS score, three individual parameters; percent of chondrocyte cell death (CCD%), Articular Cartilage Structure score (ACS), and Safranin-O staining score (Saf-O) from the new scheme were found to be significantly correlated with the total Mankin HHGS for all four observers (Table 4.7).

4.4 Discussion

This study validates the new histological grading scheme and found it in general to be more reliable and reproducible than the Mankin HHGS, which is currently the most widely used histological grading scheme for both humans and animals. The Mankin HHGS was chosen for comparison with the new scheme over others including the Glasson, et al (7) and OOCHAS (8) schemes because it has been the basis of comparison for numerous other studies. (2-4) In addition, the Mankin HHGS evaluates one section with a detailed scheme, which more closely matches the evaluation process used with the newly developed scheme. The scheme developed by Glasson, et al on the other hand, evaluates several sections with a much simpler scheme (one parameter, graded on a scale of 0-5), and therefore it would not be as easily comparable.

Observers were selected to represent a wide range of experience, both in using the Osteomeasure system and in evaluating OA severity. The results demonstrated that experience is important for obtaining reliable results, particularly for the Mankin HHGS. For example, the intra-observer reliability coefficient was low (0.590) for the Mankin HHGS for Observer 3, who was the most inexperienced evaluator. This correlates with a previous study that also showed that the least experienced observers had relatively low intra-observer reproducibilities for the Mankin HHGS. (9) Experience appeared to be less important for the new grading system, however. For example, the Articular Cartilage Integrity factor scores overall had much higher intra-observer reliability scores than the total Mankin HHGS score. For inter-observer reliability scores, the ICC model utilized in this study allows for the inter-observer reliability estimates to be generalized to the larger

population of evaluators rather than limited to the fixed set of evaluators in this study. The inter-observer reliability results indicate that having multiple observers evaluating the data using the newly devised scheme will yield the most accurate results, even though some of the observers were less experienced. However, experience in evaluating OA severity and/or using the Osteomeasure system also is important, as inter-observer reliability scores were higher when only data from Observers 1 & 4 were included in the ICC analysis. Under normal circumstances, though, it is not a reasonable expectation for multiple individuals to evaluate OA severity in a single study, particularly when multiple measurements are required, and also to expect those individuals to be experts in evaluating OA in mouse joints. The results of the present study showed that a single, inexperienced observer can produce very reliable results for the Articular Cartilage Integrity factor scores, and that a single observer will be sufficient to create reliable results using the newly developed scheme if that observer is experienced. The Mankin HHGS, however, had lower inter- observer reliabilities regardless of the level of experience or the number of observers evaluating the sections.

The extremely low intra-observer reliability score for Observer 1 for the Osteophyte factor score (-0.090) was likely because the observer changed her method of evaluating osteophytes during the second evaluation once she had identified the differences between osteophyte development in non-human primates and mice. In addition, the relatively low intra-observer reliability score for Observer 2 for the Chondrocyte Viability factor score was likely because the observer changed her mind about how she identified dead chondrocytes; during Time 1 she relied upon the

Osteomeasure computer screen to identify dead chondrocytes and take measurements, during Time 2 she identified dead chondrocytes directly from the microscope itself and correlated that to the image on the computer screen to take measurements.

Intra-observer consistency also is critical in creating reproducible results for any scheme, but especially when using a scheme as detailed as the newly developed scheme in this study. Care should be taken to set out strict definitions of changes identified within the tissues, which may be dependent on the species. For example, the low reliability scores for the Osteophyte factor score is likely because the definitions used by the new scheme to identify both axial and abaxial osteophytes in mice were developed for use in monkeys (10) and did not apply perfectly to mice. In this study, observers had at least a general knowledge of the tissues within the joint and changes that were to be evaluated, but only moderately detailed instructions were given for identifying changes within each tissue. Despite this, inter- and intra-observer reliabilities for the new scheme were acceptable and probably could be improved upon with more complete instructions.

The biggest limitation to the evaluation of the validity of both schemes is the method by which the levels of OA (normal, minimal, mild, moderate, & severe) were chosen. Unfortunately there is no "gold standard" by which OA severity can be identified. Another study by Ostergaard, et al, (2) used macroscopic evaluation such as the Collins & McElligott scale (11) to create levels of OA severity among the samples in the study, however this method is impossible to apply to a very small mouse stifle joint which cannot be evaluated macroscopically. Therefore, a histological method of categorizing OA severity was utilized in this study. However, it was redundant in that it

used an initial independent evaluation with the ACS score for each joint to place it within the proper OA severity category, and this same ACS score is part of the newly developed histological grading scheme. Despite this limitation, however, the Mankin HHGS was able to discriminate normal cartilage from OA cartilage and severe OA from normal, minimal, mild, & moderate disease in the mouse joints, which effectively reproduced the results obtained by Ostergaard, et al, using human tissue. (2) The Chondrocyte Viability and Articular Cartilage Integrity scores also had comparable validity results with those of the Mankin HHGS.

The combined results of this study show that the newly developed histological grading scheme is more reliable and as equally valid as the Mankin HHGS. These results only utilized factor scores generated by combining all of the data (15 parameters) and did not evaluate each individual parameter. Future work would include determining reproducibility and reliability of each individual parameter of the newly developed scheme and comparison of these to the Mankin HHGS. In addition, data can be gathered from an even larger number of joints from studies using other surgical or naturally induced models and various interventions to further widen the range of OA severity and potential changes that may be identified.

Table 4.1. Description of Articular Cartilage Structure scores used to classify tibial plateaus into five respective OA severity categories: normal, minimal, mild, moderate, and severe.

Articular Cartilage Structure Score	Description
Grade 0	Articular surface smooth and intact
Grade 1-3	Fibrillation and/or clefts and/or loss of cartilage involving 1/4 or less of the articular cartilage thickness involving ≤1/3, >1/3 and ≤2/3, or >2/3 of the plateau or condyle respectively
Grade 4-6	Fibrillation and/or clefts and/or loss of cartilage involving 1/2 or less of the articular cartilage thickness involving ≤1/3, >1/3 and ≤2/3, or >2/3 of the plateau or condyle respectively
Grade 7-9	Fibrillation and/or clefts and/or loss of cartilage involving >1/2 of the articular cartilage but less than full thickness involving ≤1/3, >1/3 and ≤2/3, or >2/3 of the plateau or condyle respectively
Grade 10-12	Fibrillation and/or clefts and/or loss of cartilage involving the full thickness of articular cartilage involving ≤1/3, >1/3 and ≤2/3, or >2/3 of the plateau or condyle respectively

Table 4.2. Summary of 15 parameters included in the new histological grading scheme.

Parameter (units); Abbreviation	Definition
Articular cartilage (AC) area (μm^2); AC area	Total area of articular cartilage
Articular cartilage thickness (μm); AC thick	Average articular cartilage thickness
Subchondral bone (SCB) area (μm^2); SCB area	Total area of subchondral bone
subchondral bone thickness (μm); SCB thick	Average subchondral bone thickness
Chondrocyte cell death (CCD) area (μm^2); CCD area	Total area of articular cartilage with two or more necrotic chondrocytes
Percent of chondrocyte cell death (%); CCD%	Percent of CCD area over total AC area
Number of chondrocytes; #chond	Total number of viable chondrocytes
Total AC area per viable chondrocyte (μm^2); AC/chond	AC area divided by number of viable chondrocytes
Viable AC area per viable chondrocyte (μm^2); VAC/chond	Total area of AC subtracted by CCD area, divided by total number of viable chondrocytes
Size of axial osteophytes (μm^2); Ax OP	Total area of axial osteophytes (if present)
Size of abaxial osteophytes (μm^2); Abax OP	Total area of abaxial osteophytes (if present)
Meniscal area (μm^2); Men area	Total area of weight-bearing menisci
Meniscal cell death area (μm^2); Men CCD	Total area of chondrocyte cell death within weight-bearing menisci
Articular cartilage structure score (0-12); ACS	Semi-quantitative score of articular cartilage integrity
Safranin-O staining score (0-12); Saf-O	Semi-quantitative score of loss of Safranin-O staining

Table 4.3. Summary of the Mankin HHGS scheme. A total grade of 0 indicates normal articular cartilage, a total grade of 14 indicates severe OA. (1)

Category	Subcategory	Score
Structure	normal	0
	surface irregularities	1
	pannus & surface irregularities	2
	clefts to transitional zone	3
	clefts to radial zone	4
	clefts to calcified zone	5
	complete disorganization	6
Cells	normal	0
	diffuse hypercellularity	1
	cloning	2
	hypocellularity	3
Safranin-O Staining	normal	0
	slight reduction	1
	moderate reduction	2
	severe reduction	3
	no dye noted	4
Tidemark Integrity	intact	0
	crossed by blood vessels	1
Total		**0-14**

Table 4.4. Intra-rater reliability coefficients for PCA-derived factor scores and the total Mankin HHGS score. Coefficients $\geq$0.90 are recommended for diagnostic purposes, and these are indicated in bold. Coefficients $\geq$0.80 are deemed acceptable.

	Articular Cartilage Integrity	Chondrocyte Viability	Subchondral Bone	Meniscus	Osteophytes	Total Mankin HHGS
Observer 1	**0.946**	**0.962**	**0.973**	0.863	-0.090	**0.918**
Observer 2	**0.955**	0.529	0.821	0.813	0.503	**0.904**
Observer 3	**0.978**	0.880	0.846	0.845	0.465	0.590
Observer 4	**0.900**	**0.924**	0.878	**0.911**	0.685	**0.973**

Table 4.5. Inter-rater reliability coefficients for PCA-derived factor scores and the total Mankin HHGS score. Reliability coefficients for a single evaluator and mean of four evaluators were calculated using data from all four observers (first two columns). Reliability coefficients for a single evaluator and mean of two evaluators were calculated using data from the two most experienced observers (Observers 1 & 4; second two columns). Coefficients ≥0.90 were determined to be within the acceptable range for diagnostic purposes.

	ICC for Single Evaluator (4 evaluators)	ICC for Mean of 4 Evaluators	ICC for Single Evaluator (2 evaluators)	ICC for Mean of 2 Evaluators
Articular Cartilage Integrity	**0.95**	**0.99**	**0.94**	**0.97**
Chondrocyte Viability	0.89	**0.97**	**0.95**	**0.97**
Subchondral Bone	0.82	**0.95**	**0.90**	**0.94**
Meniscus	0.78	**0.93**	0.75	0.86
Osteophytes	-0.01	-0.02	-0.08	-0.18
Total Mankin HHGS	0.68	**0.90**	0.76	0.86

Table 4.6. Area under the ROC curve (AUC) for each OA severity level using data from all four evaluators for Time 1. AUC >0.70 indicated moderately accurate classification, AUC>0.90 indicated high classification accuracy.

	Normal	Minimal OA	Mild OA	Moderate OA	Severe OA
Articular Cartilage Integrity	0.50	0.65	0.62	0.55	**0.82**
Chondrocyte Viability	**0.81**	0.54	0.51	0.68	**0.74**
Subchondral Bone	0.70	0.52	**0.86**	0.63	0.53
Meniscus	0.49	0.53	0.60	0.52	0.59
Osteophytes	0.59	0.50	0.61	0.67	0.64
Mankin HHGS	**0.85**	0.52	0.52	0.67	**0.94**

Table 4.7. Significant Spearman rank correlation coefficients between the Mankin HHGS total score and individual parameter measurements with factor loadings $\geq$0.40 on either the Articular Cartilage Integrity or Chondrocyte Viability factors.

	Observer 1	Observer 2	Observer 3	Observer 4
AC area	-0.038 (p=0.037)	NS	NS	NS
AC thickness	-0.44 (p=0.014)	NS	NS	NS
CD area	0.57 (p=0.001)	0.41 (p=0.025)	NS	NS
CD%	0.74 (p<0.001)	0.70 (p<0.001)	0.55 (p=0.002)	0.44 (p=0.014)
# chond.	-0.72 (p<0.001)	-0.65 (p<0.001)	-0.55 (p=0.002)	NS
AC/chondr.	0.50 (p=0.004)	0.45 (p=0.014)	NS	NS
VAC/chondr.	NS	0.38 (p=0.037)	NS	NS
ACS	0.83 (p<0.001)	0.79 (p<0.001)	0.40 (p=0.03)	0.80 (p<0.001)
Saf-O	0.56 (p=0.001)	0.70 (p<0.001)	0.65 (p<0.001)	0.36 (p=0.05)

Figure 4.1. Mean PCA-score and total Mankin HHGS score by OA severity level for each evaluator at Time 1. (A) Articular Cartilage Integrity factor scores, (B) Chondrocyte Viability factor scores, (C) total Mankin HHGS scores.

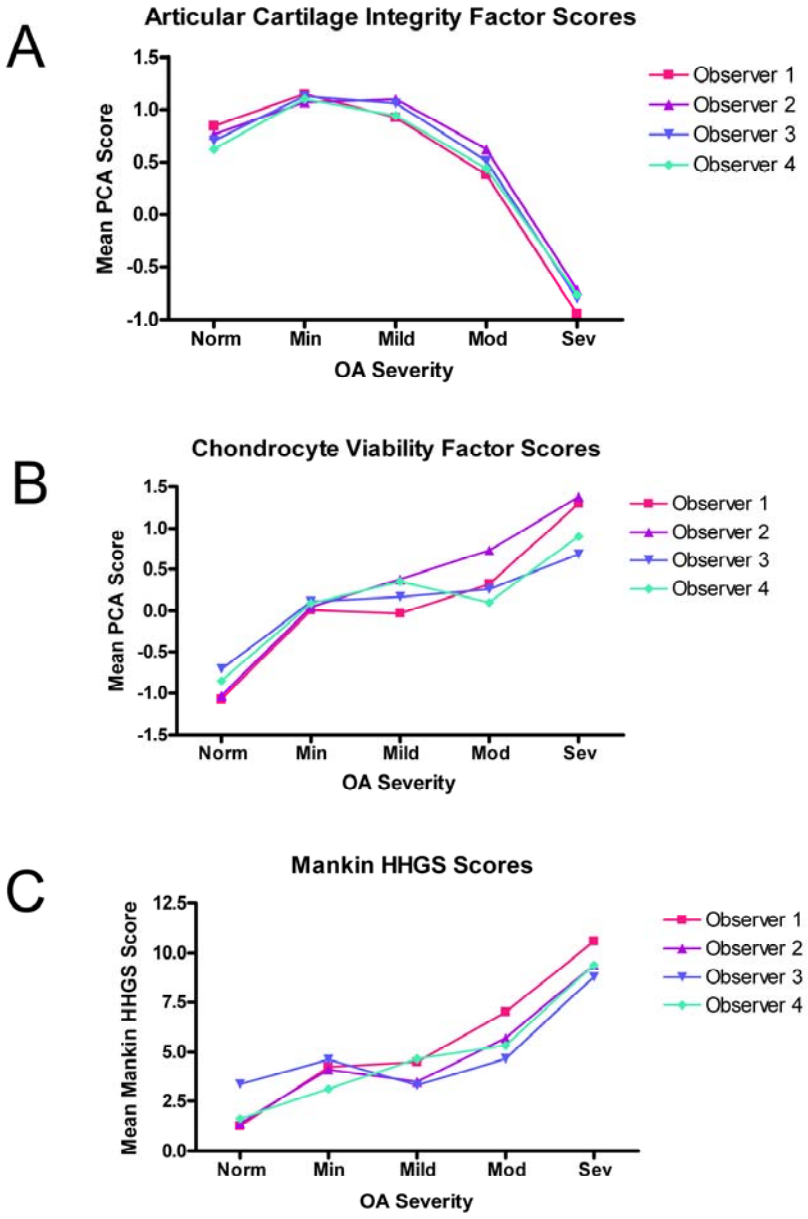

4.5 References

1. Mankin HJ, Dorfman H, Lippiello L, Zarins A. Biochemical and metabolic abnormalities in articular cartilage from osteo-arthritic human hips. II. correlation of morphology with biochemical and metabolic data. J Bone Joint Surg Am. 1971 Apr;53(3):523-37.

2. Ostergaard K, Andersen CB, Petersen J, Bendtzen K, Salter DM. Validity of histopathological grading of articular cartilage from osteoarthritic knee joints. Ann Rheum Dis. 1999 Apr;58(4):208-13.

3. Ostergaard K, Petersen J, Andersen CB, Bendtzen K, Salter DM. Histologic/histochemical grading system for osteoarthritic articular cartilage: Reproducibility and validity. Arthritis Rheum. 1997 Oct;40(10):1766-71.

4. van der Sluijs JA, Geesink RG, van der Linden AJ, Bulstra SK, Kuyer R, Drukker J. The reliability of the mankin score for osteoarthritis. J Orthop Res. 1992 Jan;10(1):58-61.

5. Weiner IB, Freedheim DK, Schinka JA, Velicer WF. Handbook of psychology. New York: Wiley; 2003.

6. Swets JA. Measuring the accuracy of diagnostic systems. Science. 1988 Jun 3;240(4857):1285-93.

7. Glasson SS, Blanchet TJ, Morris EA. The surgical destabilization of the medial meniscus (DMM) model of osteoarthritis in the 129/SvEv mouse. Osteoarthritis Cartilage. 2007 Sep;15(9):1061-9.

8. Pritzker KP, Gay S, Jimenez SA, Ostergaard K, Pelletier JP, Revell PA, et al. Osteoarthritis cartilage histopathology: Grading and staging. Osteoarthritis Cartilage. 2006 Jan;14(1):13-29.

9. Custers RJ, Creemers LB, Verbout AJ, van Rijen MH, Dhert WJ, Saris DB. Reliability, reproducibility and variability of the traditional Histologic/Histochemical grading system vs the new OARSI osteoarthritis cartilage histopathology assessment system. Osteoarthritis Cartilage. 2007 Nov;15(11):1241-8.

10. Olson EJ, Lindgren BR, Carlson CS. Effects of long-term estrogen replacement therapy on bone turnover in periarticular tibial osteophytes in surgically postmenopausal cynomolgus monkeys. Bone. 2008 May;42(5):907-13.

11. COLLINS DH, McELLIGOTT TF. Sulphate (35SO4) uptake by chondrocytes in relation to histological changes in osteoarthritic human articular cartilage. Ann Rheum Dis. 1960 Dec;19:318-30.

CHAPTER 5

GENERAL SUMMARY AND FUTURE DIRECTIONS

5.1 General Summary & Conclusions

Previous research has identified the lack of an adequate histological assessment tool for evaluating osteoarthritis (OA) severity in animals, (1-4) particularly laboratory animals such as mice, which are increasingly used in OA research. The goals of this project were: 1) develop a histological grading scheme that can reliably and reproducibly evaluate OA severity in mice; 2) apply this scheme to several mouse models of OA in which disease severity is expected to be influenced by intervention; and 3) compare the reliability and reproducibility of this scheme to pre-established histological grading schemes that are commonly utilized in OA research. This project accomplished these goals through the following three specific aims.

In Specific Aim 1, mid-coronal histological sections from 158 mouse stifle joints from five separate OA studies were globally evaluated for changes that are associated with OA, including changes not only in cartilage but also in surrounding bone and soft tissues. These studies included both surgically induced as well as naturally occurring disease and included animals with a wide range of disease severities. Changes that were consistently observed were further characterized using histomorphometric measurements or with semi-quantitative grades. The final version of this newly developed histological grading scheme included 13 quantitative measurements and 2 semi-quantitative evaluations of disease severity in mice. Data from the 15 parameters from both medial tibial plateaus of all stifle joints were combined into a single data set and were evaluated using correlation analyses and Principal Components Analysis (PCA). In the medial tibial

plateau, where OA lesions were most severe, strong correlations between the majority of the 15 parameters were identified. In the lateral tibial plateau, there were fewer correlations between the 15 parameters, likely due to a decrease in the severity of the disease in this site. PCA was then performed on the data from only the medial tibial plateaus and this analysis generated five factors that accounted for 74% of the variation within the data. Each of the five factors was composed of parameters that were related to each other and made conceptual sense. Factor 1 was composed of parameters that pertained to changes in articular cartilage integrity, including measurements of articular cartilage area and thickness and the two semi-quantitative grades. Factor 2 was composed of parameters that evaluated changes in chondrocytes, and Factors 3, 4, and 5 contained measurements of subchondral bone, weight-bearing meniscus, and periarticular osteophytes, respectively. These factors, combined with each individual parameter, allow this scheme to evaluate changes in articular cartilage, subchondral & periarticular bone, and the meniscus and provide a comprehensive histological analysis of OA in mice.

The goal of Specific Aim 2 was to apply this newly developed scheme to five studies of naturally occurring and surgically induced OA in mice to identify intervention group differences in disease severity. Two of these studies used the destabilized medial meniscus (DMM) model of surgically induced OA. (5) Two additional studies examined dietary interventions on naturally occurring OA severity using aged animals. And the goal of the fifth study was to examine the effects of a potential transgenic model of OA using the D257A mouse, which has an early aging phenotype and has only half the lifespan of wild-type littermates. (6) The scheme that was developed in Specific Aim 1

was applied to the stifle joints in all five studies. In addition, a pre-established histological grading scheme that was initially developed in humans, the Mankin Histological-Histochemical Grading System (HHGS) (7), was applied to these same joints for comparison. Finally, factor scores for each individual joint that were generated using the data generated by the newly developed scheme were assigned and provided a more global evaluation of OA severity by combining data from parameters pertaining to articular cartilage integrity, chondrocyte viability, subchondral bone, weight-bearing meniscus, and periarticular osteophytes respectively into a single factor score. These five factor scores that were generated for each individual joint could then be compared within studies or across studies.

The Mankin HHGS identified significant intervention differences in the surgically induced model of OA, in which OA lesions were most severe of all studies evaluated and was only able to identify age group differences in one naturally occurring model of OA and was unable to identify intervention group differences in naturally occurring OA. Numerous significant intervention differences were identified, however, using the newly developed scheme. A significant increase in OA severity, including a decrease in articular cartilage area and thickness and an increase in the number of dead chondrocytes was identified in the DMM joints vs. controls in both studies using this model. This scheme also identified intervention differences in articular cartilage and chondrocyte cell death in one of the dietary studies in which aged animals with naturally occurring disease were used. Finally, in the study focusing on a potential transgenic model of OA, although no significant intervention differences were noted in articular cartilage parameters, a

significant reduction in subchondral bone thickness and area was noted in the homozygotes that expressed the early aging phenotype. The results from this specific aim demonstrated that the newly developed scheme was more sensitive at detecting intervention differences in OA severity than the Mankin HHGS. In addition, by comprehensively evaluating several studies of both naturally occurring and surgically induced mouse OA, this study was also able to characterize the changes that are associated with the disease in mice.

In Specific Aim 3, the goal was to directly compare the newly developed scheme to the Mankin HHGS. This was accomplished by first identifying 30 mouse tibial plateaus that represented a wide range of disease severities. Four observers with varying experience then applied both schemes to the 30 tibial plateaus in two different sessions, separated by a period of two weeks. Intra- and inter-observer reproducibilities and the validity of both schemes were calculated. The newly developed scheme had higher intra- and inter-observer reproducibilities than the Mankin HHGS probably due, at least in part, to the objective nature of the scheme. In addition, we determined that intra-observer reproducibility of the Mankin HHGS decreased as experience decreased. Inter-observer reproducibility increased for the Mankin HHGS when data from only the two most experience observers was used in the analysis. None of these findings were true for the newly developed scheme. In fact, the least experienced observer had the highest intra-observer reproducibility when evaluating articular cartilage integrity. The Mankin HHGS was able to accurately distinguish severe OA vs. normal, minimal, mild, and moderate disease, and also accurately identified normal from osteoarthritic tissue. These results

were closely similar to those of a previous study. (2) Using data from the new scheme, the factor score evaluating articular cartilage integrity was able to distinguish severe disease from normal, minimal, mild, and moderate disease, and the factor score evaluating chondrocyte viability was as accurate as the Mankin HHGS, being able to distinguish normal from osteoarthritic tissue and severe disease from normal & less severe disease.

In summary, a comprehensive histological grading scheme for evaluating OA severity in mice was developed. The application of this scheme identified a wide range of OA lesions in multiple tissues in the mouse stifle joint. It proved to be more reliable than the well established and widely used Mankin HHGS, and was equally effective at distinguishing disease severity. The results of this study also provide a comprehensive characterization of naturally occurring and surgically induced OA in mice. Changes in several tissues were identified, including the striking contribution of decreased chondrocyte viability in murine OA, which was previously reported only in single transgenic mouse model. (8)

5.2 Future Directions

This project identified a possible role of chondrocyte cell death within the articular cartilage in the pathogenesis of OA in the mouse stifle joint. Large areas of dead chondrocytes in mice associated with OA have only been noted in one other study. (8) In the present studies, these changes often occurred prior to any identifiable damage to the articular cartilage matrix, and may provide a method of identifying early disease in this

species. Further characterization of the role and mechanism of this chondrocyte cell death may provide critical insights into the early initiation of the disease in the mouse stifle joint. Previous studies of the role of chondrocytes in the pathogenesis of OA in mice and other species have focused solely on apoptosis as the primary mechanism of cell death. However, the morphometry of the changes observed in the present study indicate that necrosis may have a more important role. Once the mechanism has been identified, molecular studies may then be completed to identify potential pathways through which the activation of cell death is occurring. In addition, this project identified a clear increase in chondrocyte cell death with age, whether via apoptosis or necrosis, in C57/Bl6 mice. This is clearly an important finding for studies using aged mice as a naturally occurring model and may also be of importance in studies that are examining surgically induced models in older animals, as these individuals have pre-existing disease that was not anticipated. A more controlled study, using C57/Bl6 mice of varying age groups, would be critical in reproducing these results. If this change is confirmed, further immunohistochemistry can be performed to attempt to identify the mechanism of cell death. DAPI (4',6-diamidino-2-phenylindole) staining, which is a fluorescent stain that strongly binds to DNA will be utilized to confirm a lack of chondrocytes in the areas of hypocellularity in articular cartilage that are evaluated in the newly developed scheme.

Hypercellularity of chondrocytes within the articular cartilage has been associated with the early stages of disease. (9-11) However, areas of hypercellularity found within the stifle joints of this study were diffuse across the entire plateau and appeared to be due to individual variability in chondrocyte density. These areas of hypercellularity never

correlated to any other changes associated with OA and often affected both femoral condyles and tibial plateaus of the same joint. In addition, if hypercellularity was a change associated with early disease, it would be expected to precede any changes in the extracellular matrix of articular cartilage as well as chondrocyte cell death. However, the areas of chondrocyte cell death that were identified, and noted above, appeared to be composed of a normal density of chondrocytes, and did not appear to be composed of an increase in the number of chondrocytes. There was also a noticeable lack of any chondrocyte clones within these stifle joints, which are often found to be associated with hypercellularity. Chondrocyte clones, or a proliferation of chondrocytes to form clusters of cells within articular cartilage, have been identified in several models of OA in osteoarthritic tissue from humans and animals, including mice. (12-16) These clones have been indicated to be a repair response to damage to the extracellular matrix of articular cartilage caused by the progression of the disease. (17) However, another study histologically evaluated C57 black mice and also noted a lack of chondrocyte cloning within osteoarthritic articular cartilage. (18) This lack of chondrocyte clones during the progression of OA may only occur in certain strains of mice, or possibly the morphology of chondrocyte clones in mice are dissimilar from other species and therefore are more difficult to identify, or are so few that the limited number of sections evaluated in this study failed to reveal any clones. Further morphological studies should be performed to identify whether clones are truly present in the joints of mice. If a lack of chondrocyte clones in these strains of mice alone were confirmed, studies would be necessary to identify whether there was a genetic mechanism that prevents these clones from forming

and may provide insight into the pathogenesis of the disease in this species and the role of chondrocytes and clones during disease progression.

In most species, including humans, it is widely accepted that initial superficial fibrillation and clefting associated with OA gradually erodes articular cartilage to the point of completely denuded bone, which is considered end-stage disease. However, tidemark clefts, such as those noted previously in hamsters (19), were identified in numerous joints within this study. Tidemark clefts form along the tidemark line (articular cartilage-calcified cartilage junction) and spread horizontally until large areas of articular cartilage detach resulting in complete loss of articular cartilage. Tidemark clefts associated with osteochondrosis in rats have been previously identified (20), but this separation of articular cartilage from the underlying calcified cartilage associated with osteoarthritis has only been identified previously in mice in a single study. (18) In addition, there is a noticeable decrease in superficial fibrillation and clefting of the articular cartilage in the OA mouse stifle joints compared to other species. These changes are remarkably different from those found in larger species, and warrant further investigation to identify the importance of tidemark clefts and their formation. The total number of tidemark clefts was initially included in the grading scheme developed in this study, however they were too few in number and only associated with severe disease to be included in the final version of the scheme. Because these tidemark clefts result in complete loss of articular cartilage, it was assumed that presence of a tidemark cleft within a joint would be reflected in the articular cartilage area and thickness measurements.

In summary, several histological changes associated with OA were identified in the mice included in this study. Tidemark clefts and changes in chondrocyte viability appear to be critical in the progression of OA in this species and further investigation into the mechanisms of these changes would assist in understanding the pathogenesis of OA in mice and potentially other species as well.

5.3 References

1. Custers RJ, Creemers LB, Verbout AJ, van Rijen MH, Dhert WJ, Saris DB. Reliability, reproducibility and variability of the traditional Histologic/Histochemical grading system vs the new OARSI osteoarthritis cartilage histopathology assessment system. Osteoarthritis Cartilage. 2007 Nov;15(11):1241-8.

2. Ostergaard K, Andersen CB, Petersen J, Bendtzen K, Salter DM. Validity of histopathological grading of articular cartilage from osteoarthritic knee joints. Ann Rheum Dis. 1999 Apr;58(4):208-13.

3. Ostergaard K, Petersen J, Andersen CB, Bendtzen K, Salter DM. Histologic/histochemical grading system for osteoarthritic articular cartilage: Reproducibility and validity. Arthritis Rheum. 1997 Oct;40(10):1766-71.

4. van der Sluijs JA, Geesink RG, van der Linden AJ, Bulstra SK, Kuyer R, Drukker J. The reliability of the mankin score for osteoarthritis. J Orthop Res. 1992 Jan;10(1):58-61.

5. Glasson SS, Blanchet TJ, Morris EA. The surgical destabilization of the medial meniscus (DMM) model of osteoarthritis in the 129/SvEv mouse. Osteoarthritis Cartilage. 2007 Sep;15(9):1061-9.

6. Kujoth GC, Hiona A, Pugh TD, Someya S, Panzer K, Wohlgemuth SE, et al. Mitochondrial DNA mutations, oxidative stress, and apoptosis in mammalian aging. Science. 2005 Jul 15;309(5733):481-4.

7. Mankin HJ, Dorfman H, Lippiello L, Zarins A. Biochemical and metabolic abnormalities in articular cartilage from osteo-arthritic human hips. II. correlation of morphology with biochemical and metabolic data. J Bone Joint Surg Am. 1971 Apr;53(3):523-37.

8. Taniguchi N, Carames B, Ronfani L, Ulmer U, Komiya S, Bianchi ME, et al. Aging-related loss of the chromatin protein HMGB2 in articular cartilage is linked to reduced cellularity and osteoarthritis. Proc Natl Acad Sci U S A. 2009 Jan 27;106(4):1181-6.

9. Baici A, Horler D, Lang A, Merlin C, Kissling R. Cathepsin B in osteoarthritis: Zonal variation of enzyme activity in human femoral head cartilage. Ann Rheum Dis. 1995 Apr;54(4):281-8.

10. Papaioannou NA, Triantafillopoulos IK, Khaldi L, Krallis N, Galanos A, Lyritis GP. Effect of calcitonin in early and late stages of experimentally induced osteoarthritis. A histomorphometric study. Osteoarthritis Cartilage. 2007 Apr;15(4):386-95.

11. Pelletier JP, Fernandes JC, Brunet J, Moldovan F, Schrier D, Flory C, et al. In vivo selective inhibition of mitogen-activated protein kinase kinase 1/2 in rabbit experimental osteoarthritis is associated with a reduction in the development of structural changes. Arthritis Rheum. 2003 Jun;48(6):1582-93.

12. Bendele AM, White SL, Hulman JF. Osteoarthrosis in guinea pigs: Histopathologic and scanning electron microscopic features. Lab Anim Sci. 1989 Mar;39(2):115-21.

13. Kouri JB, Arguello C, Quintero M, Chico A, Ramos ME. Variability in the cell phenotype of aggregates or "clones" of human osteoarthritic cartilage. A case report. Biocell. 1996 Dec;20(3):191-200.

14. Miller LM, Novatt JT, Hamerman D, Carlson CS. Alterations in mineral composition observed in osteoarthritic joints of cynomolgus monkeys. Bone. 2004 Aug;35(2):498-506.

15. Munoz-Guerra MF, Delgado-Baeza E, Sanchez-Hernandez JJ, Garcia-Ruiz JP. Chondrocyte cloning in aging and osteoarthritis of the hip cartilage: Morphometric analysis in transgenic mice expressing bovine growth hormone. Acta Orthop Scand. 2004 Apr;75(2):210-6.

16. Lahm A, Uhl M, Erggelet C, Haberstroh J, Mrosek E. Articular cartilage degeneration after acute subchondral bone damage: An experimental study in dogs with histopathological grading. Acta Orthop Scand. 2004 Dec;75(6):762-7.

17. Loeser RF. Molecular mechanisms of cartilage destruction in osteoarthritis. J Musculoskelet Neuronal Interact. 2008 Oct-Dec;8(4):303-6.

18. Takahama A. Histological study on spontaneous osteoarthritis of the knee in C57 black mouse. Nippon Seikeigeka Gakkai Zasshi. 1990 Apr;64(4):271-81.

19. Otterness IG, Chang M, Burkhardt JE, Sweeney FJ, Milici AJ. Histology and tissue chemistry of tidemark separation in hamsters. Vet Pathol. 1999 Mar;36(2):138-45.

20. Kato M, Onodera T. Morphological investigation of osteochondrosis induced by ofloxacin in rats. Fundam Appl Toxicol. 1988 Jul;11(1):120-31.

LIST OF REFERENCES

References

[homepage on the Internet]. . 2006. Available from: http://www.niams.nih.gov/Health_Info/Osteoarthritis/default.asp.

Abramson SB. Nitric oxide in inflammation and pain associated with osteoarthritis. Arthritis Res Ther. 2008;10 Suppl 2:S2.

Adams CS, Horton WE,Jr. Chondrocyte apoptosis increases with age in the articular cartilage of adult animals. Anat Rec. 1998 Apr;250(4):418-25.

Aigner T, Hemmel M, Neureiter D, Gebhard PM, Zeiler G, Kirchner T, et al. Apoptotic cell death is not a widespread phenomenon in normal aging and osteoarthritis human articular knee cartilage: A study of proliferation, programmed cell death (apoptosis), and viability of chondrocytes in normal and osteoarthritic human knee cartilage. Arthritis Rheum. 2001 Jun;44(6):1304-12.

Aigner T, McKenna L. Molecular pathology and pathobiology of osteoarthritic cartilage. Cell Mol Life Sci. 2002 Jan;59(1):5-18.

Aigner T. Apoptosis, necrosis, or whatever: How to find out what really happens? J Pathol. 2002 Sep;198(1):1-4.

Altman R, Asch E, Bloch D, Bole G, Borenstein D, Brandt K, et al. Development of criteria for the classification and reporting of osteoarthritis. classification of osteoarthritis of the knee. diagnostic and therapeutic criteria committee of the american rheumatism association. Arthritis Rheum. 1986 Aug;29(8):1039-49.

Altman R, Alarcon G, Appelrouth D, Bloch D, Borenstein D, Brandt K, et al. The american college of rheumatology criteria for the classification and reporting of osteoarthritis of the hip. Arthritis Rheum. 1991 May;34(5):505-14.

Altman R, Alarcon G, Appelrouth D, Bloch D, Borenstein D, Brandt K, et al. The american college of rheumatology criteria for the classification and reporting of osteoarthritis of the hand. Arthritis Rheum. 1990 Nov;33(11):1601-10.

Ameye LG, Young MF. Animal models of osteoarthritis: Lessons learned while seeking the "holy grail". Curr Opin Rheumatol. 2006 Sep;18(5):537-47.

Assimakopoulos AP, Katonis PG, Agapitos MV, Exarchou EI. The innervation of the human meniscus. Clin Orthop Relat Res. 1992 Feb;(275)(275):232-6.

Athanasiou KA, Agarwal A, Muffoletto A, Dzida FJ, Constantinides G, Clem M. Biomechanical properties of hip cartilage in experimental animal models. Clin Orthop Relat Res. 1995 Jul;(316)(316):254-66.

Ayral X, Pickering EH, Woodworth TG, Mackillop N, Dougados M. Synovitis: A potential predictive factor of structural progression of medial tibiofemoral knee osteoarthritis -- results of a 1 year longitudinal arthroscopic study in 422 patients. Osteoarthritis Cartilage. 2005 May;13(5):361-7.

Baici A, Horler D, Lang A, Merlin C, Kissling R. Cathepsin B in osteoarthritis: Zonal variation of enzyme activity in human femoral head cartilage. Ann Rheum Dis. 1995 Apr;54(4):281-8.

Bellamy N, Bell MJ, Goldsmith CH, Lee S, Maschio M, Raynauld JP, et al. BLISS index using WOMAC index detects between-group differences at low-intensity symptom states in osteoarthritis. J Clin Epidemiol. 2009 Nov 5.

Bendele AM. Animal models of osteoarthritis. J Musculoskelet Neuronal Interact. 2001 Jun;1(4):363-76.

Bendele AM, Hulman JF. Spontaneous cartilage degeneration in guinea pigs. Arthritis Rheum. 1988 Apr;31(4):561-5.

Bendele AM, White SL, Hulman JF. Osteoarthrosis in guinea pigs: Histopathologic and scanning electron microscopic features. Lab Anim Sci. 1989 Mar;39(2):115-21.

Boileau C, Martel-Pelletier J, Abram F, Raynauld JP, Troncy E, D'Anjou MA, et al. Magnetic resonance imaging can accurately assess the long-term progression of knee structural changes in experimental dog osteoarthritis. Ann Rheum Dis. 2008 Jul;67(7):926-32.

Bomsta BD, Bridgewater LC, Seegmiller RE. Premature osteoarthritis in the disproportionate micromelia (dmm) mouse. Osteoarthritis Cartilage. 2006 May;14(5):477-85.

Botter SM, Glasson SS, Hopkins B, Clockaerts S, Weinans H, van Leeuwen JP, et al. ADAMTS5-/- mice have less subchondral bone changes after induction of osteoarthritis through surgical instability: Implications for a link between cartilage and subchondral bone changes. Osteoarthritis Cartilage. 2009 May;17(5):636-45.

Brandt KD, Radin EL, Dieppe PA, van de Putte L. Yet more evidence that osteoarthritis is not a cartilage disease. Ann Rheum Dis. 2006 Oct;65(10):1261-4.

Bullough PG, Jagannath A. The morphology of the calcification front in articular cartilage. its significance in joint function. J Bone Joint Surg Br. 1983 Jan;65(1):72-8.

Burr DB. Anatomy and physiology of the mineralized tissues: Role in the pathogenesis of osteoarthrosis. Osteoarthritis Cartilage. 2004;12 Suppl A:S20-30.

Carlson CS, Loeser RF, Jayo MJ, Weaver DS, Adams MR, Jerome CP. Osteoarthritis in cynomolgus macaques: A primate model of naturally occurring disease. J Orthop Res. 1994 May;12(3):331-9.

Carlson CS, Loeser RF, Johnstone B, Tulli HM, Dobson DB, Caterson B. Osteoarthritis in cynomolgus macaques. II. detection of modulated proteoglycan epitopes in cartilage and synovial fluid. J Orthop Res. 1995 May;13(3):399-409.

Carlson CS, Loeser RF, Purser CB, Gardin JF, Jerome CP. Osteoarthritis in cynomolgus macaques. III: Effects of age, gender, and subchondral bone thickness on the severity of disease. J Bone Miner Res. 1996 Sep;11(9):1209-17.

Centers for Disease Control and Prevention (CDC). Prevalence and most common causes of disability among adults--united states, 2005. MMWR Morb Mortal Wkly Rep. 2009 May 1;58(16):421-6.

Chambers MG, Bayliss MT, Mason RM. Chondrocyte cytokine and growth factor expression in murine osteoarthritis. Osteoarthritis Cartilage. 1997 Sep;5(5):301-8.

Chavassieux P, Meunier PJ. Histomorphometric approach of bone loss in men. Calcif Tissue Int. 2001 Oct;69(4):209-13.

COLLINS DH, McELLIGOTT TF. Sulphate (35SO4) uptake by chondrocytes in relation to histological changes in osteoarthritic human articular cartilage. Ann Rheum Dis. 1960 Dec;19:318-30.

Custers RJ, Creemers LB, Verbout AJ, van Rijen MH, Dhert WJ, Saris DB. Reliability, reproducibility and variability of the traditional Histologic/Histochemical grading system vs the new OARSI osteoarthritis cartilage histopathology assessment system. Osteoarthritis Cartilage. 2007 Nov;15(11):1241-8.

Dalle Carbonare L, Valenti MT, Bertoldo F, Zanatta M, Zenari S, Realdi G, et al. Bone microarchitecture evaluated by histomorphometry. Micron. 2005;36(7-8):609-16.

Daubs BM, Markel MD, Manley PA. Histomorphometric analysis of articular cartilage, zone of calcified cartilage, and subchondral bone plate in femoral heads from clinically normal dogs and dogs with moderate or severe osteoarthritis. Am J Vet Res. 2006 Oct;67(10):1719-24.

de Hooge AS, van de Loo FA, Bennink MB, Arntz OJ, de Hooge P, van den Berg WB. Male IL-6 gene knock out mice developed more advanced osteoarthritis upon aging. Osteoarthritis Cartilage. 2005 Jan;13(1):66-73.

Ding C, Cicuttini F, Jones G. Tibial subchondral bone size and knee cartilage defects: Relevance to knee osteoarthritis. Osteoarthritis Cartilage. 2007 May;15(5):479-86.

Dore D, Ding C, Jones G. A pilot study of the reproducibility and validity of measuring knee subchondral bone density in the tibia. Osteoarthritis Cartilage. 2008 Dec;16(12):1539-44.

Englund M. The role of the meniscus in osteoarthritis genesis. Med Clin North Am. 2009 Jan;93(1):37,43, x.

Englund M, Guermazi A, Lohmander SL. The role of the meniscus in knee osteoarthritis: A cause or consequence? Radiol Clin North Am. 2009 Jul;47(4):703-12.

Englund M, Lohmander LS. Risk factors for symptomatic knee osteoarthritis fifteen to twenty-two years after meniscectomy. Arthritis Rheum. 2004 Sep;50(9):2811-9.

Eyre DR. Collagens and cartilage matrix homeostasis. Clin Orthop Relat Res. 2004 Oct;(427 Suppl)(427 Suppl):S118-22.

Eyre DR, Wu JJ. Collagen of fibrocartilage: A distinctive molecular phenotype in bovine meniscus. FEBS Lett. 1983 Jul 25;158(2):265-70.

Felson DT. An update on the pathogenesis and epidemiology of osteoarthritis. Radiol Clin North Am. 2004 Jan;42(1):1,9, v.

Felson DT. Risk factors for osteoarthritis: Understanding joint vulnerability. Clin Orthop Relat Res. 2004 Oct;(427 Suppl)(427 Suppl):S16-21.

Frisbie DD, Kawcak CE, Werpy NM, Park RD, McIlwraith CW. Clinical, biochemical, and histologic effects of intra-articular administration of autologous conditioned serum in horses with experimentally induced osteoarthritis. Am J Vet Res. 2007 Mar;68(3):290-6.

Glasson SS. In vivo osteoarthritis target validation utilizing genetically-modified mice. Curr Drug Targets. 2007 Feb;8(2):367-76.

Glasson SS, Blanchet TJ, Morris EA. The surgical destabilization of the medial meniscus (DMM) model of osteoarthritis in the 129/SvEv mouse. Osteoarthritis Cartilage. 2007 Sep;15(9):1061-9.

Goldring SR. The role of bone in osteoarthritis pathogenesis. Rheum Dis Clin North Am. 2008 Aug;34(3):561-71.

Goldring MB, Goldring SR. Osteoarthritis. J Cell Physiol. 2007 Dec;213(3):626-34.

Griffin TM, Huebner JL, Kraus VB, Guilak F. Extreme obesity due to impaired leptin signaling in mice does not cause knee osteoarthritis. Arthritis Rheum. 2009 Oct;60(10):2935-44.

Ham KD, Loeser RF, Lindgren BR, Carlson CS. Effects of long-term estrogen replacement therapy on osteoarthritis severity in cynomolgus monkeys. Arthritis Rheum. 2002 Jul;46(7):1956-64.

Hashimoto S, Nishiyama T, Hayashi S, Fujishiro T, Takebe K, Kanzaki N, et al. Role of p53 in human chondrocyte apoptosis in response to shear strain. Arthritis Rheum. 2009 Aug;60(8):2340-9.

Hashimoto S, Takahashi K, Amiel D, Coutts RD, Lotz M. Chondrocyte apoptosis and nitric oxide production during experimentally induced osteoarthritis. Arthritis Rheum. 1998 Jul;41(7):1266-74.

Hayami T, Pickarski M, Zhuo Y, Wesolowski GA, Rodan GA, Duong le T. Characterization of articular cartilage and subchondral bone changes in the rat anterior cruciate ligament transection and meniscectomized models of osteoarthritis. Bone. 2006 Feb;38(2):234-43.

Hill CL, Gale DG, Chaisson CE, Skinner K, Kazis L, Gale ME, et al. Knee effusions, popliteal cysts, and synovial thickening: Association with knee pain in osteoarthritis. J Rheumatol. 2001 Jun;28(6):1330-7.

Huang K, Wu LD. Aggrecanase and aggrecan degradation in osteoarthritis: A review. J Int Med Res. 2008 Nov-Dec;36(6):1149-60.

Hunter DJ, Eckstein F. Exercise and osteoarthritis. J Anat. 2009 Feb;214(2):197-207.

Hunter DJ, Felson DT. Osteoarthritis. BMJ. 2006 Mar 18;332(7542):639-42.

Hunter DJ, Lo GH, Gale D, Grainger AJ, Guermazi A, Conaghan PG. The reliability of a new scoring system for knee osteoarthritis MRI and the validity of bone marrow lesion assessment: BLOKS (boston leeds osteoarthritis knee score). Ann Rheum Dis. 2008 Feb;67(2):206-11.

Iwanaga T, Shikichi M, Kitamura H, Yanase H, Nozawa-Inoue K. Morphology and functional roles of synoviocytes in the joint. Arch Histol Cytol. 2000 Mar;63(1):17-31.

Kato M, Onodera T. Morphological investigation of osteochondrosis induced by ofloxacin in rats. Fundam Appl Toxicol. 1988 Jul;11(1):120-31.

KELLGREN JH, LAWRENCE JS, BIER F. Genetic factors in generalized osteo-arthrosis. Ann Rheum Dis. 1963 Jul;22:237-55.

Kim J, Xu M, Xo R, Mates A, Wilson GL, Pearsall AW,4th, et al. Mitochondrial DNA damage is involved in apoptosis caused by pro-inflammatory cytokines in human OA chondrocytes. Osteoarthritis Cartilage. 2009 Oct 1.

Kobayashi K, Amiel M, Harwood FL, Healey RM, Sonoda M, Moriya H, et al. The long-term effects of hyaluronan during development of osteoarthritis following partial meniscectomy in a rabbit model. Osteoarthritis Cartilage. 2000 Sep;8(5):359-65.

Kornaat PR, Ceulemans RY, Kroon HM, Riyazi N, Kloppenburg M, Carter WO, et al. MRI assessment of knee osteoarthritis: Knee osteoarthritis scoring system (KOSS)--inter-observer and intra-observer reproducibility of a compartment-based scoring system. Skeletal Radiol. 2005 Feb;34(2):95-102.

Kouri JB, Arguello C, Quintero M, Chico A, Ramos ME. Variability in the cell phenotype of aggregates or "clones" of human osteoarthritic cartilage. A case report. Biocell. 1996 Dec;20(3):191-200.

Kouri JB, Jimenez SA, Quintero M, Chico A. Ultrastructural study of chondrocytes from fibrillated and non-fibrillated human osteoarthritic cartilage. Osteoarthritis Cartilage. 1996 Jun;4(2):111-25.

Kuhn K, D'Lima DD, Hashimoto S, Lotz M. Cell death in cartilage. Osteoarthritis Cartilage. 2004 Jan;12(1):1-16.

Kujoth GC, Hiona A, Pugh TD, Someya S, Panzer K, Wohlgemuth SE, et al. Mitochondrial DNA mutations, oxidative stress, and apoptosis in mammalian aging. Science. 2005 Jul 15;309(5733):481-4.

Lahm A, Uhl M, Erggelet C, Haberstroh J, Mrosek E. Articular cartilage degeneration after acute subchondral bone damage: An experimental study in dogs with histopathological grading. Acta Orthop Scand. 2004 Dec;75(6):762-7.

Laprade RF, Wentorf FA, Olson EJ, Carlson CS. An in vivo injury model of posterolateral knee instability. Am J Sports Med. 2006 Aug;34(8):1313-21.

Little CB, Barai A, Burkhardt D, Smith SM, Fosang AJ, Werb Z, et al. Matrix metalloproteinase 13-deficient mice are resistant to osteoarthritic cartilage erosion but not chondrocyte hypertrophy or osteophyte development. Arthritis Rheum. 2009

Loeser RF. Molecular mechanisms of cartilage destruction in osteoarthritis. J Musculoskelet Neuronal Interact. 2008 Oct-Dec;8(4):303-6.

Lozano J, Saadat E, Li X, Majumdar S, Ma CB. Magnetic resonance T(1 rho) imaging of osteoarthritis: A rabbit ACL transection model. Magn Reson Imaging. 2009 Jun;27(5):611-6.

Luther JK, Cook CR, Cook JL. Meniscal release in cruciate ligament intact stifles causes lameness and medial compartment cartilage pathology in dogs 12 weeks postoperatively. Vet Surg. 2009 Jun;38(4):520-9.

Lutzner J, Kasten P, Gunther KP, Kirschner S. Surgical options for patients with osteoarthritis of the knee. Nat Rev Rheumatol. 2009 Jun;5(6):309-16.

MacCONAILL MA. The movements of bones and joints; the synovial fluid and its assistants. J Bone Joint Surg Br. 1950 May;32-B(2):244-52.

Mankin HJ, Dorfman H, Lippiello L, Zarins A. Biochemical and metabolic abnormalities in articular cartilage from osteo-arthritic human hips. II. correlation of morphology with biochemical and metabolic data. J Bone Joint Surg Am. 1971 Apr;53(3):523-37.

Marijnissen AC, Vincken KL, Vos PA, Saris DB, Viergever MA, Bijlsma JW, et al. Knee images digital analysis (KIDA): A novel method to quantify individual radiographic features of knee osteoarthritis in detail. Osteoarthritis Cartilage. 2008 Feb;16(2):234-43.

Maroudas AI. Balance between swelling pressure and collagen tension in normal and degenerate cartilage. Nature. 1976 Apr 29;260(5554):808-9.

Mason RM, Chambers MG, Flannelly J, Gaffen JD, Dudhia J, Bayliss MT. The STR/ort mouse and its use as a model of osteoarthritis. Osteoarthritis Cartilage. 2001 Feb;9(2):85-91.

Messner K, Fahlgren A, Ross I, Andersson B. Simultaneous changes in bone mineral density and articular cartilage in a rabbit meniscectomy model of knee osteoarthrosis. Osteoarthritis Cartilage. 2000 May;8(3):197-206.

Miller LM, Novatt JT, Hamerman D, Carlson CS. Alterations in mineral composition observed in osteoarthritic joints of cynomolgus monkeys. Bone. 2004 Aug;35(2):498-506.

Miller PD. The role of bone biopsy in patients with chronic renal failure. Clin J Am Soc Nephrol. 2008 Nov;3 Suppl 3:S140-50.

Mistry D, Oue Y, Chambers MG, Kayser MV, Mason RM. Chondrocyte death during murine osteoarthritis. Osteoarthritis Cartilage. 2004 Feb;12(2):131-41.

Moojen DJ, Saris DB, Auw Yang KG, Dhert WJ, Verbout AJ. The correlation and reproducibility of histological scoring systems in cartilage repair. Tissue Eng. 2002 Aug;8(4):627-34.

Moussavi-Harami SF, Pedersen DR, Martin JA, Hillis SL, Brown TD. Automated objective scoring of histologically apparent cartilage degeneration using a custom image analysis program. J Orthop Res. 2009 Apr;27(4):522-8.

Munoz-Guerra MF, Delgado-Baeza E, Sanchez-Hernandez JJ, Garcia-Ruiz JP. Chondrocyte cloning in aging and osteoarthritis of the hip cartilage: Morphometric analysis in transgenic mice expressing bovine growth hormone. Acta Orthop Scand. 2004 Apr;75(2):210-6.

Naito K, Watari T, Muta T, Furuhata A, Iwase H, Igarashi M, et al. Low-intensity pulsed ultrasound (LIPUS) increases the articular cartilage type II collagen in a rat osteoarthritis model. J Orthop Res. 2009 Oct 6;28(3):361-9.

Nayak SK, Panesar PS, Kumar H. p53-induced apoptosis and inhibitors of p53. Curr Med Chem. 2009;16(21):2627-40.

NIH consensus statement on total knee replacement. NIH Consens State Sci Statements. 2003 Dec 8-10;20(1):1-34.

Noble J, Hamblen DL. The pathology of the degenerate meniscus lesion. J Bone Joint Surg Br. 1975 May;57(2):180-6.

O'Driscoll SW, Keeley FW, Salter RB. The chondrogenic potential of free autogenous periosteal grafts for biological resurfacing of major full-thickness defects in joint surfaces under the influence of continuous passive motion. an experimental investigation in the rabbit. J Bone Joint Surg Am. 1986 Sep;68(7):1017-35.

O'Driscoll SW, Keeley FW, Salter RB. Durability of regenerated articular cartilage produced by free autogenous periosteal grafts in major full-thickness defects in joint surfaces under the influence of continuous passive motion. A follow-up report at one year. J Bone Joint Surg Am. 1988 Apr;70(4):595-606.

Oegema TR,Jr, Carpenter RJ, Hofmeister F, Thompson RC,Jr. The interaction of the zone of calcified cartilage and subchondral bone in osteoarthritis. Microsc Res Tech. 1997 May 15;37(4):324-32.

Oka H, Muraki S, Akune T, Mabuchi A, Suzuki T, Yoshida H, et al. Fully automatic quantification of knee osteoarthritis severity on plain radiographs. Osteoarthritis Cartilage. 2008 Nov;16(11):1300-6.

Olson EJ, Lindgren BR, Carlson CS. Effects of long-term estrogen replacement therapy on bone turnover in periarticular tibial osteophytes in surgically postmenopausal cynomolgus monkeys. Bone. 2008 May;42(5):907-13.

Olson EJ, Wentorf FA, McNulty MA, Parker JB, Carlson CS, LaPrade RF. Assessment of a goat model of posterolateral knee instability. J Orthop Res. 2008 May;26(5):651-9.

Ostergaard K, Andersen CB, Petersen J, Bendtzen K, Salter DM. Validity of histopathological grading of articular cartilage from osteoarthritic knee joints. Ann Rheum Dis. 1999 Apr;58(4):208-13.

Ostergaard K, Petersen J, Andersen CB, Bendtzen K, Salter DM. Histologic/histochemical grading system for osteoarthritic articular cartilage: Reproducibility and validity. Arthritis Rheum. 1997 Oct;40(10):1766-71.

Otterness IG, Chang M, Burkhardt JE, Sweeney FJ, Milici AJ. Histology and tissue chemistry of tidemark separation in hamsters. Vet Pathol. 1999 Mar;36(2):138-45.

Papaioannou NA, Triantafillopoulos IK, Khaldi L, Krallis N, Galanos A, Lyritis GP. Effect of calcitonin in early and late stages of experimentally induced osteoarthritis. A histomorphometric study. Osteoarthritis Cartilage. 2007 Apr;15(4):386-95.

Parfitt AM. Bone histomorphometry: Proposed system for standardization of nomenclature, symbols, and units. Calcif Tissue Int. 1988 May;42(5):284-6.

Pastoureau P, Leduc S, Chomel A, De Ceuninck F. Quantitative assessment of articular cartilage and subchondral bone histology in the meniscectomized guinea pig model of osteoarthritis. Osteoarthritis Cartilage. 2003 Jun;11(6):412-23.

Pelletier JP, Fernandes JC, Brunet J, Moldovan F, Schrier D, Flory C, et al. In vivo selective inhibition of mitogen-activated protein kinase kinase 1/2 in rabbit experimental osteoarthritis is associated with a reduction in the development of structural changes. Arthritis Rheum. 2003 Jun;48(6):1582-93.

Peterfy CG, Guermazi A, Zaim S, Tirman PF, Miaux Y, White D, et al. Whole-organ magnetic resonance imaging score (WORMS) of the knee in osteoarthritis. Osteoarthritis Cartilage. 2004 Mar;12(3):177-90.

Pineda S, Pollack A, Stevenson S, Goldberg V, Caplan A. A semiquantitative scale for histologic grading of articular cartilage repair. Acta Anat (Basel). 1992;143(4):335-40.

Price JS, Oyajobi BO, Russell RG. The cell biology of bone growth. Eur J Clin Nutr. 1994 Feb;48 Suppl 1:S131-49.

Pritzker KP, Gay S, Jimenez SA, Ostergaard K, Pelletier JP, Revell PA, et al. Osteoarthritis cartilage histopathology: Grading and staging. Osteoarthritis Cartilage. 2006 Jan;14(1):13-29.

Radin EL, Rose RM. Role of subchondral bone in the initiation and progression of cartilage damage. Clin Orthop Relat Res. 1986 Dec;(213)(213):34-40.

Roos H, Karlsson J. Anterior cruciate ligament instability and reconstruction. review of current trends in treatment. Scand J Med Sci Sports. 1998 Dec;8(6):426-31.

Rosenberg L. Chemical basis for the histological use of safranin O in the study of articular cartilage. J Bone Joint Surg Am. 1971 Jan;53(1):69-82.

Saris DB, Lafeber FP, Bijlsma JW, Dhert WJ, Verbout AJ. Cartilage repair by tissue engineering not successful in arthritic knees. Proc Orthop Res Soc. 2001:0200.

Schulze-Tanzil G, Muller RD, Kohl B, Schneider N, Ertel W, Ipaktchi K, et al. Differing in vitro biology of equine, ovine, porcine and human articular chondrocytes derived from the knee joint: An immunomorphological study. Histochem Cell Biol. 2009 Feb;131(2):219-29.

Schunke M, Tillmann B, Bruck M, Muller-Ruchholtz W. Morphologic characteristics of developing osteoarthrotic lesions in the knee cartilage of STR/IN mice. Arthritis Rheum. 1988 Jul;31(7):898-905.

Spahn G, Muckley T, Klinger HM, Hofmann GO. Whole-organ arthroscopic knee score (WOAKS). BMC Musculoskelet Disord. 2008 Nov 24;9:155.

Swets JA. Measuring the accuracy of diagnostic systems. Science. 1988 Jun 3;240(4857):1285-93.

Takahama A. Histological study on spontaneous osteoarthritis of the knee in C57 black mouse. Nippon Seikeigeka Gakkai Zasshi. 1990 Apr;64(4):271-81.

Taniguchi N, Carames B, Ronfani L, Ulmer U, Komiya S, Bianchi ME, et al. Aging-related loss of the chromatin protein HMGB2 in articular cartilage is linked to reduced cellularity and osteoarthritis. Proc Natl Acad Sci U S A. 2009 Jan 27;106(4):1181-6.

van der Kraan PM, van den Berg WB. Osteophytes: Relevance and biology. Osteoarthritis Cartilage. 2007 Mar;15(3):237-44.

van der Sluijs JA, Geesink RG, van der Linden AJ, Bulstra SK, Kuyer R, Drukker J. The reliability of the mankin score for osteoarthritis. J Orthop Res. 1992 Jan;10(1):58-61.

Wachsmuth L, Keiffer R, Juretschke HP, Raiss RX, Kimmig N, Lindhorst E. In vivo contrast-enhanced micro MR-imaging of experimental osteoarthritis in the rabbit knee joint at 7.1T1. Osteoarthritis Cartilage. 2003 Dec;11(12):891-902.

Wakamatsu E, Sissons HA. The cancellous bone of the iliac crest. Calcif Tissue Res. 1969;4(2):147-61.

Walker PS, Erkman MJ. The role of the menisci in force transmission across the knee. Clin Orthop Relat Res. 1975;(109)(109):184-92.

Weiner IB, Freedheim DK, Schinka JA, Velicer WF. Handbook of psychology. New York: Wiley; 2003.

Whitehouse WJ. The quantitative morphology of anisotropic trabecular bone. J Microsc. 1974 Jul;101(Pt 2):153-68.

Ytrehus B, Carlson CS, Ekman S. Etiology and pathogenesis of osteochondrosis. Vet Pathol. 2007 Jul;44(4):429-48.